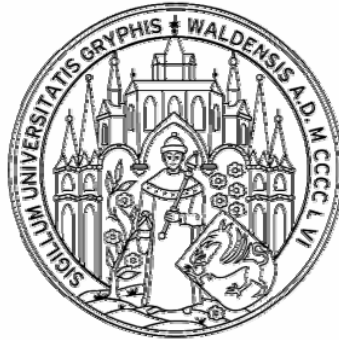


LANDSLIDE HAZARD ASSESSMENT IN MUONGLAY, VIETNAM APPLYING GIS AND REMOTE SENSING



Dissertation

in

fulfillment of the academic degree

doctor rerum naturalium (Dr. rer. nat.)

at the Faculty of Mathematics and Natural Sciences

Ernst-Moritz-Arndt-University Greifswald

Nguyen Quoc Khanh

born on 02, Sept, 1975

in Hanoi, Vietnam

Greifswald, 2009

Dekan:

1. Gutachter :

2. Gutachter:

Tag der Promotion:.....

Acknowledgment

The present thesis is the final output of my four-year study. I am grateful to numerous people who contributed towards shaping this dissertation.

I would like first to thank my supervisors, Prof. Dr. Reinhard Zölitz (Greifswald University, Germany), Prof. Dr. Nguyen Ngoc Thach (Hanoi University of Sciences), for their excellent guidance for my doctoral research. I would particularly like to thank Professor Reinhard Zölitz for providing me with the opportunity to work in the best conditions, and to Professor Nguyen Ngoc Thach for his assistance about geosciences. Their observations and comments helped me to establish the overall direction of research and move forward with investigation in depth, without which this study would not have completed.

Next I am very grateful for the 4-year-financial supporting from Ministry of Education and Training of Vietnam (MOET) and the German Academic Exchange Service (DAAD) for me to do this Ph.D. work. I am also highly appreciated the organization for my Ph.D. work between Vietnam Institute of Geosciences and Mineral Resources (VIGMR), Hanoi University of Science (HUS) and Greifswald University.

Special thanks to Dr. Le Quoc Hung, chief of Remote Sensing and Geomatics Department, Vietnam Institute of Geosciences and Mineral Resources, Dr. Nguyen Thanh Long for the data and sharing their experience with me to make this thesis possible. I would like to express my high appreciation to my colleagues, Dr. Nguyen Quoc Dinh, MSc. Do Minh Hien, PhD. Nguyen Thi Hai Van, Mrs. Nguyen Thi Phin, MSc. Le Nguyen Hoang, Mr. Luu Thanh Binh, Mr. Trinh Thanh for their excellent remote sensing and GIS technical assistance and data preparation. Especially, my sincere thanks also go to Dr. Pham Vu Luyen for their valuable cooperation during preparation of various maps and data.

During the time of studying, I owed a lot of gratitude to Mr. Vuong Van, Mr. Wessel from the Moskito Company for their contributions in GIS knowledge. My gratitude is due to Mr. J. Hartleib, for his spirit encouragement and sharing some of his enormous GIS experience and computer skills with me.

Thanks to all who collaborated and helped me by supporting to work in the best conditions. Thanks to all members of project 322.

Finally, my family with their endless love and all friends of mine are the great encouragements for me during this Ph.D. work.

ERKLÄRUNG

Hiermit erkläre ich, dass diese Arbeit bisher von mir weder an der Mathematisch - Naturwissenschaftlichen Fakultät der Ernst - Moritz - Arndt - Universität Greifswald noch einer anderen wissenschaftlichen Einrichtung zum Zwecke der Promotion eingereicht wurde.

Ferner erkläre ich, dass ich diese Arbeit selbständig verfasst und keine anderen als die darin angegebenen Hilfsmittel benutzt habe.

NGUYEN QUOC KHANH

STATEMENT OF ORIGINAL AUTHORSHIP

I, Khanh Q. NGUYEN, hereby state that the work contained in this assignment has not previously been submitted for assessment, either in whole or in part, by either myself or any other student at either Faculty of Mathematics and Sciences, Ernst-Moritz-Arndt-University of Greifswald or at any other tertiary institution except where explicitly acknowledged.

To the best of my knowledge and belief, the assignment contains no material which has been previously published or written by another person except where due reference is made.

ABSTRACT

Muong Lay is one of the important social and economic areas in Northwestern Vietnam. Landslides occur frequently in the area and seriously affect local livelihoods and living conditions. Therefore, the problem of landslide hazard and mitigation for a sustainable development of this area is significant. The spatial analysis of landslide hazard assessment in the mountainous regions in Muong Lay is important to address this development challenge.

The study firstly aims to produce the causal factor maps by verifying digital data. These factors then will be applied in a methodology based on statistical methods such as: “bivariate statistical analysis” and “multivariate statistical analysis” approach to calculate the susceptibility level of each class of each factor to landslide. The integration of Geographic Information System (GIS) and Remote Sensing (RS) for landslide hazard zonation and assessment is a valid approach. In these researches various methods for image integration and information extraction have been analysed and evaluated in detail.

This study shows the procedure for establishing a landslide hazard map for the Muong Lay area based on two methods: “Statistical index” and “Multiple linear regression”, applied by Van Westen (1993) and Carrara (1983). An inventory landslide map and nine factor maps (i.e., rainfall, slope degree, weathering, geological, geomorphology, lineament density, drainage density, landcover and elevation) were collected, established, stored and managed in definite GIS. After crossing the inventory landslide map and factor map, a cross-table was formed. Statistical analysis attribute fields of cross-table allowed for the calculation of a landslide density and forming a weight values for all classes of the factor map. The weight maps were formed from 9 factor maps. By combining (adding) nine maps of weight values, a weight map was created. Calculating the histogram of weight maps allows selecting boundary values to classify one into several classes, for example: very low hazard, low hazard, moderate hazard, high hazard and very high hazard.

The classified weight map provides for a new landslide hazard map of the Muong Lay area. The landslide hazard map supplies the assessment and prediction with the information about the scale and place of the landslide potential. The study not only estimated the accuracy of landslide hazard mapping results based on criteria considering the number of landslide occurrences (observed landslide), but also compared it with previous results of the research area. It also estimated the predicted results were accurate or inaccurate. Based upon this methodology, the hypothesis and predicted results were validated and very reliable. The areas of landslide probability of the different landslide susceptibility classes are considered to be both accurate and very reliable. The results of

the experiments have shown that the integration of GIS and remote sensing improved significantly the quality and effectiveness of the landslide hazard assessment.

This study focuses on the application of GIS and RS to landslide hazard assessment, especially for support of GIS modeling to landslide hazard susceptibility for Muong Lay area. By using Remote sensing with LandSat TM image and aerial photos of scale 1:50,000 and using statistical models with GIS-software's ENVI3.4, ILWIS3.0, PCI9.0 and ARC/GIS9.1, the study tries to evaluate and estimate the landslide in relation with naturally different elements of natural conditions such as geology, geomorphology, geology-engineering, tectonics, hydrology, rainfall, etc...

The goal of this study is to produce a landslide hazard map at the medium scale of 1:50,000 that identify geographic areas where future landslides are most likely to occur. Knowing such locations, planners and engineers can design good roads and other infrastructure project with fuller awareness of the risks in most vulnerable areas. By developing and applying reliable and accurate methods for assessing landslide hazard, it is possible to enhance planning strategies leading to disaster mitigation, economic losses reduction and safer communities and environments building. The primary aim of this thesis is to recognize and map the landslide hazard in Muong Lay, North-West of Vietnam in order to reduce loss of lives, property damage and social and economic disruption from slope movements.

TABLES OF CONTENT

ACKNOWLEDGMENT	2
ABSTRACT	4
TABLE OF CONTENT	6
LIST OF FIGURES	9
LIST OF TABLES	12
LIST OF ABBREVIATIONS	13
CHAPTER 1. INTRODUCTION	14
1.1. GENERAL	14
1.2. THE DEVELOPMENT CHALLENGE	14
1.3. RESEARCH OBJECTIVES	17
1.3.1. Main objectives	17
1.3.2. Specific Objectives	17
1.4. CONTENTS	18
1.5. THE STUDY AREA DESCRIPTION	18
1.5.1. Location	18
1.5.2. Climate	19
1.5.3. Terrain features	21
1.5.4. Land use in the study area	21
1.5.5. River and stream systems	22
1.5.6. Soil and rock in the study area	22
1.5.7. Landslide in the study area	23
CHAPTER 2. DEFINITION OF LANDSLIDE AND LANDSLIDE HAZARD MAPPING	25
2.1. DEFINITION OF LANDSLIDE HAZARD	25
2.1.1. Concepts about landslide	25
2.1.2. Landslide types	25
2.1.3. Processes of Landslide	29
2.1.4. Landslide causes	31
2.1.4.1. Geological causes	31
2.1.4.2. Morphological causes	32
2.1.4.3. Physical causes	33
2.1.4.4. Human causes	34
2.1.4.5. Three cause most of the damaging landslides	34
2.1.5. How to Reduce the Effects of Landslides	36
2.1.6. Hazard, risk and vulnerability	36

2.1.7. Landslide hazard maps	36
2.2. LANDSLIDE HAZARD ZONATION MODELS	37
2.2.1. Definition	37
2.2.2. Some popular deterministic models for landslide zonation	38
2.2.3. Scale of mapping for landslide hazard zonation	40
CHAPTER 3. REMOTE SENSING AND GEOGRAPHIC INFORMATION SYSTEM (GIS) IN LANDSLIDE HAZARD ASSESSMENT	41
3.1. REMOTE SENSING APPROACHES FOR LANDSLIDE HAZARD ASSESSMENT	41
3.1.1. Genaral	41
3.1.2. Pre-Processing	44
3.1.2.1. Radiometric correction	44
3.1.2.2. Geometric correction	45
3.1.3. Image Processing	45
3.1.3.1. Lineament extraction	45
3.1.3.1.1. <i>Edge enhancement</i>	46
3.1.3.1.2. <i>Lineament extraction</i>	46
3.1.3.2. Land cover	48
3.1.4. Aerial-photos for landslide occurence mapping	51
3.2. GEOGRAPHIC INFORMATION SYSTEM (GIS) APPROACHES FOR LANDSLIDE HAZARD ASSESSMENT	52
3.2.1. Genaral	52
3.2.2. Digital Elevation model (DEM)	54
3.2.3. GIS and Statistical models	55
3.2.3.1. GIS modelling methods	55
3.2.3.2. Models of the Overall Estimation of Landslide Susceptibility	59
CHAPTER 4. LANDSLIDE HAZARD ASSESSMENT IN MUONG LAY AREA	60
4.1. EXISTING LANDSLIDE IN MUONG LAY	60
4.1.1. Landslide inventory mapping	60
4.1.2. Landslide occurence map of Muong Lay	63
4.2. DATA LAYER PREPARATIONS	67
4.2.1. Geological factor	69
4.2.2. Weathering crust factor	71
4.2.3. Geomorphological factor	73
4.2.4. Lineament density factor	76
4.2.5. Elevation factor	77
4.2.6. Slope degree factor	79

4.2.7. Drainage density factor	80
4.2.8. Landcover factor	81
4.2.9. Rainfall factor	82
4.3. APPLICATION OF STATISTICAL ANALYSIS APPROACHES FOR LANDSLIDE HAZARD MAPPING IN MUONG LAY	85
4.3.1. Bivariate statistical and multivariate statistical approaches	85
4.3.2. Statistical index method for landslide susceptibility	91
4.3.3. Multiple linear regression method for landslide susceptibility	92
CHAPTER 5. RESULTS AND DISCUSSION	94
5.1. ANALYSIS RESULTS OF STATISTICAL INDEX METHOD	94
5.1.1. Weighted factors	94
5.1.1.1. Weighted factors of slope degree	94
5.1.1.2. Weighted factors of weathering crust	95
5.1.1.3. Weighted factors of geological	96
5.1.1.4. Weighted factors of geomorphology	98
5.1.1.5. Weighted factors of lineament density	99
5.1.1.6. Weighted factors of elevation	101
5.1.1.7. Weighted factors of drainage density	102
5.1.1.8. Weighted factors of landcover	103
5.1.1.9. Weighted factors of rainfall	105
5.1.2. Landslide hazard zonation map of statistical index method	106
5.2. ANALYSIS RESULTS OF MULTIPLE LINEAR REGRESSION METHOD	111
5.2.1. Variables description	111
5.2.2. Regression coefficients	113
5.2.3. Landslide hazard zonation map of multiple linear regression method	115
5.3. ACCURACY OF PREDICTION RESULTS	118
5.4. DISCUSSION	123
CHAPTER 6. CONCLUSIONS AND RECOMMENDATIONS	126
6.1. CONCLUSIONS	126
6.2. RECOMMENDATIONS	127
REFERENCES	128
CURRICULUM VITAE	139

LIST OF FIGURES

Figure 1-1.	Landslide damage on road transport system in North-western Vietnam	15
Figure 1-2.	Human fatalities (right) and damages to crops (left) in North-western Vietnam	16
Figure 1-3.	The study area, Muong Lay, Viet nam	19
Figure 1-4.	The monthly temperature of 2004	20
Figure 1-5.	The monthly rainfall of Muong Lay	20
Figure 1-6.	The Landslide map of North-West of Vietnam	24
Figure 2-1.	The parts of a landslide	26
Figure 2-2.	These schematics illustrate the major types of landslide movement that are described within this article	27
Figure 3-1.	The satellite image of Muong Lay area (LandSat TM, dated 20th February 1999); a) band1; b) band2; c) band3; d) band4 e) band5; f) band6; g) band7; h) LandSat TM True-color Composite; i) LandSat TM False-color Infrared Composite (bands 4, 7, 1 as RGB)	44
Figure 3-2.	Radiometric correction in Pre-processing	45
Figure 3-3.	Geometric correction in Pre-processing	46
Figure 3-4.	Edge enhancement in Image processing	47
Figure 3-5.	Image Processing: Lineament extraction.	48
Figure 3-6.	The map of lineament extraction of Muong Lay	48
Figure 3-7.	The flowchart of lineament mapping	49
Figure 3-8.	The flowchart of landcover mapping	50
Figure 3-9.	Setting up sample patterns for classification (Key areas)	51
Figure 3-10.	Flowchart of the supervised classification with Maximum Likelihood Algorithm	52
Figure 3-11.	The information of regions of interest (ROIs)	52
Figure 3-12.	The structure of GIS: a) hardware, b) software, and c) data of GIS	54
Figure 3-13.	Digital Elevation Models (DEM) of Muong Lay area	56
Figure 3-14.	Simplified flowchart of the statistical analysis: This flowchart illustrates the various terms that will be used in next chapter	60
Figure 4-1.	Flow chat of landslide zonation	62
Figure 4-2	a) A aerial-photo; b) 3D view of 30 image pairs of MuongLay area (pixel size 0.5 m/pix)	63
Figure 4-3.	Examples of a landslide happening in Ban Moi, Muong Tung, Muong Lay. a) Signs of landslide concern on aerial photograph; b) Photo-landslide observed outside the field	63
Figure 4-4.	Examples of a landslide happening in Ma Lu Thang, Muong Lay. (a) Signs of landslide concern on aerial photograph; (b) Photo-landslide observed outside the field	64
Figure 4-5.	Some pictures of landslide occurrences in Muong Lay. a) Landslide in Ho Muc, Pa Ham, Muong Cha; b) Landslide in Xa Long, Huoi Leng, Muong Cha	64
Figure 4-7.	Landslide occurrence map of Muong Lay	68

Figure 4-8:	<i>The Geological map of Muong Lay</i>	71
Figure 4-9.	<i>The Weathering crust map of Muong Lay area</i>	72
Figure 4-10.	<i>The Geomorphological map of Muong Lay area</i>	75
Figure 4-11.	<i>Lineament density map of Muong Lay</i>	78
Figure 4-12.	<i>The elevation map of Muong Lay</i>	79
Figure 4-13.	<i>The map of slope classes in the study area</i>	80
Figure 4-14.	<i>Drainage density map of Muong Lay</i>	82
Figure 4-15.	<i>Landcover map of Muong Lay</i>	83
Figure 4-16.	<i>Location sketch of hydrometeorology stations in Muong Lay, Lai Chau province and surroundings</i>	84
Figure 4-17.	<i>The map distributed rainfall average year of Muong Lay with monitoring period of 9 years (from 1996 to 2005)</i>	85
Figure 4-18.	<i>Flowchart of landslide hazard zonation techniques</i>	87
Figure 4-19.	<i>Simplified flowchart for bivariate statistical analysis (adopted from Westen 2003)</i>	89
Figure 4-20.	<i>Multivariate statistical analysis flowchart (adopted from Westen 2004)</i>	90
Figure 4-21.	<i>Schematic representation of statistical index method implemented in GIS</i>	93
Figure 4-22.	<i>Schematic representation of multiple linear regression method implemented in GIS</i>	94
Figure 5-1.	<i>The weight index of each class of slope factor</i>	96
Figure 5-2.	<i>The weight index of each class of weathering factor</i>	97
Figure 5-3.	<i>The weight index of each class of engineering geology factor</i>	99
Figure 5-4.	<i>The weight index of each class of Geomorphological factor</i>	100
Figure 5-5.	<i>The weight index of each class of lineament density factor</i>	101
Figure 5-6.	<i>The weight index of each class of elevation factor</i>	103
Figure 5-7.	<i>The weight index of each class of drainage density factor</i>	104
Figure 5-8.	<i>The weight index of each class of landcover factor</i>	105
Figure 5-9.	<i>The weight index of each class of rainfall factor</i>	106
Figure 5-10.	<i>The frequency histogram in natural break method</i>	109
Figure 5-11.	<i>The map of landslide susceptibility index of Muong Lay</i>	110
Figure 5-12.	<i>Landslide hazard zonation map from Statistical index method</i>	111
Figure 5-13.	<i>The map of landslide susceptibility index of Muong Lay</i>	116
Figure 5-14.	<i>The frequency histogram in natural break method</i>	117
Figure 5-15.	<i>Landslide hazard zonation map from multiple linear regression method</i>	118
Figure 5-16.	<i>Curves of the observed landslide accumulation versus cumulative areal percentage of increased landslide susceptibility</i>	120
Figure 5-17.	<i>Example of some landslides overlaying the final LSZ map</i>	120
Figure 5-18.	<i>Landslide hazard zonation map with observed landslides. a) Landslide hazard map from statistical index model; b) Landslide hazard map from multiple linear regression model</i>	122

<i>Figure 5-19.</i>	<i>Bar chart showing the distribution of various hazard zones</i>	<i>124</i>
<i>Figure 5-20.</i>	<i>The final Landslide Hazard Zonation map of Muong Lay</i>	<i>125</i>

LIST OF TABLES

Table 1-1.	<i>Average values of rainfall parameters in 1994-2007 in Muong Lay</i>	20
Table 1-2.	<i>The statistical of landslide hazard in Muong Lay, Dien Bien province</i>	23
Table 2-1.	<i>Types of landslides. Abbreviated version of Varnes' classification of slope movements.</i>	26
Table 3-1.	<i>The spectral bands for the Landsat 7 TM satellite</i>	43
Table 3-3.	<i>Some major characteristics of visual and digital lineament extraction</i>	47
Table 3-4.	<i>Characteristics of landslide susceptibility</i>	57
Table 4-1.	<i>Quantitative landslide classification with corresponding number of slides in Muong Lay</i>	65
Table 4-2.	<i>List of landslide occurrences in Muong Lay</i>	66
Table 4-3.	<i>Some remarkable features of geological</i>	70
Table 4-4.	<i>The average year of rainfall of 14 hydrometeorology stations from 1996 to 2005 (10 year)</i>	84
Table 5-1.	<i>Distribution of landslide and susceptibility classes of slope degree</i>	95
Table 5-2.	<i>Distribution of landslides and susceptibility classes of weathering crust</i>	96
Table 5-3:	<i>Distribution of landslide and susceptibility units of geological factor</i>	98
Table 5-4.	<i>Distribution of landslides and susceptibility classes of geomorphology</i>	99
Table 5-5.	<i>Distribution of landslide and susceptibility classes of lineament factor</i>	101
Table 5-6.	<i>Distribution of landslide and susceptibility classes of elevation factor</i>	102
Table 5-7.	<i>Distribution of landslide and susceptibility classes of density drainage</i>	103
Table 5-8.	<i>Distribution of landslide and landcover classes</i>	105
Table 5-9.	<i>Distribution of landslide and rainfall classes</i>	106
Table 5-10.	<i>Lists the weighted values of nine factors</i>	107
Table 5-11.	<i>The areas of different landslide hazard zones based on the statistical index method</i>	110
Table 5-12.	<i>Frequency ratios of all classes of weathering crust, geological, and geomorphological factors</i>	113
Table 5-13.	<i>Statistics characterizations description of all variables</i>	114
Table 5-14.	<i>Results of multiple linear regression model</i>	115
Table 5-15.	<i>The areas of different landslide hazard zones based on the multiple linear regression method</i>	117
Table 5-16.	<i>Comparison of different landslide mapping methods</i>	119
Table 5-17.	<i>Summary of the prediction accuracy of the LSZ map</i>	122
Table 5-18.	<i>The hazard value ranges used for the classification of LHZ map</i>	124

LIST OF ABBREVIATIONS

DEM	Digital Elevation Model
ETM	Enhanced Thematic Map
GIS	Geographic Information Systems
GPS	Global Positioning System
LANDSAT	Land remote sensing satellite
LATP	Long-term annual total precipitation
LSC	Landslide susceptibility class
LSI	Landslide susceptibility index
LSZ	Landslide susceptibility zonation
LHZ	Landslide hazard zonation
NDVI	Normalized Difference Vegetation Index
PCA	Principal Component Analysis
RS	Remote Sensing
SPOT	Satellite Pour l'Observation de la Terre
TM	Thematic Map
VIGMR	Vietnam Institute of Geosciences and Mineral Resources
USGS	U.S. Geological Survey

CHAPTER 1: INTRODUCTION

1.1. GENERAL

Landslide in mountainous areas is a serious hazard. It affects the lives and livelihoods of locals and local economies and can have intergeneration psychological effects that can take decades to heal. As mountain villagers increasingly degrade forest resources and seek out opportunities in foothills and lowlying areas, the threat and potential risk of landslides to human life and livelihoods has increased over past century.

Muong Lay is one of the important social-economic areas in northwestern Vietnam. Landslides occur frequently in the area and seriously affect local living conditions. Therefore, the problem of landslide hazard and mitigation for a sustainable development of this area is significant. The spatial analysis of landslide hazard assessment in the mountainous regions in Muong Lay is important to address this development challenge.

Within the spatial analysis, GIS with its analytical data storage and cartographic capacities allows a relatively quick and easy landslide hazard assessment for the given region. Therefore, it has been applied extensively to landslide hazard research studies, particularly those undertaken over the last decade. The most often applied approaches using GIS techniques are based on statistic methods especially based on statistical method such as "Statistical index" method and "Multiple linear regression" method of Van Westen (1993) and Carrara (1983).

This research used GIS) and RS to research and assess landslide hazards, developing maps of landslide potentiality in Muong Lay area. This method has high efficacy in interpreting and zoning landslide hazard and predicting the landslide with more reliability, quickness and lower cost. This research will help the designing, planning, migration and resettlement, especially for the social and economic development in Muong Lay area (in particular) and for Vietnam (in general).

1.2. THE DEVELOPMENT CHALLENGE

Muong Lay area of Dien Bien province, Vietnam is a region highly affected by landslides and mudslides. These landslides occur persistently and endanger the lives and livelihoods of thousands of households, most of which are ethnic minority and live in poverty. Blocks

of landslides with thousands to millions tones of soil are the material supply for mudslides (Tuyet, 1999). Landslides and mudslides occur annually in Muong Lay. Long and heavy rain in Muong Lay generated landslides in streams of Nam He, Huoi Lo, Huoi Leng, Huoi Phan in 1990, 1994, 1996 with, with giant size that blocks of ten thousand to millions m³ dumped creating natural-fender of brooks (Tuyet, 1999). Landslides and mudslides in Muong Lay injured more than 300 peoples, led to the evacuation 177 people, damaged thousands of home, destroyed roads, bridges, and factories, and buried ten thousand hectares of defendant garden fields. It caused over US\$200 million in damages. (source: Statistical Office of Lai Chau province).



Figure 1-1. Landslide damage on road transport system in North-western Vietnam

With the above reasons, this thesis selected Muong Lay as the typical region of landslides for researching, assessing and proposing methods to minimize damages caused by landslide hazard and enhancing the socio-economic development for this region. It also contains practical information useful for prevention and control measures to minimize the potential risks of landslides, contributed to socio-economic planning, and current and future resettlement plans for villages in the Muong Lay area affected by large-scale hydroelectrical development (e.g., Son La Dam).



Figure 1-2. Human fatalities (right) and damages to crops (left) in North-western Vietnam

1.3. RESEARCH OBJECTIVES

1.3.1. Main objectives

The purpose of this study is to develop an integrated approach for landslide hazard assessment in Muong Lay, Vietnam area by using Geographical Information System (GIS) combined with Remote Sensing (RS). The thesis aims to contribute to the analysis of spatial landslide susceptibility in mountainous regions such as Muong Lay and similar areas. The thesis also seeks to affirm scientific significance on selection and application of advanced treatment method systems for landslides in the catchment basin of Son La hydroelectric dam.

1.3.2. Specific Objectives

In this study, the author shows the procedure for establishing of the landslide hazard map for Muong Lay area based on "Statistical index method" and "Multiple linear regression method" applied by Van Westen (1993) and Carrara (1983). Based on materials of field-work and gathered in the last time a landslide hazardous map had been established. These materials are inventory landslide map and 9 other factors maps: rainfall, slope degree, weathering, geological, geomorphological, lineament density, drainage density, landcover and elevation. These materials are established, stored and managed in definite GIS. After crossing the inventory landslide map and factor map, a cross-table was formed. A statistical analysis attribute fields of cross-table allows calculating a landslide density and forming a weight values for every classes of factor map. In results, the 9 weight maps were formed from 9 factor maps. By combining (adding) 9 maps of weight values a weight map was created. Calculating the histogram of weight maps allows selecting boundary values to classify one into some classes, for example: very low hazard, low hazard, moderate hazard, high hazard and very high hazard. The classified weight map is the landslide hazard map of Muong Lay area. The landslide hazard map supplies the assessment and prediction with information about a scale and place of the landslide potential.

The author has applied information technology (RS and GIS) and predicting models to fit Vietnam conditions. By using of Remote sensing with LandSat TM image and aerial photos of scale 1:50'000 and using of statistic models with GIS-software's ENVI3.4, ILWIS3.0, PCI9.0, ARCGIS9.1, the study tries to evaluate and estimate the landslide in relation with naturally different elements of natural conditions such as geology, geomorphology, geology-engineering, tectonics, hydrology, etc...

Existing landslides are mapped on large scale topographic base maps by interpreting of aerial photographs. Investigations are helpful in checking the sizes and shapes of

landslides, to identify the types of movements and materials involved, and to determine the activity (active, dormant, etc.) of failed slopes.

1.4. CONTENTS

This thesis is divided into six chapters. Chapter 1 provides a short overview of the research area and objectives of the study. Chapter 2 presents the landslide hazard and method. Chapter 3 introduces the methodology supported by GIS and RS. Chapter 4 presents the landslide hazard assessment in Muong Lay area including Existing Landslide and Landslide-Susceptibility Mapping in Muong Lay. Chapter 5 discusses the results of relationship of the landslide and various factors. Finally, Chapter 6 summarizes the main results and recommendations of the study.

1.5. STUDY AREA DESCRIPTION

1.5.1. Location

Muong Lay is located in the Northwest of Vietnam, covers between 21°45' and 22°08' north latitude, between 102°58' and 103°12' East longitude. Its altitude is about 160-1980 meters (m) above sea level.

Coordinates lat/long:	System of UTM, Zone 48:
21°45' - 22°08' North latitude	Y: from 2410000 to 2446600
102°58' - 103°12' East longitude	X: from 292000 to 312400

Muong Lay consists of 3 wards and 3 communes: Le Loi ward; Song Da ward; La Nay ward, Lay Nua commune, Muong Tung commune and Huoi Leng commune. Muong Lay lies completely in the catchment of Nam Lay river, about 90 km north of Dien Bien, about 70 km north of Lai Chau town, and about 500 km to the north-west Hanoi. It is described in figured 1-3. The research area is about 553 km² large and 14,379 people reside in or around the Muong Lay town.

Twenty-four ethnic groups live in the province, nearly all of which are considered poor. In general, people in North-West Vietnam suffer more difficulties than people in other, less remote regions of the country.

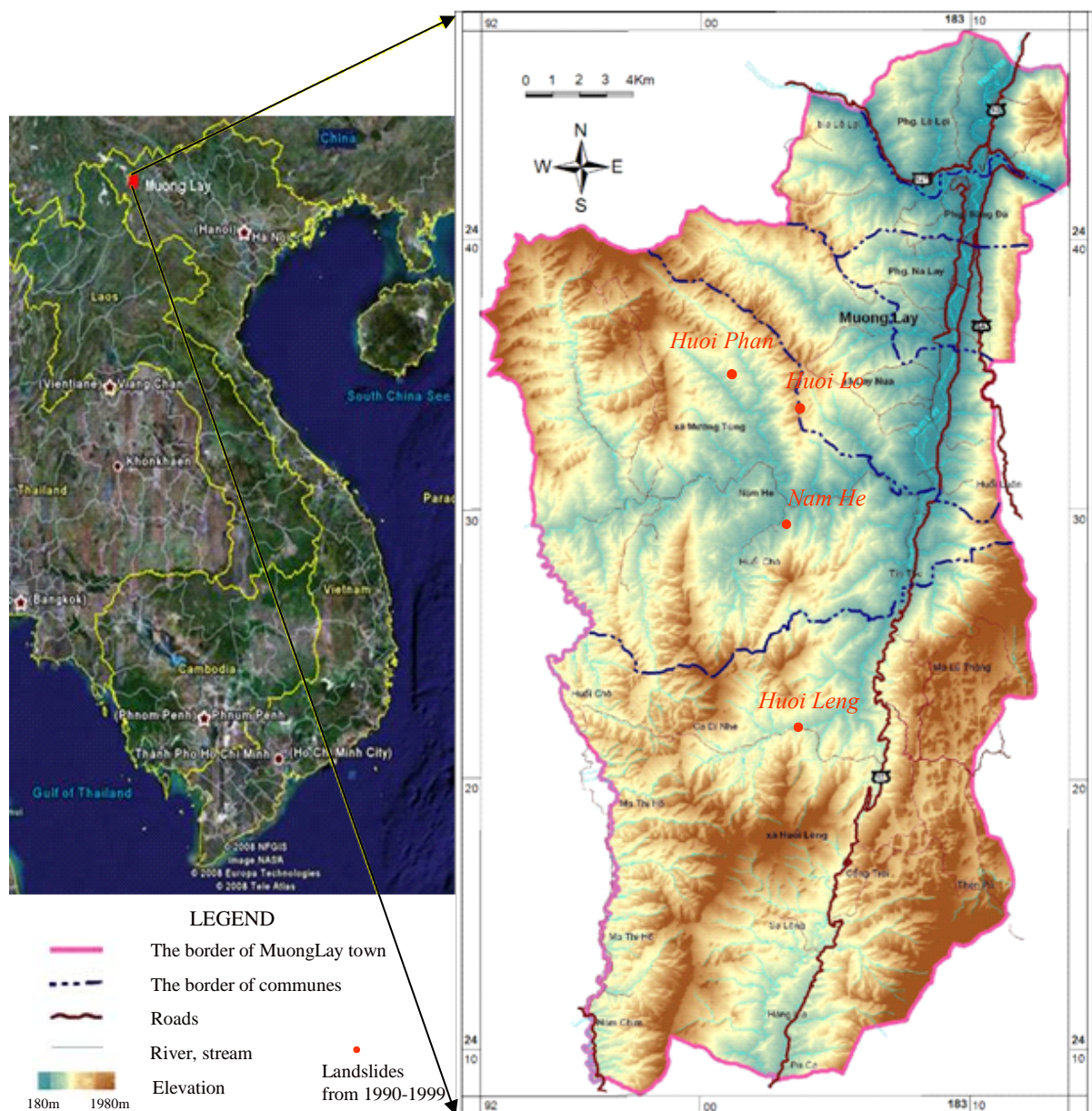


Figure 1-3. The Muong Lay Vietnam study area

1.5.2. Climate

Muong Lay lies on the tropical climate with strong monsoon influence that is a considerable amount of sunny days and high rate of rainfall and humidity. The climate here is very severe and different in areas of the city. January and February are the coolest months with usual temperature of $15.5-16.5^{\circ}\text{C}$, a long fog, sometimes the temperature is down to $<10^{\circ}\text{C}$, snowing. While June and July are the hottest featuring with temperature around $27-30^{\circ}\text{C}$ (Figure 1-4), sometimes the temperature is up to 40°C . The average temperature is about 25.1°C (Tuyet, 1999).

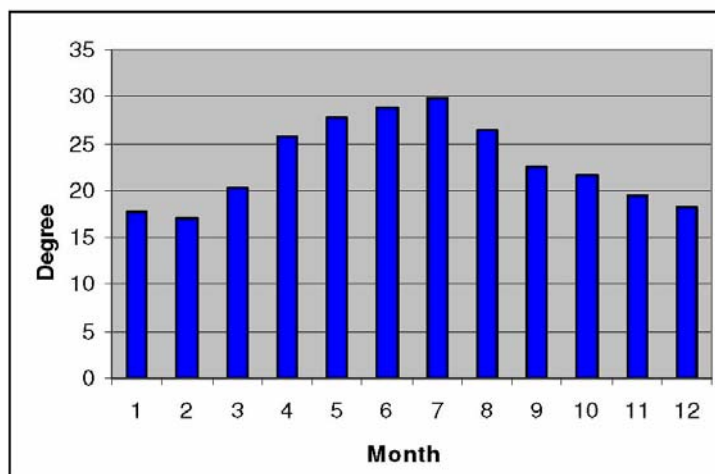


Figure 1-4. The monthly temperature of 2004

There are pretty well defined dry and wet season. The dry season lasts from September to March (figure 1-5), (Source: *Statistical office of Lai Chau province, 2004*). The rainy season, normally begins March or April then continues to August or September. In this season, there are series of continual rains, which sometimes last all the week. The later months of the wet season, particularly April and September bring much heavier rains causing the province a victim of numerous typhoons. The total annual precipitation in Muong Lay is over 1600-2800mm per year (*Tuyet, 1999*).

Table 1-1. Average values of rainfall parameters in 1994-2007 in Muong Lay
(Statistical office of Lai Chau province, 2007)

Month Station	I	II	III	IV	V	VI	VII	VIII	IX	X	XI	XII
Muong Lay	26.9	36.3	59.7	134.5	257.6	437.7	467.8	371.3	145.6	90.6	51.0	25.2

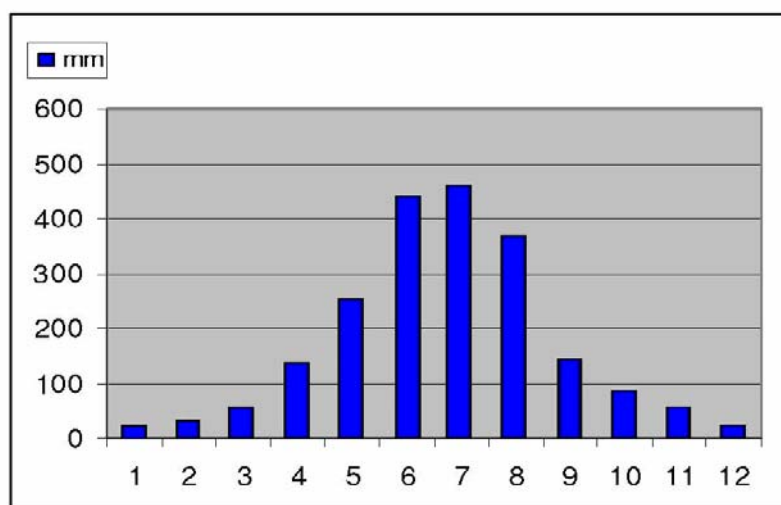


Figure 1-5. The monthly rainfall of Muong Lay
(Source: *Statistical office of Lai Chau province, 2007*)

1.5.3. Terrain features

The terrain in Muong Lay is rather complicated. In general, the altitude decreases gradually from West to East. The study area (Figure 1-3) can be divided into 3 parts, i.e. mountainous, hilly, and plain areas, of which the mountainous part occupies most of the total area (80%). Generally, the mountainous part is strongly dissected and steep, and characterized by high mountain tops with altitudes ranging from 160 to 1980 m. The highest mountain is Phu Dao (1980 m). The plains are valleys Nam La and Nam Lay. The hills are dispersed between the mountains and the plains (*Tuyet, 1999*).

Terrain of this province is pretty complicated. High mountain, strongly dissected and slope, especially in the western part are the particular relief features of the province. It suddenly changes from mountainous regions to narrow plains at coastal areas of the eastern part. Besides, the plain is connected to the sea only by only stream and river system. The dominant terrain feature of this plain is the large group of lagoons that lie behind the coastal sand dunes. In general, its terrain decreases gradually from west to east. The area is dominated by slopes ranging from 15° to 35° while steep slopes greater 35° occupy a much smaller area. The west of the province is mainly made up by hilly and mountainous regions which occupy 70 % of the total area. Mountains and hills with slope gradient from 15° to 30° occupy approximately 80 % of the total area. Slightly slope relief from 3° to 8° and plains occupy about 15 %. The remaining 5% of the total area contains mostly, sand dunes and sand bars along the coastal area (*Tuyet, 1999*).

1.5.4. Land use in the study area

Land use in the research area varies depending on the relief; types of soil, climate and human activities. Major land-use patterns in the mountainous regions comprise of the various types of vegetation such as tropical forest with trees, shrubs and grasses while in the coastal plains, the dominant land use is agriculture, primarily paddy rice. The natural vegetation is now replaced strongly by man-made activities such as wet rice, fruit – tree or timber.

According to statistical data, forests used to occupy approximately 30 % to 35 % of the total research area. However, many forest regions have been deforested for firewood and agricultural development (*Statistical office in Lai Chau province, 2007*). The analysis of remote sensing image (LandSat TM, 1999-2000) have shown a considerable decreasingly amount of quantity, quality and structure of land use patterns in the region in comparison to previous documents. This is an important factor that facilitates erosion, floods and landslide events.

Vegetation plays a very important role in landslide mechanism. In this study, four types of land use are considered: agriculture, forest, shrub and bared hills, and village and buildup

areas. In the research area, forest, and shrubs and bare hill areas are dominant on respectively 27.2% and 67.1% of the area. The large area of shrubs and bare hills is very favorable for landslides to occur. In recent years, the natural vegetation has been strongly altered by man-made activities such as agriculture and timber production. Because people clear the forest and leave the soil bare, there is a high risk of landslides.

1.5.5. River and stream systems

The Muong Lay's topography is characterized by mountains, while smaller parts are hills and plains. Therefore, the rivers or streams have short lengths and steep longitudinal morphometries, which abruptly changes into gentle slopes in the plains (*Tuyet, 1999*).

Muong Lay catchment is part of the Da River. Hence, the streams tend to flow toward Da River. There are four main rivers in the research area: Da River, Nam Lay River, Nam Muc and Nam Na River. There are streams in the research area: Nam He, Nam Chim, Nam Cay, Nam Luong, Nam Khan, Huoi Tong (*Tuyet, 1999*).

1.5.6. Soil and rock in the study area

Soils and rocks in this research area are distributed in different locations within MuongLay area. Some remarkable features of geology are described by the Geology Department of Vietnam (2007) and (*Tuyet, 1999*) as below:

- Soils, which dominantly constitute of the pebbles, cobble, gravel, sand, silt, clay and organic materials, are mostly located near the central area. These soils have different origins, mainly from sediment processes of the river, sea, marsh or wind. They belong to the Quaternary.
- The rock groups are distributed in mountainous regions in the whole of the area.
- Three major groups of rock are presented: sedimentary rock, metamorphic rock and magmatic rock. The components of sedimentary rock group are limestone, silic-limestone, sandstone, quartzite...The dominant constitute of metamorphic rocks group are shale, silicate schist, gneiss, quartzite and mica schist. They have been subjected to high levels of weathering causing favorable conditions for landslide occurrences.
- The first group of rocks originated from the Jurassic, Triassic, Permian, Devonian and Silurian-Devonian period. They are strongly foliated and sheared, showing very high weathering at most location at the western part of this province. The second group of rocks belong Neo-Proterozoic period (NPnc). The last group of rocks is group of intrusive and extrusion magmatic rock including granite, granosyenite, syenitdiorite, gabro, gabronorite and dunite. In general, the two last groups of rock are folded, faulted and sheared into various slope degree (*Tuyet, 1999*).

1.5.7. Landslides in the study area

Landslides in this region still happen persistently. Blocks of landslides with thousands to millions of tones of soil are the material supply for mudslides. Landslides and mudslides happen continuously in Muong Lay. Especially in 1990, 1994, 1996 with long and heavy rain in Muong Lay, landslides live in streams of Nam He, Huoi Lo, Huoi Leng, Huoi Phan with giant size that blocks of ten thousand to millions m³ dumped creating natural-fender of brooks (*Tuyet, 1999*). Landslides and mudslides in Muong Lay wounded more than 300 peoples, departed 177 peoples, completely damaged thousands of houses, destroyed road-ways and bridges, 15 agency manufactories, ten of thousand hectares of the defendant garden fields, buried drifts, estimated about 200 million of US dollars in damages. (*Source: Statistical office of Lai Chau province*).

Table 1-2. The statistical of landslide hazard in Muong Lay, Dien Bien province
(Source: Committee of the communes, province of Dien Bien, 1996 and Institute of Geology, 2005)

Year	Location of landslide	Size	Damage	Risk
Muong Lay town				
1990	- Huoi Lo - Huoi Tung	Large; Length: 1000m Width: 200m; Depth: 1-2m		
1994	Huoi Lo stream	Length: 500m Width: 200m; Deep: 1-2m	-Stuck the traffic -Killed people by mudslide and flash flood	Can continue to happen
1999	Huoi Luan stream	Long: 500m; Wide: 20-50m Depth: 1-3m	-Created mudslide and flash flood -Damaged hydro-electricity	Continue to happen in next year
2005	Muong Lay	180x75x20m	-Broke and stuck the traffic -Broke the concrete bund	Continue to happen often
Cha To commune				
1995	Pa Oi	Length: 300m Area: 2ha		Continue
Huoi Leng commune				
1992	Ban Huoi Tong	Length: 100m Depth: 0.4		Continue
1995	Ban Then Pe	Length: 200m Width: 40		Can continue to happen
1994-2003	Huoi Leng	Extremely large	Created flash flood and mudslide, 1994, 1996	
2005	Ma Thin Ho	25x20x10m	-Broke and stuck the traffic	often
Cha Nua commune				
1994	-De tinh 1	Length: 500m; Width: 100m Depth: 100m		Can continue to happen
1994	-Doi san bay	Long: 300m; Wide: 90m Depth: 60m		Can continue to happen
Lay Nua commune				
1991	Huoi Hai stream	Long: 1000m Width: 1000m Depth: 2m	Barred stream	Continue
2002	Huoi Lo Huoi Phan	-There are six large of landslide; -There are six large of landslide, 200x50x15m	Barred stream	Continue
Muong Tung commune				
1991-1995	Huoi En, Ban Tin Toc	Length: 1000m Width: 20-30m	-Broke 500m ² of fish pond and 2000m ² of rice-field	Continue
1995	500m distance to Tin Toc 500m in stream distance to Nam He	Length: 40m Width: 200m	-Broke 1ha of afforest -Broke 1ha of rice-field	Can continue to happen
Xa Tong commune				
2005	Xa tong_1 Xa tong_2 Xa tong_3	20x15x4m 22x14x3m 25x15x5m	-Made dam -Made dam, flash flood -Made dam, flash flood	Can continue to happen

The table 1-2 is the statistical of landslide hazard in Muong Lay, Dien Bien province. (Source: Committee of communes and provinces of Dien Bien, 1996). Moreover, landslide still happen in annually closing all the roads of Muong Lay go long to road of number 12, from MaThinHo to Muong Lay town, from Huoi Leng, Muong Tung, Lay Nua to Lai Chau townlet. Landsliding destroyed houses, broke bridges, drains, and destroyed road-ways. The figure 1-6 shows the data collection for researching the Landslide map of the North-West of Vietnam, with a map scale of 1:50'000 (Source: Tuyet, 1999), based on materials of field-work and gathered in the last time the landslide map had been established by Do Tuyet.

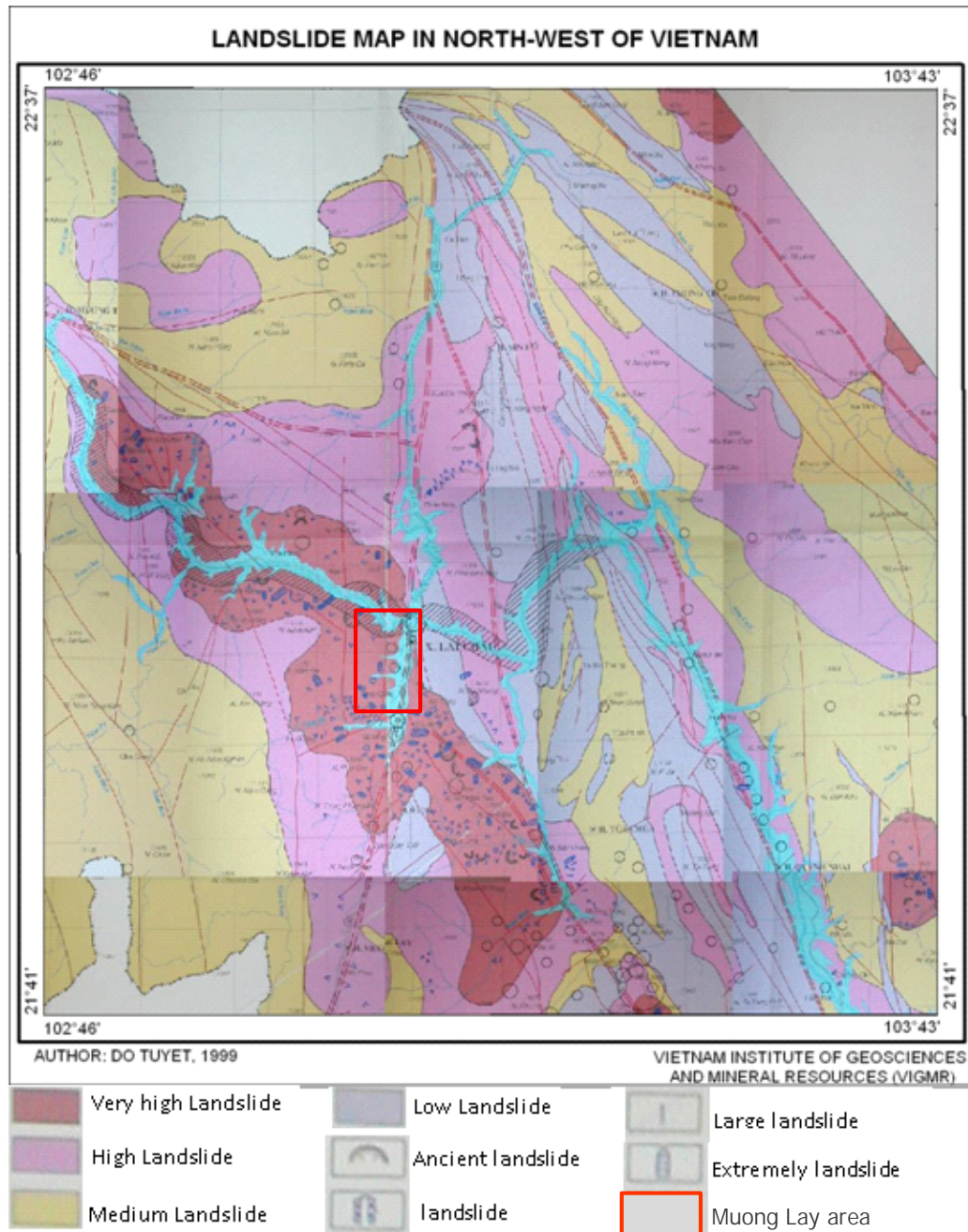


Figure 1-6. The Landslide map of North-West of Vietnam (Source: Tuyet, 1999)

CHAPTER 2.

DEFINITION OF LANDSLIDE AND LANDSLIDE HAZARD MAPPING

This chapter is mainly written according to *Varnes (1978); Van Westen (1993, 1997, 1998, 2004); Cruden (1996); Davis (1986); Long (2008); Hung (2002); and Thien (2004).*

2.1. DEFINITION OF LANDSLIDE HAZARD

2.1.1. Concepts about landslide

Land sliding is one of the many natural processes that shape the surface of the earth. Only when landslides threaten mankind do they represent a hazard. Landslides belong to a much broader group of slope processes referred to as mass movement. The definition of mass movement includes all those processes that involve the outward or downward movement of slope-forming materials under the influence of gravity. Some mass movement processes, such as soil creep, are almost imperceptibly slow and diffuse while other, such as landslides, are capable of moving at high velocity, discrete, and have clearly identifiable boundaries, often in the form of shear surfaces (*Crozier, 1989*). Landslides are a manifestation of slope instability. In particular, it identifies those aspects of landslides that make them hazardous and analyses the vulnerability of elements at risk in the face of landslide activity.

2.1.2. Landslide types

The term "landslide" describes a wide variety of processes that result in the downward and outward movement of slope-forming materials including rocks, soils, artificial fills, or a combination of these. The materials may move by falling, toppling, sliding, spreading, or flowing. Figure 2-1 shows a graphic illustration of a landslide, with the commonly accepted terminology describing its features (*Varnes, 1978*).

The various types of landslides can be differentiated by the kinds of materials involved and the mode of movement. A classification system based on these parameters is shown in Table 2-1. Other classification systems incorporate additional variables, such as the rate of movement and the water, air, or ice content of the landslide material.

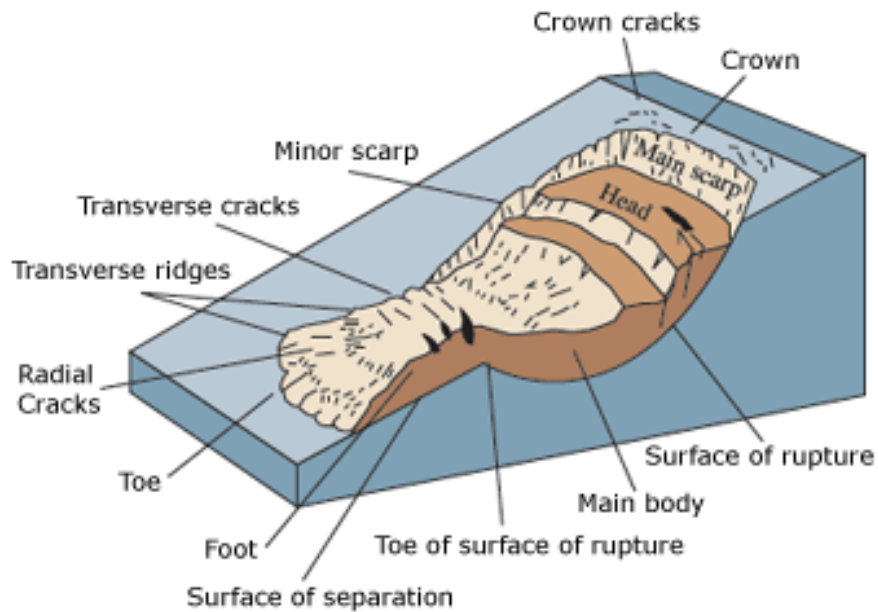


Figure 2-1. The parts of a landslide (Source: USGS, <http://landslides.usgs.gov>)

Table 2-1. Types of landslide, abbreviated version of Varnes' classification of slope movements (*Varnes, 1978*).

Type of movement		Type of material		
		Bedrock	Soil	
			Coarse	Fine
Falls		Rock fall	Debris fall	Earth fall
Topples		Rock topple	Debris topple	Earth topple
Slides	Rotational	Rock slump	Debris slump	Earth slump
	Translational	Rock block slide; rock side	Debris block slide; Debris side	Earth block slide; Earth side
Lateral spreads		Rock spread	Debris spread	Earth spread
Flows		Rock flow (deep creep)	Debris flow (soil creep)	Earth flow (soil creep)
Complex slope movements (e.g., combination of two or more types)				

Although landslides are primarily associated with mountainous regions, they can also occur in areas of generally low relief. In low-relief areas, landslides occur as cut-and-fill failures (roadway and building excavations), river bluff failures, lateral spreading landslides, collapse of mine-waste piles (especially coal), and a wide variety of slope failures associated with quarries and open-pit mines. The most common types of landslides are described as follows and are illustrated in figure 2-1 and figure 2-2.

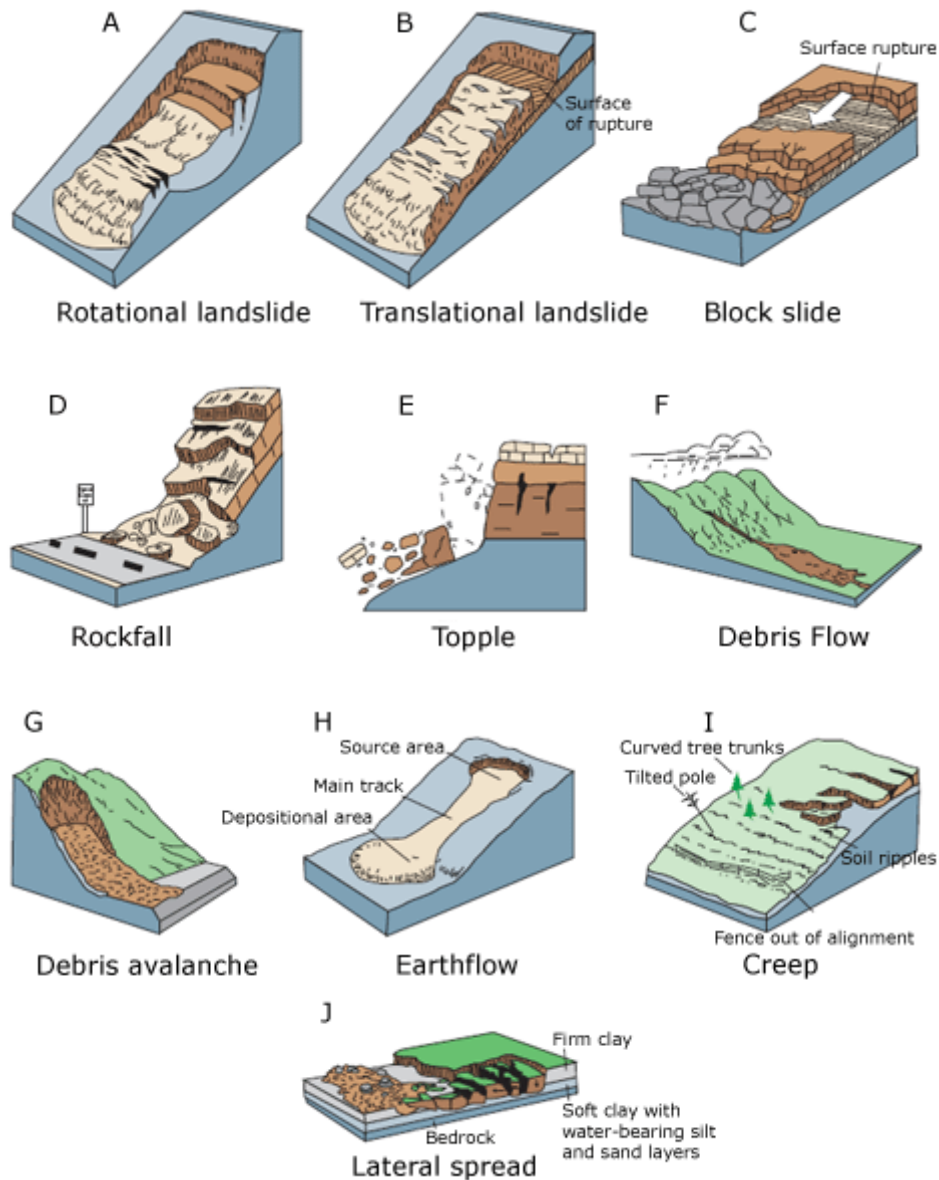


Figure 2-2. These schematics illustrate the major types of landslide movements described within this article. (Source: USGS, <http://landslides.usgs.gov>)

Slides: Although many types of mass movements are included in the general term "landslide", the more restrictive use of the term refers only to mass movements, where there is a distinct zone of weakness that separates the slide material from more stable underlying material. The two major types of slides are rotational slides and translational slides. Rotational slide: This is a slide in which the surface of rupture is curved concavely upward and the slide movement is roughly rotational about an axis that is parallel to the ground surface and transverse across the slide (fig. 2-2A). Translational slide: In this type of slide, the landslide mass moves along a roughly planar surface with little rotation or backward tilting (fig. 2-2B). A block slide is a translational slide in which the moving mass consists of a single unit or a few

Falls: Falls are abrupt movements of masses of geologic materials, such as rocks and boulders that become detached from steep slopes or cliffs (fig. 2-2D). Separation occurs along discontinuities such as fractures, joints, and bedding planes and movement occurs by free-fall, bouncing, and rolling. Falls are strongly influenced by gravity, mechanical weathering, and the presence of interstitial water.

Topples: Toppling failures are distinguished by the forward rotation of a unit, or units about some pivotal point below, or low in the unit under the actions of gravity and forces exerted by adjacent units, or by fluids in cracks (fig. 2-2E).

Flows: There are five basic categories of flows that differ from one another in fundamental ways.

a. Debris flow: A debris flow is a form of rapid mass movement in which a combination of loose soil, rock, organic matter, air, and water mobilizes as slurry that flows down slope (fig. 2-2F). Debris flows include <50% fines. Debris flows are commonly caused by intense surface-water flow, due to heavy precipitation or rapid snowmelt that erodes and mobilizes loose soil or rock on steep slopes. Debris flows also commonly mobilize from other types of landslides that occur on steep slopes, are nearly saturated, and consist of a large proportion of silt- and sand-sized material. Debris-flow source areas are often associated with steep gullies, and debris-flow deposits are usually indicated by the presence of debris fans at the mouths of gullies. Fires that denude slopes of vegetation intensify the susceptibility of slopes to debris flows.

b. Debris avalanche: This is a variety of very rapid to extremely rapid debris flow (fig. 2-2G).

c. Earth flow: Earth flows have a characteristic "hourglass" shape (fig. 2-2H). The slope material liquefies and runs out, forming a bowl or depression at the head. The flow itself is elongate and usually occurs in fine-grained materials or clay-bearing rocks on moderate slopes and under saturated conditions. However, dry flows of granular material are also possible.

d. Mudflow: A mudflow is an earth flow consisting of material that is wet enough to flow rapidly and that contains at least 50 percent sand, silt, and clay sized particles. In some instances, for example in many newspaper reports, mudflows and debris flows are commonly referred to as "mudslides."

e. Creep: Creep is the imperceptibly slow, steady, downward movement of slope-forming soil or rock. Movement is caused by shear stress sufficient to produce permanent deformation, but too small to produce shear failure. There are generally three types of creep: (1) seasonal, where movement is within the depth of soil affected by seasonal changes in soil moisture and soil temperature; (2) continuous, where shear

are reaching the point of failure as other types of mass movements. Creep is indicated by curved tree trunks, bent fences or retaining walls, tilted poles or fences, and small soil ripples or ridges (fig. 2-2I).

Lateral spreads: Lateral spreads are distinctive because they usually occur on very gentle slopes or flat terrain (fig. 2-2J). The dominant mode of movement is lateral extension accompanied by shear or tensile fractures. The failure is caused by liquefaction, the process whereby saturated, loose, incoherent sediments (usually sands and silts) are transformed from a solid into a liquefied state. Failure is usually triggered by rapid ground motion, such as that experienced during an earthquake, but can also be artificially induced. When coherent material, either bedrock or soil, rests on materials that liquefy, the upper units may undergo fracturing and extension, and may subside, translate, rotate, disintegrate, or liquefy and flow. Lateral spreading in fine-grained materials on shallow slopes is usually progressive. The failure starts suddenly in a small area and spreads rapidly. Often the initial failure is a slump, but in some materials movement occurs for no apparent reason. Combination of two or more of the above types is known as a complex landslide.

2.1.3. PROCESSES OF LANDSLIDES

“The processes involved in slope movements comprise a continuous series of events from cause to effect” (Varnes, 1978). The section follows Varnes’s distinction that the three broad types of landslide processes are those that

- Increase shear stresses
- Contribute to low strength and
- Reduce material strength

2.1.3.1. Increase shear stresses

Shear stresses can be Increase by processes that lead to removal of lateral support, by the imposition of surcharges, by transitory stresses resulting from explosions or earthquakes, and by uplift or tilting of the land surface.

a. Removal of support:

The toe of a slope can be removed by erosion, steepening the slope. Typical agents are streams and material at depth within the displacing mass results in its extrusion or, if the base of the spread has liquefied, in its outward flow.

b. Imposition of surcharges:

The addition of material can result in increases of both the length and the height of slope. Water can be added by precipitation, both rain and snow; by the flow of surface and groundwater into the displacing mass; and even by the growth of glaciers. Surcharges can

be added by the movement of landslides onto the slope, by volcanic activity, and by the growth of vegetation. Anthropogenic surcharges include construction of fills, stockpiles, and waste dumps; structural weight; and water from leaking canals, irrigation system, reservoirs, sewers, and septic tanks.

c. Transitory stresses

The local stress field within a slope can be greatly changed by transitory stresses from earthquakes and explosions (both anthropogenic and volcanic). Smaller transitory changes in the stress field can result from storms and from human activity such as driving and the passage of heavy vehicles.

d. Uplift or tilting

Uplift or tilting may be caused by tectonic forces or by volcanic processes. In either case, this type of increased shear stress may be associated with earthquakes, which themselves can trigger landslides. The melting of the extensive Pleistocene ice sheets has caused widespread uplift in temperate and circumpolar regions.

Uplift of an area of the earth's surface generally causes steepening of slopes in the area as drainage responds by increased incision. The cutting of valleys in the uplifted area may cause valley rebound and accompanying fracturing and loosening of valley walls with inward shear along flat-lying discontinuities. The fractures and shears may allow the buildup of pore-water pressures in the loosened mass and eventually lead to landsliding.

2.1.3.2. Contribute to low strength

Low strength of the earth or rock material that make up a landslide may reflect inherent material characteristics or may result from the presence of discontinuities within the soil or rock mass

a. Material characteristics

Material may be naturally weak or may become weak as a result of common natural processes such as saturation with water. Organic material and clays have low natural strengths. Rocks that have decomposed to clays by chemical weathering (weathered volcanic tuffs, schists, and serpentines, for example) develop similar properties.

Besides the material of the individual particles of which the material is composed, the arrangement of these particles (the fabric of the material) may cause low material strengths. Sensitive of material, which lose strength when disturbed, generally have loose fabrics or textures.

b. Mass characteristics

The soil or rock mass may be weakened by discontinuities such as faults, bedding surfaces, foliations, cleavages, joints, fissures, shears, and shear zones. Contrasts in

bedded sedimentary sequences - such as stiff, thick beds over-lying weak, plastic, thin beds or permeable sands (or sandstones) alternating with weak, impermeable clays (or shales) – are sources of weakness.

2.1.3.3. Reduce material strength

Clays are particularly prone to weathering processes and other physico-chemical reactions. Hydration of clay minerals result in loss of cohesion, a process often associated with softening of fissured clays. Fissuring of clays may be due to drying or to release of vertical and lateral restraints by erosion or excavation. The exchanges of ions within clay minerals with those in the pore water of the clays may lead to substantial changes in physical properties of some clay. Electrical potentials set up by these chemical reactions or by other processes may attract water to the weathering front.

The effects of extremes of temperature caused by severe weather are not confined to clays. Rocks may disintegrate under cycles of freezing and thawing or thermal expansion and contraction. Dry weather may cause desiccation cracking of weak or weather rock along preexisting discontinuities, such as bedding planes. Wet weather may dissolve natural rock cements that hold particles together. Saturation with water reduces effective intergranular pressure and friction and destroys capillary tension.

2.1.4. LANDSLIDE CAUSES

2.1.4.1. Geological causes

Geological causes are such as: Weak materials ; Sensitive materials ; Weathered materials ; Sheared materials ; Jointed or fissured materials ; Adversely oriented discontinuity (bedding, schistosity, fault, unconformity, contact, and so forth) ; Adversely oriented structural discontinuity (fault, unconformity, contact, etc.) ; Contrast in permeability; Contrast in stiffness (stiff, dense materials over plastic materials); Thickness of weathering crust; aspect of bed-rock; etc.

It is clear that there exists an association between slope instability and different types of regolith materials (*Sidle, Ochiai, 2006*). However, this association may be strong or weak largely depending upon the type of regolith material. Examples of a strong association between landslides and different types of regolith materials were given by many researchers (*Thomson, 1971; Yokota, Iwamatsu, 1999*). Weathering alters the mechanical, mineralogical and hydrologic attributes of the regolith, and, hence, is an important factor of slope instability in many settings (*Maharaj, 1995; Yokota, Iwamatsu, 1999*).

Another important geological factor in landslide hazard investigation is unstable bedding sequences. This can occur when mass movement on bedding planes is triggered when either pore water pressures develop at the interface between two different alternating

regoliths (e.g., sandstone and clay stone), or the strength of the clay deposit is weakened by water infiltrating through the overlying regolith layer. Hence, landslides often occur when there is heavy rainfall for a long period. Four unstable bedding sequences are commonly identified (*Sidle, Ochiai, 2006*): (1) alternating bedding of hard and soft rocks, (2) highly altered and permeable regolith overlaying relatively low permeability substrate, (3) thin soils overlaying bedrock or till, and (4) hard cap rock (with fissures and fractures) overlaying deeply weathered rocks.

The relative strength of the regolith is strongly influenced by past tectonic setting as well as contemporary weathering (*Long, 2008*). Especially, geotectonic contribute to slope instability by fracturing, faulting, jointing and deforming foliation structures (*Long, Khanh, 2008*). Hence, faults, lineaments, or both are usually taken into account in landslide hazard assessments.

2.1.4.2. Morphological causes

Morphological causes are such as: Tectonic or volcanic uplift ; Glacial rebound ; Fluvial erosion of slope toe ; Wave erosion of slope toe ; Glacial erosion of slope toe ; Erosion of lateral margins ; Subterranean erosion (solution, piping) ; Deposition loading slope or its crest ; Vegetation removal (by forest fire, drought).

Slope gradient

Slope gradient is important with regard to landslide initiation. In most studies of landslides, the slope gradient is taken into account as a principal causative or trigger factor (*Long, 2008*). Slope gradients are sometimes considered as an index of slope stability, and because of the availability of a digital elevation model (DEM) can be numerically evaluated and depicted spatially (*O'Neill, Mark, 1987; Gao, 1993*). Not only is slope gradient important to landslides, but other dynamic environmental factors also exerting major influences. For example, rapid landslides and debris flows can occur even in particular regions of low slope gradient. This shows that geomorphic, hydrologic, geologic, petrologic, and possibly other factors are important determinants of slope stability as well.

Slope shape

Slope shape has a strong influence on slope stability in steep terrain by concentrating or dispersing surface and primarily subsurface water in the landscape. There are three basic hydro geomorphic slope units: divergent, planar or straight, and convergent. In general, the divergent or convex landform is the most stable in steep terrain, followed by planar hill slope segment and convergent or concave hill slope (least stable). The main reason is related to the landform structure affecting largely the concentration or dispersion of surface and subsurface water. Convergent hill slope tends to concentrate subsurface water into small areas of the slope, thereby generating rapid pore water pressure increase

during storms or periods of rainfall. If pore pressures develop in the hollow, the soil shear strength will reduce to a critical level and a landslide can occur. Hence, hollows are susceptibility sites for initiation of debris slides and debris flows (*Hack, Goodlett, 1960; Dietrich, Dunne, 1978; Benda, Cundy, 1990*).

Aspect and attitude

Slope aspect strongly affects hydrologic processes via evapotranspiration and thus affects weathering processes and vegetation and root development, especially in drier environments (*Sidle, Ochiai, 2006*). Such aspect characteristics which increase the landslide failure, that have been decided in previous studies (*Churchill, 1982; Gao, 1993; Hylland, Lowe, 1997*). The strong statistical relationships between elevation and landslide occurrence have been cited in many studies (*Pachauri, Pant, 1992; Dai, Lee, 2002; Lineback, et al., 2001*). In general, altitude or elevation are usually associated with landslides by virtue of other factors such as slope gradient, lithology, weathering, precipitation, ground motion, soil thickness and land use. For example, higher mountainous areas often experience larger volumes of precipitation, both rain and snow falls.

2.1.4.3. Physical causes

Physical causes are such as: Intense rainfall; prolonged exceptional precipitation; Rapid drawdown (of floods and tides); Earthquake; Volcanic eruption; Thawing; Shrink-and-swell weathering.

One of the major factors in the triggering of landslides is seismicity. For the main part seismically generated landslides usually do not differ in their morphology and internal processes from those generated under no seismic conditions. However, they tend to be more widespread and sudden. The most abundant types of earthquake-induced landslides are rock falls and slides of rock fragments that form on steep slopes. However, almost every other type of landslide is possible, including highly disaggregated and fast-moving falls, more coherent and slower-moving slumps block slides, earth slides, and lateral spreads and flows that involve partly to completely liquefied material (*Keefer, 2002*). Rock falls, disrupted rock slides, and disrupted slides of earth and debris are the most abundant types of earthquake-induced landslides, whereas earth flows, debris flows, and avalanches of rock, earth, or debris typically transport material the farthest. There is one type of landslide that is essential uniquely limited to earthquakes, i.e. liquefaction failure which can cause fissuring or subsidence of the ground. Liquefaction involves the temporary loss of strength of sands and silts which behave as viscous fluids rather than as soils. This can have devastating effects during large earthquakes.

Some of the largest and most destructive landslides known have been associated with volcanoes. These can occur either in association with the eruption of the volcano itself, or as a result of mobilization of the very weak deposits formed as a consequence of volcanic activity. Essentially, there are two main types of volcanic landslide: lahars and debris avalanches, the largest of which are sometimes termed flank collapses.

2.1.4.4. Human causes

Human causes are such as: Excavation of slope or its toe; Loading of slope or its crest; Drawdown (of reservoirs); Deforestation; Irrigation; Mining; Artificial vibration; Water leakage from utilities; Construction of highways and railroads.

Landslides may result directly or indirectly from the activities of people. But any attempt to address all activities by people that induce landslide occurrences will be incomplete. Therefore, only some examples will be given:

- Undercutting during construction of highways and railroads increases the average slope gradients, and increases the chance of slope failure.
- Overloading of hill slopes by housing construction is common. This extra weight may increase the chance of slope failure; altering the hydrology may have dramatic effects on hill slope stability.
- Clear cutting of trees promotes soil erosion and weakens the support of soils by tree roots. It also reduces evapotranspiration and raises the water tables.
- Vibrations occurring in consequence of natural (earthquake) or artificial (machine activities, underground explosions) causes.

2.1.4.5. Three most common causes of the damaging landslides

Although there are multiple types of causes of landslides, the three that cause most of the damaging landslides around the world are these:

Landslides and Water

Slope saturation by water is a primary cause of landslides. This effect can occur in the form of intense rainfalls, snowmelts, changes in ground-water levels, and water-level changes along coastlines, earth dams, and the banks of lakes, reservoirs, canals, and rivers.

Land sliding and flooding are closely allied because both are related to precipitation, runoff, and the saturation of ground by water. In addition, debris flows and mudflows usually occur in small, steep stream channels and often are mistaken for floods; in fact, these two events often occur simultaneously in the same area.

Landslides can cause flooding by forming landslide dams that block valleys and stream channels, allowing large amounts of water to back up. This causes backwater flooding and, if the dam fails, subsequent downstream flooding. Also, solid landslide debris can "bulk" or add volume and density to otherwise normal stream flow or cause channel blockages and diversions creating flood conditions or localized erosion. Landslides can also cause overtopping of reservoirs and/or reduce capacity of reservoirs to store water.

Landslides and Seismic Activity

Many mountainous areas that are vulnerable to landslides have also experienced at least moderate rates of earthquake occurrence in recorded times. The occurrence of earthquakes in steep landslide-prone areas greatly increases the likelihood of landslides will occur, due to ground shaking alone or shaking-caused dilation of soil materials, which allows rapid infiltration of water. The 1964 Great Alaska Earthquake caused widespread land sliding and other ground failure, which caused most of the monetary loss due to the earthquake. Other areas of the United States, such as California and the Puget Sound region in Washington, have experienced slides, lateral spreading, and other types of ground failure due to moderate to large earthquakes. Widespread rock falls also are caused by the loosening of rocks as a result of ground shaking. Worldwide, landslides caused by earthquakes kill people and damage structures at higher rates than in the United States.

Landslides and Volcanic Activity

Landslides due to volcanic activity are some of the most devastating types. Volcanic lava may melt snow at a rapid rate, causing a deluge of rock, soil, ash, and water that accelerates rapidly on the steep slopes of volcanoes, devastating anything in its path. These volcanic debris flows reach great distances, once leaving the flanks of the volcano. They can damage structures in flat areas surrounding the volcanoes. The 1980 eruption of Mount St. Helens, in Washington triggered a massive landslide on the north flank of the volcano, the largest landslide in recorded times.

Landslide and Mitigation

Vulnerability to landslide hazards is a function of location, type of human activity, usage, and frequency of landslide events. The effects of landslides on people and structures can be lessened by total avoidance of landslide hazard areas or by restricting, prohibiting, or imposing conditions on hazard-zone activity. Local governments can reduce landslide effects through land-use policies and regulations. Individuals can reduce their exposure to hazards by educating themselves on the past hazard history of a site and by making inquiries to planning and engineering departments of local governments. They can also obtain the professional services from an engineering geologist, a geotechnical engineer,

or a civil engineer, who can properly evaluate the hazard potential of a site, built or unbuilt.

2.1.5. How to Reduce the Effects of Landslides

The hazard from landslides can be reduced by avoiding construction on steep slopes and existing landslides, or by stabilizing the slopes. Stability increases when ground water is prevented from rising in the landslide mass by (1) covering the landslide with an impermeable membrane, (2) directing surface water away from the landslide, (3) draining ground water away from the landslide, and (4) minimizing surface irrigation. Slope stability is also increased when a retaining structure and/or the weight of a soil/rock beam are placed at the toe of the landslide or when mass is removed from the top of the slope.

2.1.6. Hazard, risk and vulnerability

Hung (2002) and Thien (2004) have written:

In order to provide a systematic approach to study landslides, Varnes, 1984 defined various types of hazards, risks & vulnerability.

- **Natural hazard**, the probability of occurrence of a potentially damaging phenomenon within a specific period of time and within a given area.
- **Vulnerability**, the degree of loss to a given element or set of elements resulting from the occurrence of a natural phenomenon of a given magnitude.
- **Element at Risk**, the population, properties, economic activities etc. at risk in a given area.
- **Risk**, the expected degree of loss due to a particular natural phenomenon. Hence it is a product of hazard and vulnerability.

2.1.7. Landslide Hazard Maps

Four principal types of information describing the various classes of landslides are portrayed by different landslide maps prepared by Varnes (1978) and Cruden (1996): (a) inventories of existing landslides, (b) landslide hazard expressed as landslide susceptibility or landslide potential maps, (c) landslide risk maps, and (d) landslide zone maps. The maps can be either qualitative or quantitative in their preparation.

- a. **Landslide-inventory maps**, the most basic landslide maps, portray the location of prior failure. Because one clue to the location of future land sliding is the distribution of past movement, maps that show existing landslides are helpful in predicting the hazard. Inventory maps do not necessarily distinguish fresh movements, but in any one year some of the mapped slides-or more frequently, portions of them-may become active. A landslide inventory reveals the extent of past movement and thus

the probable locus of some future activity within those landslides, but it does not indicate the likelihood of failure for the much larger area between mapped landslides. For this, hazard, risk or zone maps are required.

- b. **Landslide-hazard maps** describe an unstable condition arising from the presence or likely future occurrence of slope failure. There are two general types of landslide-hazard maps, each of which provides a different level of information and detail:
 - Landslide-susceptibility maps describe the relative likelihood of future land sliding based solely on the intrinsic properties of a locale or site. Prior failure (from a landslide inventory), rock or soil strength, and steepness of slope are the three site factors that most determine susceptibility.
 - Landslide-potential maps describe the likelihood of land sliding (susceptibility) jointly with the occurrence of a triggering event (opportunity). Potential commonly is based on the three factors determining susceptibility plus an estimate or measure of the probability (likelihood of occurrence) of a triggering event such as earthquake or excessive rainfall.
- c. **Landslide-risk maps** describe landslide potential jointly with the expected losses to life and property if a failure was to occur. The potential for landslide damage to a road system, for example, can be evaluated by considering the exposure of the roads to different levels of landslide hazard and the vulnerability of the roads to consequent damage. Similarly, the risk of excessive sedimentation in streams and other ecological damage can be evaluated by considering the landslide hazard jointly with the properties of streams and their sensitivity.
- d. **Landslide-zone maps** depict areas with a higher probability of land sliding, within which specific actions are mandated by California law prior to any development. These maps typically are binary in nature (a given site is either in or out of the zone) and are designed for use as planning tools by non-geoscientists. Zone maps may be derived from landslide potential or susceptibility, but some have been based simply on slope gradient or landslide-inventory maps.

Landslide hazard, risk and zone maps are prepared in many ways, increasingly involving complex manipulations of multiple criteria by computer. Because the value of landslide maps can be judged only by whether they correctly predict the locations of future failures, effectiveness of the different approaches to constructing them is difficult to evaluate.

2.2. LANDSLIDE HAZARD ZONATION MODELS

2.2.1. Definition

Although by definition the term *landslide* is used for mass movements occurring along a

well defined sliding surface, it has been used in literature as the most general term for all kinds of mass movements, including some with little or no true sliding, such as rock-falls, topples, and debris flows (Varnes, 1984). In this context, *mass movement* is used subsequently as a synonymous term for landslide, similar to *slope movement*.

Zonation refers to the division of the land surface into areas and the ranking of these areas according to degrees of actual or potential hazard. Hence landslide hazard zonation shows potential hazard of landslides or other mass movements on a map, displaying the spatial distribution of hazard classes. In general three basic principles or fundamental assumptions guide all zonation studies (Varnes, 1984):

- **The past and the present are keys to the future:** Natural slope failures in the future will most likely occur where geologic, geomorphic and hydraulic situations have led to past and present failures. Thus, we have the possibility to estimate the features of potential future failure. The absence of past and present failures doesn't mean that failures will not occur in the future.
- **The main conditions that cause landslides can be identified:** The basic causes of slope failure can be recognized, are fairly well known from several case studies and the effects of them can be rated or weighed. It's possible to map and correlate the contributing factors to each other.
- **Degrees of hazard can be estimated:** If the conditions and processes that promote instability can be identified, it is often possible to estimate their relative contribution and give them some qualitative or semi-quantitative measure. Thus, a summary of the degree of potential hazard in an area can be built up, which depends on the number of failure inducing factors present, their severity, and their interaction.

2.2.2. Some popular deterministic models for landslide hazard zonation

The infinite slope model is a static stability model in which local stability conditions are determined by the means of the local equilibrium along a potential slip surface. Other models couple the infinite slope stability model with more or less complex rainfall infiltration models (Montgomery, Dietrich, 1994; Dietrich, et al., 1995; Terlien, et al., 1995).

Shallow landsliding stability model (SHALSTAB): a model that combines a hydrologic model (O'Loughlin, 1986) with an infinite slope stability equation, the Mohr-Coulomb failure law (Bolt, et al., 1975), for the prediction of slope instabilities based upon the minimum amount of steady-state rainfall required to trigger land sliding. Its required inputs are obtained from a DEM that is widely available within the U.S. and a few representative values of geotechnical parameters, such as soil bulk density, internal angle of friction and water table depth. This model calculates pore pressures for steady-state saturated water flow parallel to the slope plane.

Stability index mapping (SINMAP) model is based upon similar SHALSTAB's principles (Pack, *et al.*, 1998). The main difference between these two models is that SHALSTAB assumes zero soil cohesion because of the spatial and temporal heterogeneity of soil cohesion (and therefore the difficulty in obtaining values) and because assuming a zero cohesion value results in the most conservative estimate of slope instability (Dietrich, *et al.*, 2001). However, new versions of the model do allow for the inclusion of soil cohesion.

Transient response model developed by Iverson (2000) uses unsaturated flow to calculate pore pressures and vertical flow. The International Institute for Aerospace Survey and Earth Sciences (ITC) has developed a GIS called the Integrated Land and Water Information System (ILWIS) that has modules incorporated in the GIS for deterministic instability zonation (Van Westen, 1997). The Level I Stability Analysis (LISA) prepared for the U.S. Forest Service by Hammond *et al.* (1992) uses average estimates for geotechnical parameters in their model.

Models based on distribution of seismically induced landslides are specific, physically based models developed for predicting the effects of seismic shaking on the stability of slopes over large areas, or to explain the known distribution of seismically induced landslides (Miles, Ho, 1999; Luzi, Pergalani, 2000; Jibson, *et al.*, 1998). Some of the most reliable approaches extend the Newmark method designed for estimating the stability of dams or embankments subject to seismic shaking to the stability of individual slopes (Newmark, 1965; Wilson, 1993).

Physically based models to simulate rock fall processes developed by Van Westen, Alzate (1990) and by Guzzetti *et al.* (2002), are based on a DEM and spatially distributed information on the location of the source areas of rock falls, and of the energy lost at impact points and where boulders are rolling, to simulate in three dimensions rock fall phenomena for areas ranging from a few thousands of square meters to several hundreds of square kilometers (Guzzetti, *et al.*, 2002). Results of the model include: (i) the extent and location of the areas potentially subject to rock falls, and (ii) estimates of the maximum velocity and of the maximum distance to the ground of the falling rocks. This information can be combined to obtain quantitative estimates of landslide hazards (Crosta, *et al.*, 2004; Guzzetti, *et al.*, 2004).

Statistical models to determine spatial landslide instability are used to describe the functional relationships between instability factors and the past and present distribution of slope failures (Carrara, 1983). The approach is indirect and provides quantitative results suitable to the quantitative assessment of landslide hazard. Statistical analyses are popular because they provide a more quantitative analysis of slope instability and have the ability to examine the various effects of each factor on an individual basis. Statistical analyses of slope instability can include *bivariate and multivariate methods*.

More advanced methods employ a variety of classifications techniques such as fuzzy systems (Davis, Keller, 1997; Chung, Fabbri, 2001; Juang, et al., 1992; Chi, et al., 2002), neural networks (Gomez, Kavzoglu, 2005; Long, 2008; Lee, et al., 2004), and expert systems (Pistocchi, et al., 2002).

2.2.3. Scale of mapping for landslide hazard zonation

There are several techniques for landslide hazard zonation making use of GIS that can be applied. Therefore the appropriate scales on which the data is collected and the final result presented vary considerably. More detailed hazard maps require more detailed input data. Thus the objectives of the analysis and the required accuracy of the input data determine the scale.

The following scales of analysis have been differentiated for landslide hazard zonation according to the definition by the International Association of Engineering Geologists 1976: National scale ($< 1:1'000'000$); Regional scale ($1:100'000 - 1:1'000'000$); Medium scale ($1:25'000 - 1:100'000$); and Large scale ($1:2'000 - 1:25'000$). The detail at **national scale** is very low, covering an entire country. The aim is to generate awareness among national policy makers and the public and to indicate problematic areas. The maps at **regional scale** are intended for agencies in charge of agricultural, urban or infrastructure planning and may indicate areas where severe land sliding problems can threaten different facilities. Detail is still low, covering large areas of 1000 km² or more, like a large catchment area or a political entity of the country.

Areas covered at **medium scale** have an extent of several 10km² to several 100km², including a municipality or smaller catchment area. As main characteristics in terms of detail morphometric features, such as slope angle or curvature, are distinguished within bigger units, be it a geologic, land use or terrain unit. Additionally a precise landslide distribution map is obtained from aerial photo interpretation. A field campaign emphasizes quantitative description and additional information about the mass movements themselves and sliding relevant factors. **Large scale** hazard analyses are used at site investigation level, covering several square kilometers, like a town or part of a city. The methodology is based on detailed geotechnical knowledge. Detailed fieldwork is indispensable and may be accomplished by laboratory analysis. Playing with different scenarios of triggering factors, like rain or horizontal seismic acceleration, critical mass movement areas can be identified in this way.

CHAPTER 3.

REMOTE SENSING AND GEOGRAPHIC INFORMATION SYSTEM IN LANDSLIDE HAZARD ASSESSMENT

Nowadays, GIS has been widely used in landslide hazard assessment (*Brabb, 1984; Carrara, 1991; Aleotti, Chowdhury, 1999; Dai, et al., 2001*). Hazard zonation is the basis for any further disaster management project. Many types of information needed for this kind of analysis have an important spatial component. The scarce availability of spatial data in developing countries makes remote sensing (aerial photo, satellite imagery) useful to acquire this information in an appropriate cost/time ratio. GIS has strong functions for spatially distributed data processing and analysis. Using GIS gives the possibility to integrate qualitative as well as quantitative data and to collect, store, transform, analyze and display the huge amount of geographically referenced information needed for evaluation. (*Long, 2008*).

3.1. REMOTE SENSING APPROACHES FOR LANDSLIDE HAZARD ASSESSMENT

3.1.1. General

Remote sensing (RS) is the science of acquiring, processing and interpreting images that records the interaction between electromagnetic energy and matter. RS is the instrumentation, techniques and methods to observe the Earth's surface at a distance and to interpret the images or numerical values obtained in order to acquire meaningful information of particular objects on Earth. Remote sensing is defined as "the science of obtaining information about an object area, or phenomenon through the analysis of data acquired by a device that is not in direct contact with the object, area or phenomenon under investigation, except perhaps with energy emitted from the sensor".

Shrestha (1991) stated RS as comparison the measurement and recording of electromagnetic energy reflected from or emitted by the Earth's surface and relating of such measurement to the nature and properties of surface materials. In a general sense, remote sensing includes all the activities from recording, processing, analyzing, interpretation and finally obtaining useful information from the data generated by the remote sensing system.

Abdel-Salam (1982) noticed that soils derived from the same parent rock deposited in the same way, occupying similar topographic positions and having properties that appeared in the aerial photographs in similar patterns. While predictions concerning soil texture, structure and genetic soil groups could not be identified only from photo images. In other words, photo interpretation should imply a combination of photo and field studies.

The program of Landsat is a joint effort of the U.S. Geological Survey (USGS) and the National Aeronautics and Space Administration (NASA) to gather the Earth resource data using a series of satellites. Landsat's mission is to establish and execute a data acquisition strategy that ensures the repetitive acquisition of observations over the Earth's land mass, coastal boundaries, and coral reefs and to ensure that the data acquired are of maximum utility in supporting the scientific objective of monitoring changes in the Earth's land surface.

Thematic Mapper (TM) bands 1, 5 and 7 collect reflected energy, band 6 collects emitted energy. The TM sensor has a spatial resolution of 120 m for the thermal-IR band and 30 m for the six reflective bands. The newest satellite, Landsat, carries the Enhanced Thematic Mapper plus (ETM+), with 30 m visible and IR bands, a 60 m spatial resolution thermal band, and a 15 m panchromatic band.

Table 3-1. The spectral bands for the Landsat TM satellite
(Modified from Irish, 2000 and Noonan, 1999).

Band	Spectral range (μm)	Ground resolution (m)	Electromagnetic region	Generalized application
1	0.45-0.52μm	30m	Visible Blue	Coastal water mapping, Differentiation of vegetation from soils
2	0.52-0.60μm	30m	Visible Green	Assessment of vegetation vigor
3	0.63-0.69μm	30m	Visible Red	Chlorophyll absorption for vegetation differentiation
4	0.76-0.90μm	30m	Near Infrared	Biomass surveys and Delineation of water bodies
5	1.55-1.75μm	30m	Middle Infrared	Vegetation and soil moisture measurements
6	10.4-12.5μm	60m	Thermal	
7	2.08-2.35μm	30m	Middle Infrared	Hydrothermal mapping

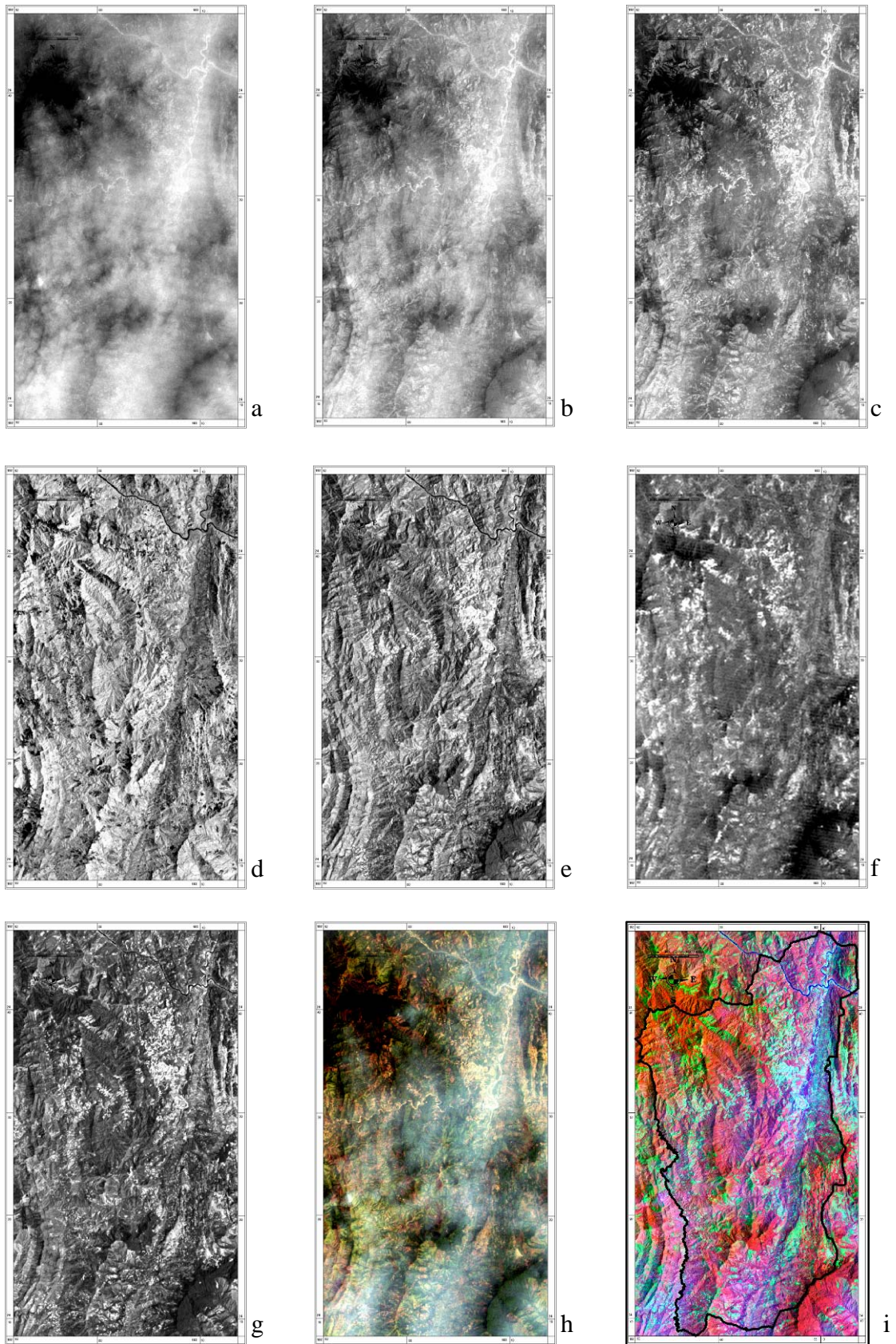


Figure 3-1. The satellite image of Muong Lay area (LandSat TM, dated 20th February 1999); a) band1; b) band2; c) band3; d) band4 e) band5; f) band6; g) band7; h) LandSat TM True-color Composite; i) LandSat TM False-color Infrared Composite (bands 4, 7, 1 as RGB)

In order to facilitate the integration technique of multi-sensor image data, pre-processing operations and image processing are required. The pre-processing step involves haze correction of the Landsat image and the georeferencing of all images to a real world coordinate system on a cartographic projection. The image processing step provides a methodology that is implemented to achieve the anticipated aims of this research.

Figure 3-7 shows the step involved in pre-processing and image processing. This methodology is created based on the principles of remote sensing technology.

3.1.2. Pre-processing

- The pre-processing is used to correct the radiometric and geometric distortion for scanned Landsat images.
- It uses Calibration Utilities functions available in ENVI 3.5 software.
- Database of remote sensing is used in this thesis are satellite imagery LandSat TM with acquisition date on February, 20th 1999 was used to interpret the information about land use and land cover and lineament extracted.

3.1.2.1. Radiometric correction

The effect of unequal detector sensitivities causes line-to-line striping in Landsat MSS and TM imagery. There is a striping of 6 lines periodicity in Landsat MSS and 16 lines periodicity in Landsat TM. Generally, the atmosphere induces radiometric distortions originating from scattering or absorption, which results in wavelength dependent multiplicative and additive noise. The scattering of electromagnetic radiation results in haze, which has an additive effect to the DN values. Since haze is wavelength dependent, its influence differs per band. It is highest in the blue band and lowest in the IR band.



Figure 3-2. Radiometric correction in Pre-processing

3.1.2.2. Geometric correction

Remote sensing imagery is inherently subject to geometric distortions. Geometric distortions are caused by earth curvature, atmospheric refraction, sensor motion and imaging distortion. The geometric registration process involves identifying the image coordinates (i.e. row, column) of several clearly discernible points called *ground control points* (or GCPs) and matching them to their true positions in ground coordinates (e.g. latitude, longitude). The true ground coordinates are typically measured from a map either in paper or digital format. This is *image-to-map registration*. (Figure 3-3).

In order to correct the original distorted image, a procedure called *resampling* is used to determine the digital values to place in the new pixel locations of the corrected output image.

The resampling process calculates the new pixel values from the original digital pixel values in the uncorrected image. Pixels are assigned in the output space on a choice within nearest neighbor, bilinear or cubic interpolation techniques. *Nearest neighbor resampling* uses the digital value from the pixel in the original image which is nearest to the new pixel location in the corrected image. This is the simplest method and does not alter the original values, but may result in some pixel values being duplicated while others are lost.

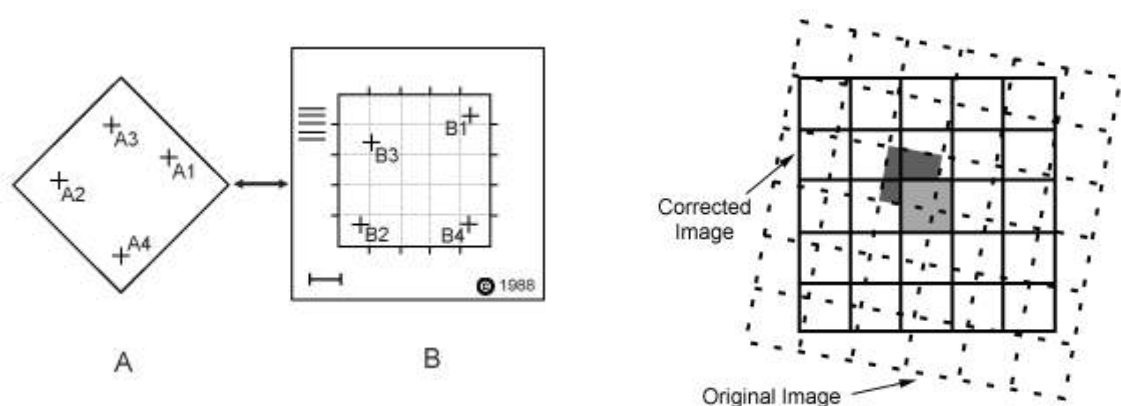


Figure 3-3. Geometric correction in Pre-processing

3.1.3. Image processing

3.1.3.1. Lineament extraction

Lineaments are any linear features that can be picked out as lines (appearing as such or evident because of contrasts in terrain or ground cover on either side) in aerial or space imagery. Lineaments are usually faults, joints, or boundaries between stratigraphic formations.

3.1.3.1.1. Edge enhancement

In general, linear features are formed by edges. More typically, edges are marked by subtle brightness differences that may be difficult to recognize. Digital filters have been developed specifically to enhance edges in images, they fall into two categories: directional filters and nondirectional filters. Laplacian filters are nondirectional filters because they enhance linear features having almost any orientation in an image. The exception applies to linear features oriented parallel with the direction of filter movement; these features are not enhanced. The exception applies to linear features oriented parallel with the direction of filter movement; these features are not enhanced. Directional filters are used to enhance specific linear trends in an image. (Figure 3-4).

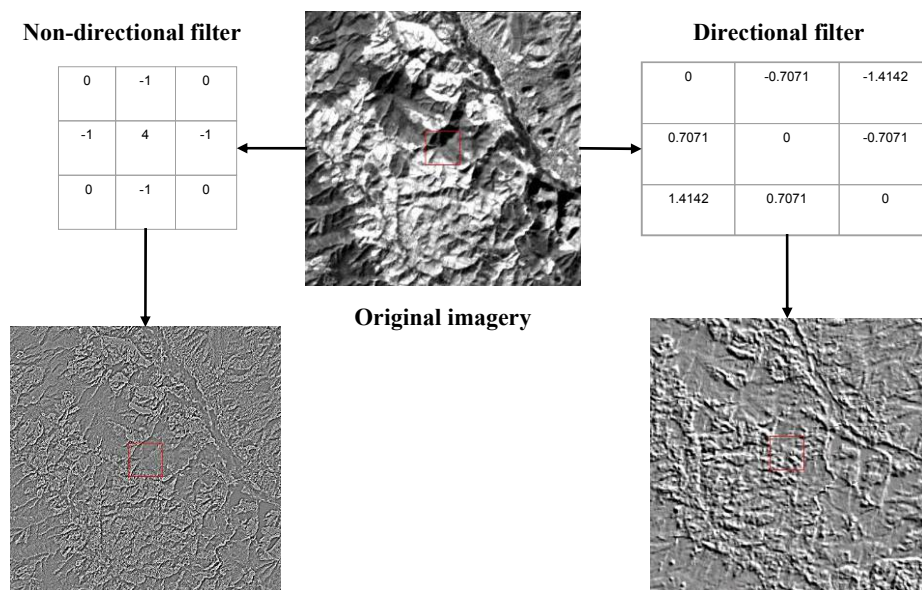


Figure 3-4. Edge enhancement in Image processing

3.1.3.1.2. Lineament extraction

There are two common ways of lineament extraction: *visual process* and *digital process* (table 3-3). Both of them have certain advantages and disadvantages (Hung, 2001).

Table 3-3. Some major characteristics of visual and digital lineament extraction.

Visual process	Digital process
Depends on the quality of the image	Depends on the quality of the image
Depends on the complexity of the research area	Totally depends on the complexity of
Strongly depends on human experience	Totally depends on the function of the software
Takes a lot of time	Very quickly
Strongly effected by human subjectiveness	Little effected by human subjectiveness
Easy to distinguish the kind of lineament (tectonic	Can not recognize the kind of lineament, so the result
Simple but subjective	Complex but objective

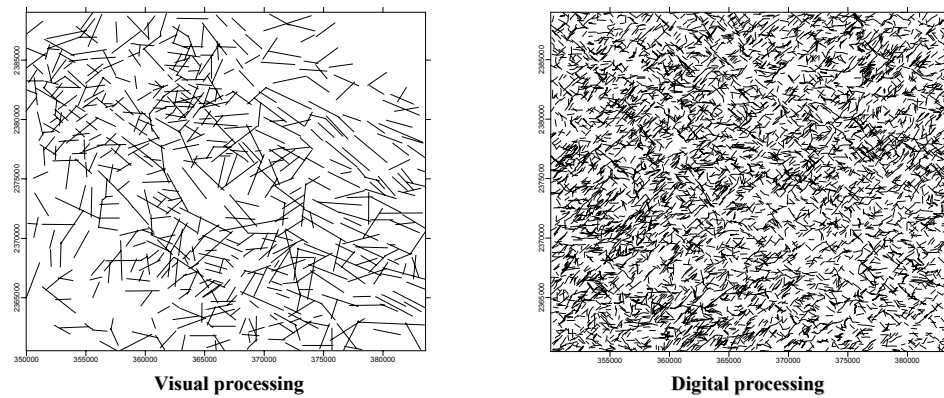


Figure 3-5. Image Processing: Lineament extraction.

However, in this study, the author chooses the method of automatically lineament extraction from remote sensing Landsat TM image by PCI software 9.1. (Lineament extraction tool). Landsat TM image editing is common radiometric correction and Geometric correction (according to coordinate of river system) as well as carried out steps enhances image quality before that carry out for automatically lineament extraction.

Later to proceed with work to filter the "false" lineament. Then undertaking is interpolated from ILWIS software 3.3 to establish the final map of lineament density. Process established maps of lineament density are shown in the picture below.

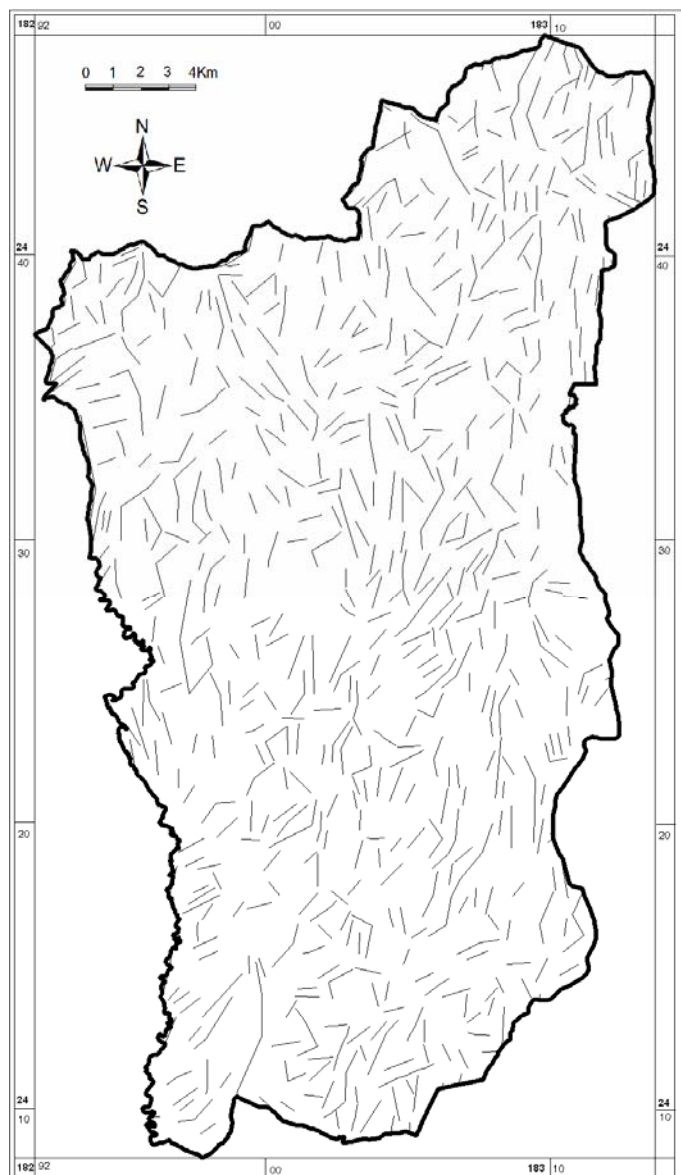


Figure 3-6. The map of lineament extraction of Muong Lay

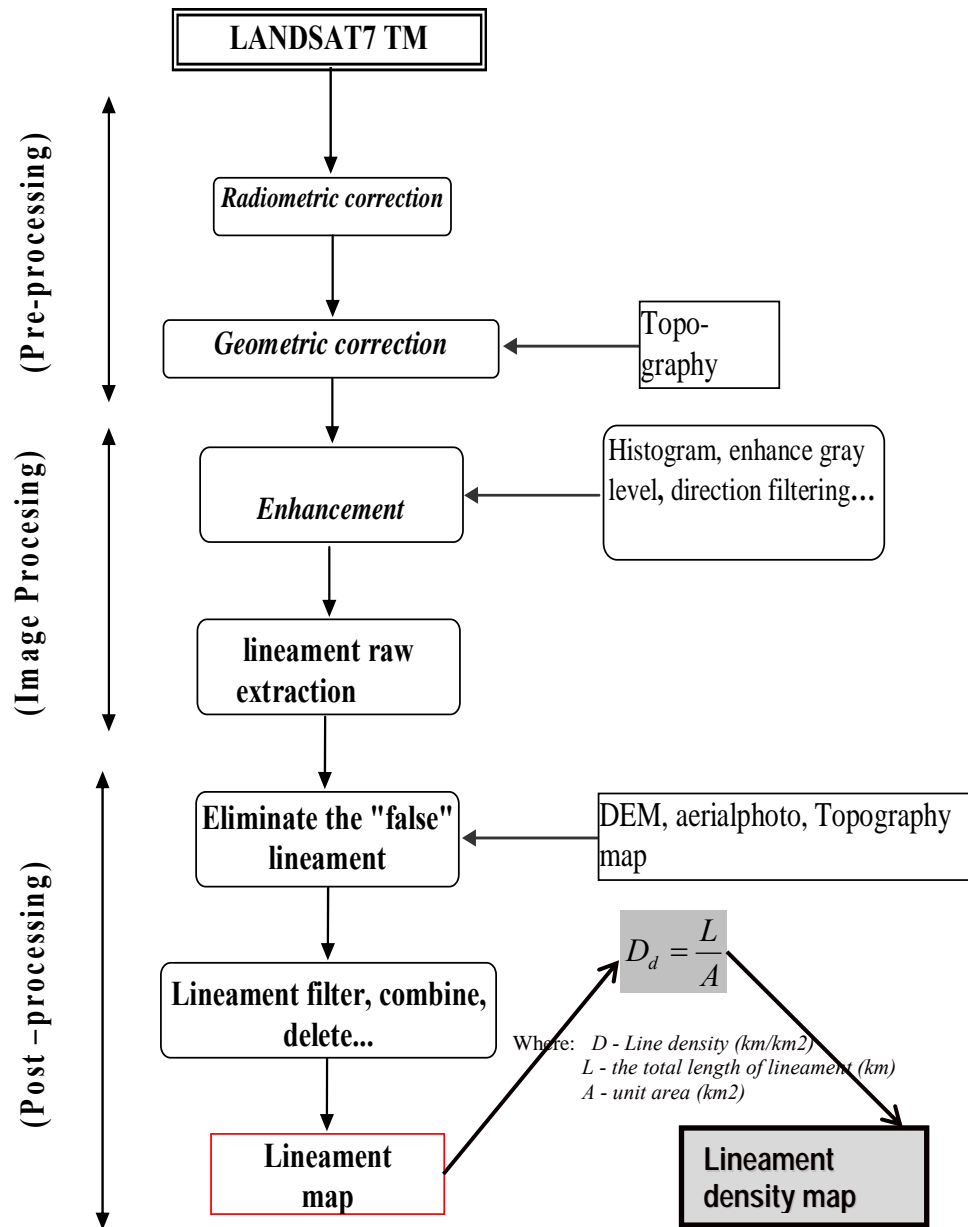


Figure 3-7. The flowchart of lineament mapping

3.1.3.2. Landcover

Input data to establish the landcover map is LandSat TM image of 20 February 1999 (Path/row: 125/48) covering the research area (Figure 3-1). The process for Remote Sensing image to landcover mapping of the research area is described in the picture below (Figure 3-7). In this study, the classification method is supervised that was used to processing and classifying for the landcover. Software used to process and analyze is the ENVI 4.3. Landsat TM image editing is common radiometric correction and Geometric correction (according to coordinate of river system) as well as carried out steps enhances image quality before that carry out for the landcover mapping.

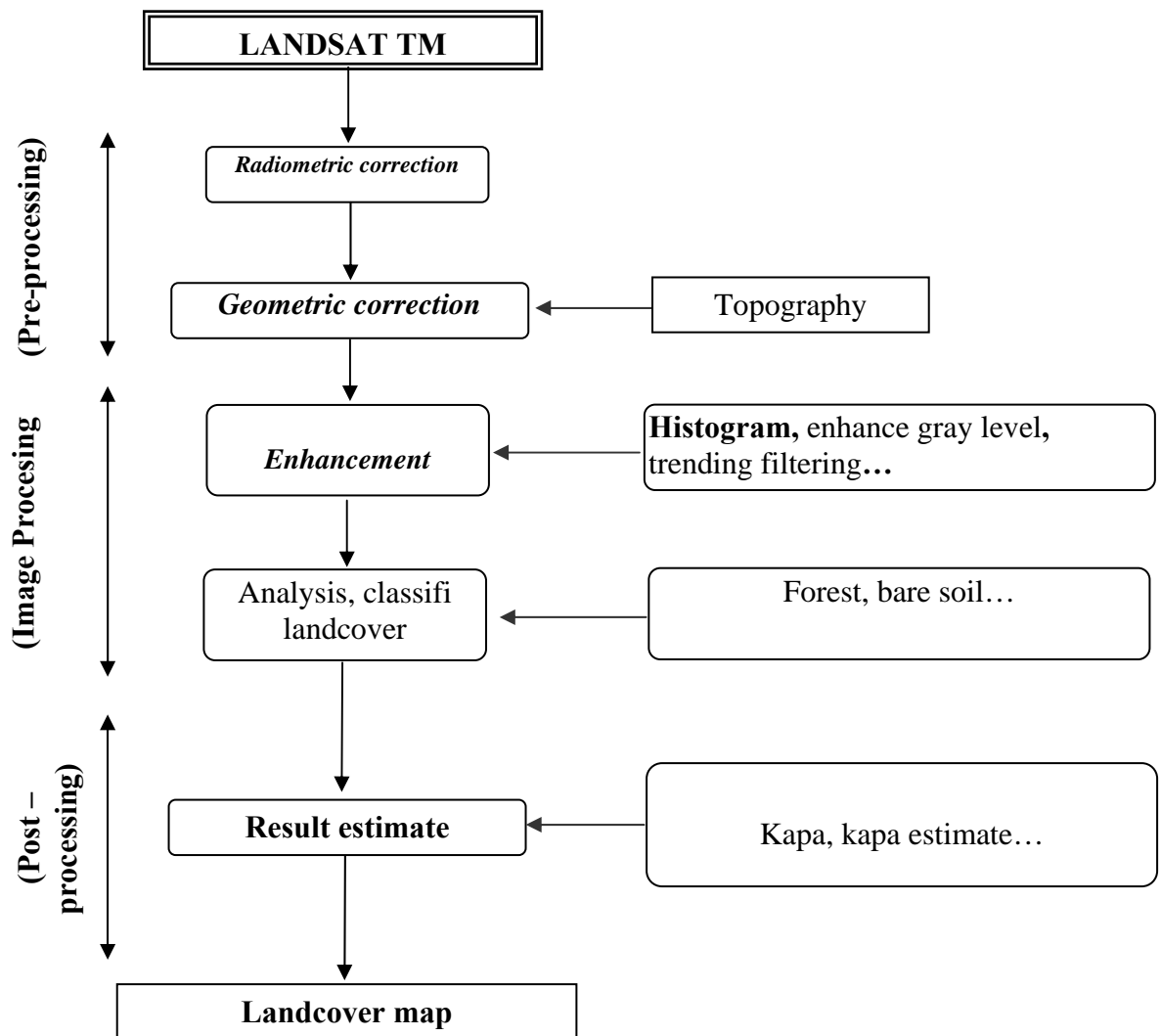


Figure 3-8. The flowchart of landcover mapping

Supervised classification has been used in this study. Supervised classification of multispectral remote sensing imagery is commonly used for land cover determination. Supervised classification requires that the user select training areas for use as the basis for classification. It is important that these classes be a homogenous sample of the respective class, but at the same time includes the range of variability for that class. Thus more than one training area is used to represent a particular class.

The ENVI main menu, there are seven of the supervised classification methods in the pull-down menu (Parallelepiped, Minimum Distance, Mahalanobis Distance, Maximum Likelihood, Spectral Angle Mapper, Binary Encoding, or Neural Net in which the Maximum Likelihood method is common used with high accuracy.

The supervised classification method is classified by the expert's supervision based on the understanding of objects in space research areas and attached to the sample classification. After the classes are determined by rules of expert's classification, the

classification is conducted based on the sample classification of classes and follow one of the supervised classification methods in upper, also known as regions of interest (ROIs).

The supervised classification should have to go through these steps:

- Setting up sample patterns for classification. The purpose of this step is to find areas with the same spectral values and sets them to class objects that we know on the field or on the source of collecting data.
- The next step is aggregation groups and removes groups which do not choose the right to create groups of right spectral for the final classification.

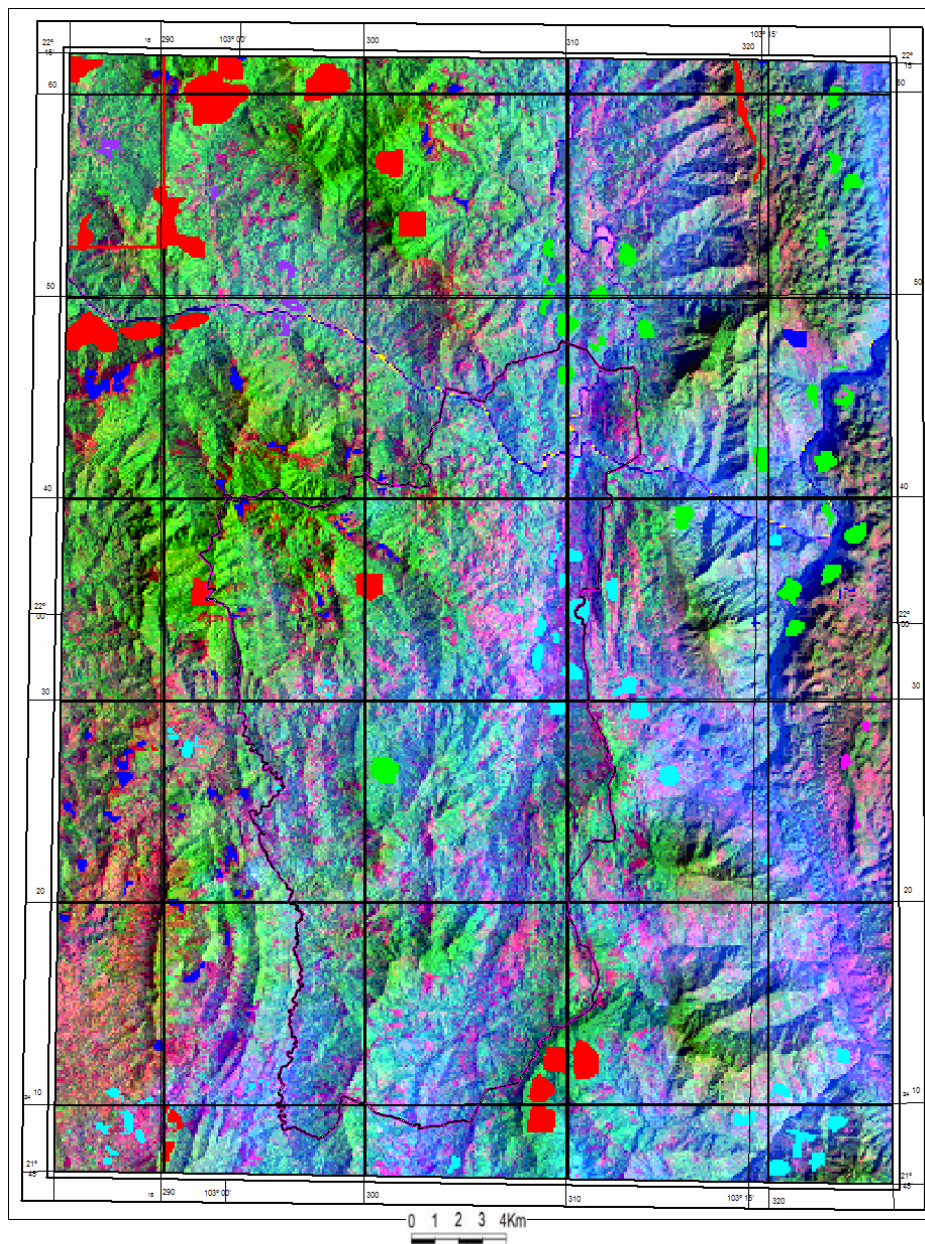


Figure 3-9. Setting up sample patterns for classification (Key areas)

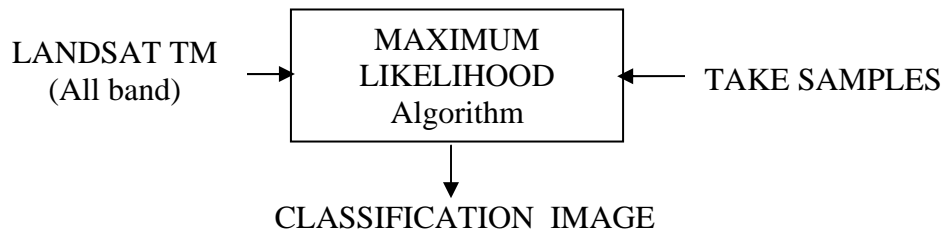


Figure 3-10. Flowchart of the supervised classification with Maximum Likelihood algorithm

ROI Name	Color	Pixels	Polygons	Polylines	Points	Fill	Orien	Space
0	Sea Green	0	0/0	0/0	0	Solid	45	0.10
Grass and bare h	Blue	18,055	72/18,055	0/0	0	Solid	45	0.10
Forage crops	Cyan	21,288	54/21,288	0/0	0	Solid	45	0.10
Shrub and bush	Magenta	1,724	15/1,724	0/0	0	Solid	45	0.10
Young forest	Purple	2,759	5/2,759	0/0	0	Solid	45	0.10
Sustained forest	Red	54,456	33/54,456	0/0	0	Solid	45	0.10
* Mixed forest	Green	23,906	32/23,906	0/0	0	Solid	45	0.10

Figure 3-11. The information of regions of interest (ROIs)

After conducting classification with supervised method, the author has evaluated the accuracy of the results by Kappa factor. With $k > 0.8$, the result analyzed is quite reliable and serves for the next researches of work.

3.1.4. Aerial-photos for landslide occurrence mapping

Remote sensing techniques greatly aid in the investigation of landslides, on both local and regional scales. Although these cannot replace fieldwork, for interdisciplinary research strategies and testing of reliability of landslide prediction models, remote sensing techniques do offer an additional tool from which we can extract information about landslide causes and occurrences. The landslide information extracted from remotely sensed products is mainly related to morphology, vegetation and hydrologic conditions of a slope. Especially, stereo-remote sensing products reveal the true morphodynamical features of landslides. Other remote sensing data for landslide inventory mapping are: LANDSAT (*Honda, et al., 2002*), SPOT (*Yamaguchi, et al., 2003*), IRS-1 (*Nagarajan, et al., 2000*), ASTER's 14 multi-spectral bands, IKONOS or Quickbird (*Petley, et al., 2002*).

Photogram metrical methods using aerial photos are very useful for identification of landslides. Such methods have now become standard procedures that can be carried out by most landslide research groups. Moreover, comparing aerial photographs of an area can give an indication of the frequency and extent of landslide events. When using photographs it is important to use photographs from different periods, as often land

development can display the presence of landslide features. Looking at the different periods, landslide causes can be detected and evaluated. Fookes et al. (1991) give excellent applications of aerial photogrammetric for landslide detection.

3.2. GEOGRAPHIC INFORMATION SYSTEM (GIS) APPROACHES FOR LANDSLIDE HAZARD ASSESSMENT

3.2.1. General

Geographic Information Systems (GIS), as a computer-based system for data capture, input, manipulation, transformation, visualization, combination, query, analysis, modeling and output, with its excellent spatial data processing capacity, has attracted great attention in natural disaster assessment (*Carrara, 1983*).

Using GIS can also ease the problem of slope stability analysis if a GIS-based geotechnical analysis model is used. With GIS, the methods for mapping landslide hazard can be briefly classified into three groups: qualitative methodologies, statistical methodologies and geotechnical model-based methodologies. Generally, qualitative approaches are based entirely on the judgment of those conducting the susceptibility or hazard assessment (*Van Westen, 1993*). The input data are usually derived from assessment during field visits, possibly supported by aerial photo interpretation. Because of the lack of a concrete physical concept with slope failure, qualitative approaches are seldom used as a guide for large-scale areas.

The statistical approach is an indirect method in which either a predictive function or index is derived from a combination of weighted factors. The relative contribution of each factor is obtained by means of statistical analyses (bivariate and multivariate). Using GIS makes these over layering operations much easier and largely explains the increasing popularity of the statistical approach, which closely parallels the ever-increasing application of GIS techniques. Deterministic, or physically based, models are based on the physical laws of conservation of mass, energy and momentum. The parameters used in these models can be determined in the field or in the laboratory. Most deterministic models employed in civil engineering and the engineering geology are site-specific and do not consider the spatial distribution of the input parameters. Models that consider the spatial distribution of input parameters are called deterministic distributed models. Deterministic distributed models require maps that give the spatial distribution of the input data. GIS is a tool for collecting, storing, retrieving, transforming, manipulating and displaying spatially distributed data, and therefore it is frequently used in distributed deterministic modeling.

- All GIS have hardware, software and data (Figure 3-8)
- It is primarily designed for the collection, storage and analysis of objects and phenomena where geographic location is an important characteristic for analysis.

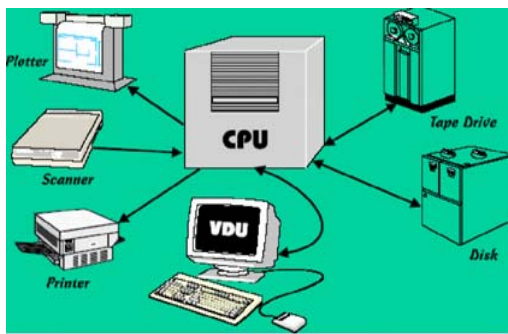
- A computer system for GIS consists of hardware, software and procedures designed to support the data capture, processing, analysis, modeling and display of geospatial data.

In general, a GIS should satisfy the following four criteria:

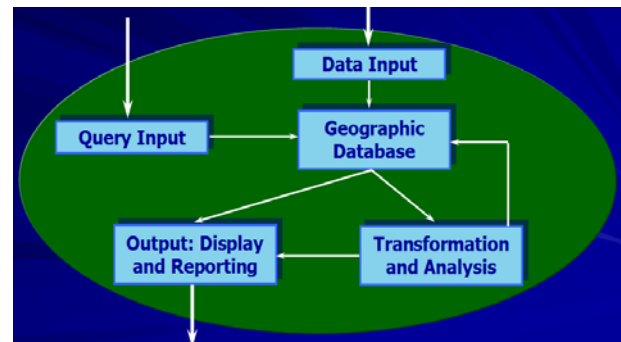
- Data input
- Data management (data storage and retrieval)
- Manipulation and analysis
- Output (Visualization)

Functionalities of GIS

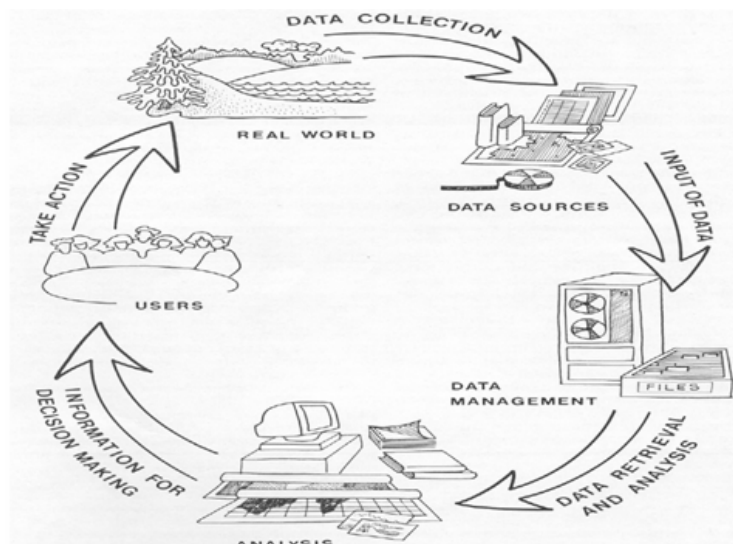
- Collecting, storing, retrieving, transforming, manipulating and displaying spatially distributed data
- Automatically synthesizing layers of geographic data
- Updating a database of spatial entities
- Spatial searching and overlaying
- Displaying of geospatial data
- Analysis spatial data
- Statistic methods



a)



b)



c)

Figure 3-12. The structure of GIS: a) hardware, b) software, and c) data of GIS

3.2.2. Digital Elevation Model (DEM)

Digital Elevation Models (DEMs) are a type of raster GIS layer. Raster GIS represents the world as a regular arrangement of locations. In a DEM, each cell has a value corresponding to its elevation. The fact that locations are arranged regularly permits the raster GIS to infer many interesting associations among locations: Which cells are upstream from other cells? Which locations are visible from a given point? Where are the steep slopes? One of the most powerful applications of DEMs is adding synthetic hillshading to maps so that the map reader may see the relationship between terrain and other things you may be mapping.

A Digital Elevation Model (DEM) is a raster of elevation values. Rasters represent the world as regular arrangements of pixels (cells). Rasters lend themselves to systematic analysis of the relationships among places and their properties.

For example, a Raster GIS can calculate many useful derivatives of elevation, such as: Slope or Aspect - the direction of slopes.

Synthetic Hill shade calculated from a DEM is a great way to create visualizations of terrain with other semi-transparent themes. DEMs can also be used to create 3-D scenes or to create contour which may be exported to CAD programs.

Common uses of DEMs include:

- Extraction terrain parameters
- Modeling of water flow or mass movement (for example avalanches and landslides)
- Creation of relief maps
- Rendering of 3D visualizations.
- Creation of physical models (including raised-relief maps)
- Rectification of aerial photography or satellite imagery.
- Reduction (terrain correction) of gravity measurements (gravimetric, physical geodesy).
- Terrain analyses in geomorphology and physical geography
- Geographic Information Systems (GIS)
- Engineering and infrastructure design
- Global positioning systems (GPS)
- Line-of-sight analysis
- Base mapping
- Flight simulation
- Precision farming and forestry
- Surface analysis
- Intelligent transportation systems (ITS)
- Auto safety / Advanced Driver Assistance Systems (ADAS)

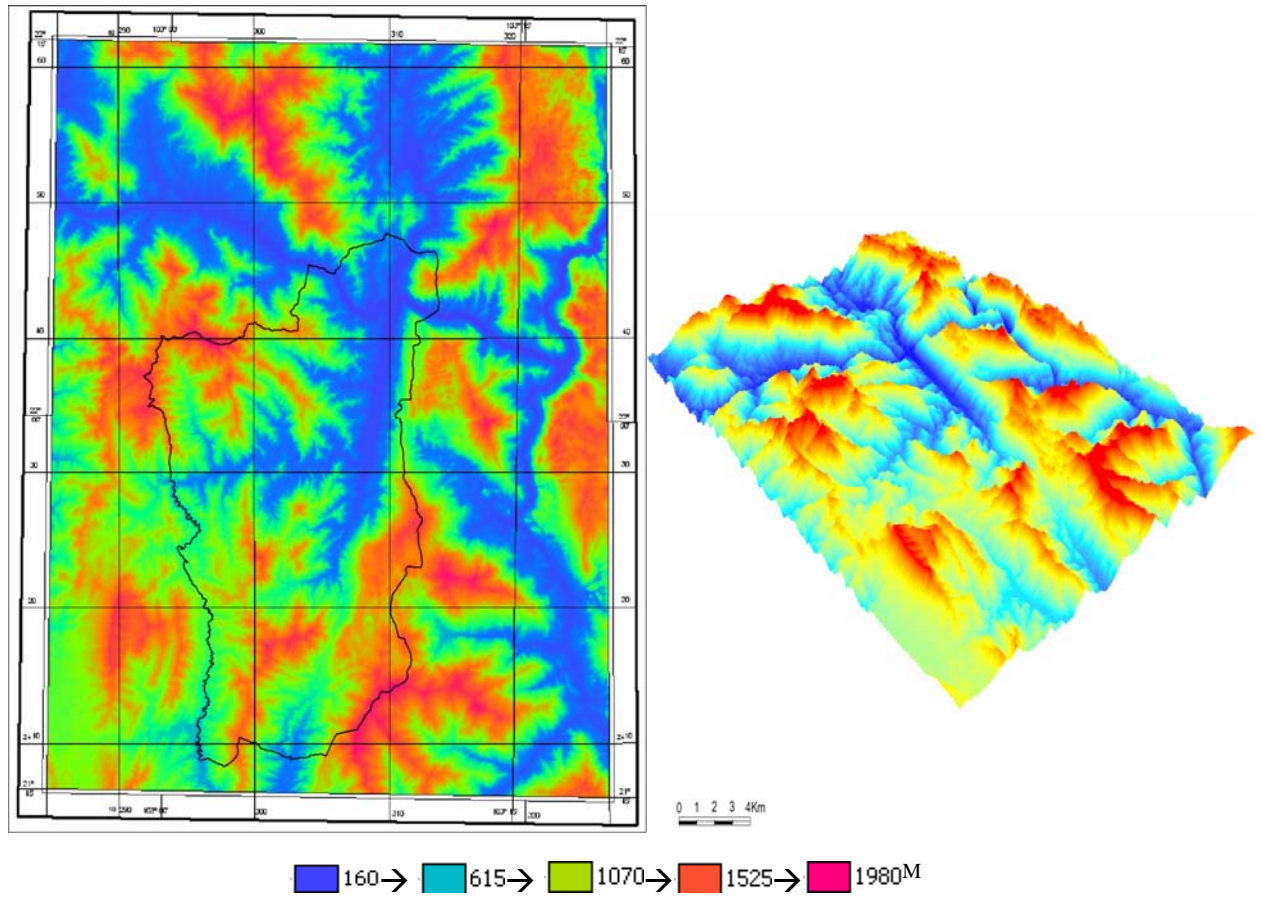


Figure 3-13. Digital Elevation Models (DEM) of Muong Lay area

3.2.3. GIS and Statistical models

3.2.3.1. GIS modeling methods

GIS methods for modeling slope instability have been employed by different investigators throughout the world. Reviews outlining the methods were given by Brabb (1984), Varnes (1984).

Literature review reveals that methods for ranking slope instability factors and assigning different susceptibility levels can be divided into: (1) qualitative or quantitative, and (2) direct or indirect (Soeters, *et al.*, 1996; Guzzetti, *et al.*, 1999).

Qualitative methods are subjective, ascertain susceptibility heuristically, and portray susceptibility levels using descriptive (qualitative) terms. Quantitative methods produce numerical estimates, i.e. probabilities of the occurrence of landslide phenomena in any susceptibility zone (Guzzetti, *et al.*, 2005). Only quantitative methods are suited to the quantitative evaluation of landslide hazard.

Direct mapping methods are those that identify the spatial distribution of instability directly from existing landslides and/or specific knowledge of areas of potential instability. A direct method consists of the (direct) geomorphologic mapping of landslide susceptibility in the

field from aerial photographs or from satellite images (*Nossin, 1989*). Indirect mapping methods are those that use factors relevant to land sliding to estimate potential instability. Indirect methods for landslide susceptibility assessment are essentially stepwise. Guzzetti et al. (2005) determined the requirements of Indirect methods as: (1) the recognition and mapping of landslides over a target region or a subset of it (i.e. the training area), which is obtained by preparing a landslide inventory map; (2) the identification and mapping of the physical factors which are directly or indirectly correlated with slope instability (the instability factors, or independent variables); (3) an estimate of the relative contribution of the instability factors in generating slope failures; (4) the classification of the land surface into domains of different levels of susceptibility; and (5) the assessment of the model performance.

The most common approaches proposed in the literature can be grouped into five main categories (*Van Westen, 1993; Soeters, Van Westen, 1996; Aleotti, Chowdhury, 1999; Guzzetti, et al., 1999*), namely: (1) direct geomorphologic mapping; (2) analysis of landslide inventories; (3) heuristic or index based methods; (4) statistical methods, including neural networks, fuzzy logic and expert systems; and (5) process based conceptual models (Table 3-4).

Table 3-4. Characteristics of landslide susceptibility (*Van Westen, 1993*)

	Direct	Indirect	Qualitative	Quantitative
Geomorphologic mapping	√		√	
Analysis of inventories		√		√
Heuristic (index-based)		√	√	
Statistical modeling		√		√
Process based (conceptual)		√		√

Geomorphologic mapping

The geomorphologic approach is employed to display the spatial variability of slope instability through either direct or indirect mapping. Direct mapping methods are those that identify the spatial distribution of instability directly from existing landslides and/or specific knowledge of areas of potential instability. Indirect mapping methods are those that use factors relevant to land sliding to estimate potential instability. The geomorphologic approach mainly relies on the ability of the investigator to recognize actual and potential slope failures, including their evolution and possible consequences (*Cardinali, et al., 2002*). This method can provide very reliable results.

Analysis of inventories

Landslide occurrences are usually determined through the interpretation of aerial photographs and/or field surveys, and then digitized directly into an instability map using a GIS. The analysis of landslide inventories attempts to predict future patterns of instability directly from the past distribution of landslide deposits. A landslide inventory map provides spatial information on instability directly from the mapping of previous landslides. The analysis of this distribution can lead to the extrapolation to other areas of possible future instabilities and classification into a final instability map. This can be accomplished by preparing landslide density maps, i.e. maps showing the percent of area covered by landslide deposits or the number of landslide events over a region (*Guzzetti, et al., 1994*). Different types of landslide density maps can be prepared, depending on the type of mapping unit and the filtering techniques used to determine the density (*Guzzetti, 2000*). In a GIS, landslide inventories can be accompanied by a table showing different attributes of the landslide such as type of movement, type of material, activity, depth (*Soeters, Van Westen, 1996*) as well as the certainty of identification and direction of movement (*Wieczorek, 1984*). Most often, inventory maps are an additional piece of information used as input factors and/or validation assessments for the other methods described later. As straightforward as it is to develop, an inventory map is an invaluable component of any slope instability zonation.

Heuristic (index-based) method

An index-based approach is an indirect (or semi-direct), mostly qualitative method that relies heavily on the a priori knowledge of landslides and their processes in a region. Therefore, its reliability depends on how well and how much the investigator understands the geomorphologic processes acting upon the terrain. Instability factors are classified, ranked and weighted according to their assumed or expected importance in causing mass movements. Based on this information, heuristic and subjective decision rules are established to define possibly unstable areas and to zone landslide susceptibility

accordingly (*Montgomery, Dietrich, 1994; McClelland, et al., 1997; Lee, et al., 2002*). In the index-based approach, the method used for combining various factor maps to obtain a map of slope instability is known as a qualitative map combination, and has become a very popular method of slope instability zonation due to its ease of use and lack of fieldwork needed to develop a required landslide inventory. The advantage of this method is that a landslide inventory is not needed because the weights are assigned based on the field knowledge of an experienced geomorphologist. Moreover, the use of GIS for the weighting assignments and overlays makes this method fast and easy to use provided the needed data are available.

However, experts' subjectivity strongly influences the resulting map of landslide susceptibility, although subjectivity is not necessarily bad, particularly if it is based on the opinion of an expert. Nonetheless, subjectivity adds to the uncertainty of the model. To limit this problem, the expected importance of each instability factor can be obtained "objectively" by investigating the relative abundance of landslides (*Pachauri, et al., 1998*), or from regression analysis (*Long, 2008*).

Process based models

Process based (deterministic or physically based) models for the assessment of landslide susceptibility rely upon the understanding of the physical laws controlling slope instability. In general, due to lack of information or poor understanding of the physical laws controlling landslide initiation and development, only simplified, "conceptual" models are considered. These models are indirect and provide quantitative results, which may or may not be suited for quantitative landslide hazard assessment depending on the types of output. Reviews of the literature reveal that process based models are developed mostly to study a particular type of landslide (e.g., shallow soil slips, debris flows, or rock falls), or to investigate the effect of a specific trigger, i.e. an intense rainfall period or an earthquake.

Process based models attempt to extend spatially the simplified stability models widely adopted in geotechnical engineering. These models calculate the stability of a slope using parameters such as normal stress, angle of internal friction, cohesion, pore water pressure, seismic acceleration, external weights, etc. Most commonly, computation results in a factor of safety, i.e. an index expressing the ratio between the local stabilizing and driving forces. Values of the index greater than one indicate stability of the slope, and values less than one identify unstable conditions. A safety factor of exactly one indicates the meta-stable condition produced by equivalence of stabilizing and driving forces.

3.2.3.2. Models of the Overall Estimation of Landslide Susceptibility

Landslides are the result of the interaction of complex factors; therefore the spatial prediction of landslide susceptibility is a difficult task. As mentioned in the paragraphs above, there are two basic approaches for such a study. One approach uses statistics to compute the weighting values based on the relationship of the factors with existing landslides. Hazard can be estimated by statistical correlation with factors considered to correlate with landslide (Thien, 2004).

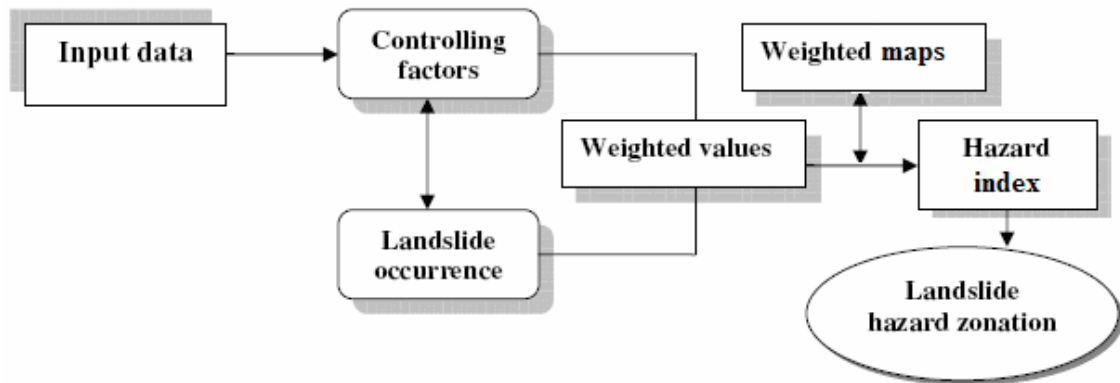


Figure 3-14. Simplified flowchart of the statistical analysis: This flowchart illustrates the various terms that will be used in next chapter.

The other approach is the qualitative map combination where relative weighing values are assigned to the factors and their classes on the basis of field knowledge and experience. Therefore the method relies heavily on the professional experience of the experts; they involve a great level of subjectivity, so the maps produced by different researchers can be very different.

In this thesis, the author has adopted a statistical approach for the model. Simply, the model can be illustrates by the scheme as figure 3-14. The author have used this model because reasons such as: data availability; transparence of the method easy to follow the different steps; very successful for other projects and other investigation areas, for example: *“Geological hazard risk assessment in Ha Giang, Cao Bang, Tuyen Quang and Bac Kan province.”*, *“Applying GIS for assessment Water and Land resources in Son La hydroelectric and surrounding”*, *“Apply remote sensing analysis method and GIS in researching geological hazards in Central of Vietnam from Quang Binh to Phu Yen”*, etc... All of the projects above are made by Vietnam Institute of Geosciences and Mineral resources.

CHAPTER 4.

LANDSLIDE HAZARD ASSESSMENT IN MUONG LAY AREA

4.1. EXISTING LANDSLIDE IN MUONG LAY

4.1.1. Landslide inventory mapping

A landslide inventory map identifies the definite and probable areas of existing landslides, and is the most basic requirement for a landslide hazard assessment. The product of a landslide inventory map is a spatial distribution of landslides as points or to scale. Landslide inventory maps can be and often are used as a basis for other landslide hazard zonation techniques or for an elementary form of a hazard map. A typical landslide inventory map is based on aerial photograph interpretation, ground survey, and/or a database of historical movements within the area. These maps, however, only provide information for a short period of time, and they provide no insight into temporal changes in landslide distribution (*Hung, 2002; Long, 2008*).

In landslide hazard assessment, the historic information on landslide occurrences is by far the most important, as this gives insight into the frequency of the phenomena, the types involved, the volumes and the damage that has been caused. Landslide inventory maps, derived from historic archives, field data collection, interviews and image interpretation are essential but unfortunately often deficient. Despite the fact that the quality of historical evidence is strongly dependent on recorded procedures and available records, this approach provides an indication of at least the minimum level of landslide activity in an area. The issue of using historical data in natural hazard assessments was discussed by Guzzetti (1994), Glade (2001), and was specifically addressed to landslides by Glade (2001), Bozzano (1996) and Guzzetti (2000).

Generally, widely used methods for making a landslide inventory map are field investigations and remote sensing techniques. By fieldwork surveys, evidence of current and former land sliding can be determined from slope morphology, sedimentary deposits, or impact features (e.g. deformed trees). As this type of evidence deteriorates or is obliterated progressively with time, care has to be taken in establishing long-term trends in occurrence. A wide range of both relative and absolute methods has been employed for dating of field evidence (*Lang, et al., 1999*). A number of papers dealing with the determination of frequency and magnitude of occurrence from field evidence can be found in Mathew et al. (1997).

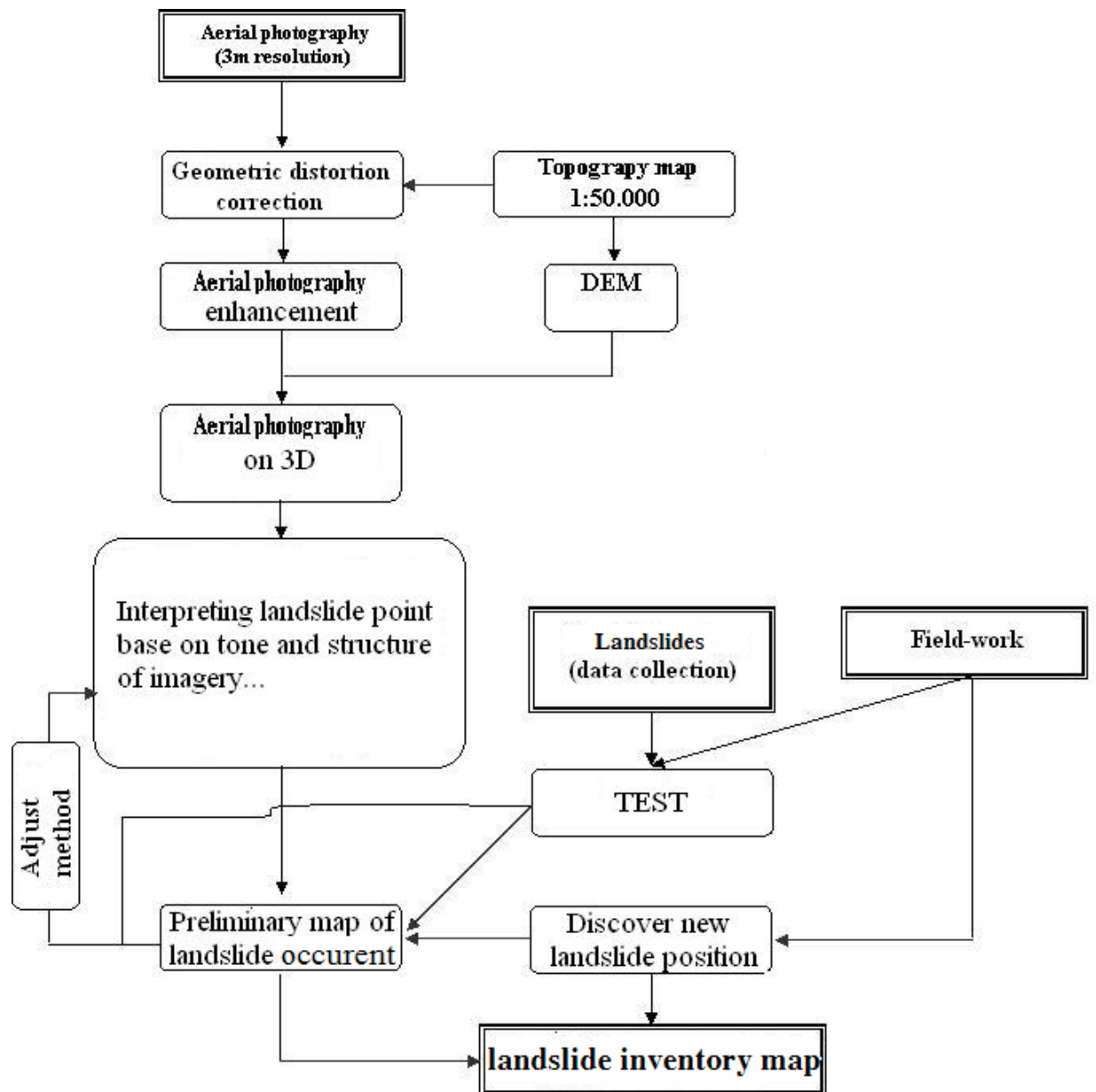


Figure 4-1. Flowchart of landslide zonation

The aerial-photos using in this thesis were acquired in November 2001 at the scale of 1:25000. After the photography, the color film was developed and scanned at 1000dpi using the photogrammetric scanner. The photographic session was carried out by a company and a series of digital images were acquired to cover roughly the same area covered by a pair of large format aerial photograph. Figure 4-1 is 30 image pair aerial-photos used for landslide inventory mapping.

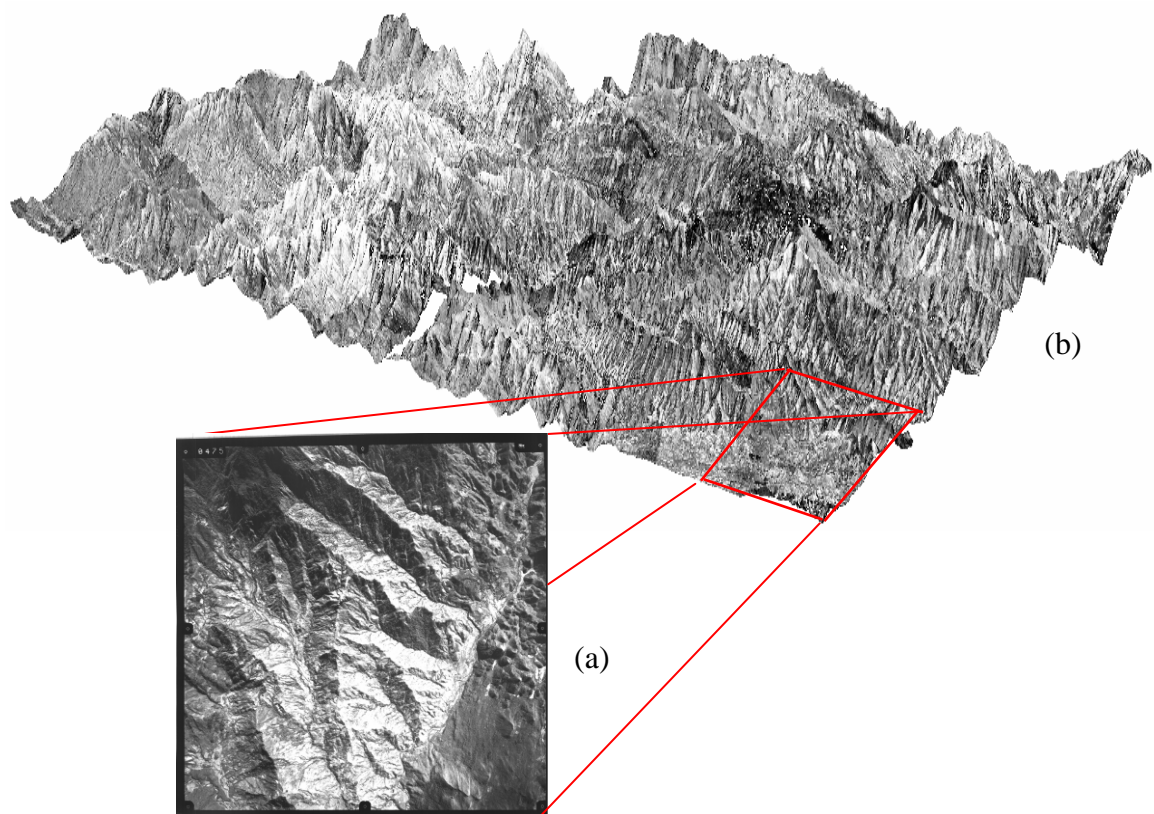


Figure 4-2. a) A aerial-photo; b) 3D view of 30 image pairs of MuongLay area (pixel size 0.5 m/pix)

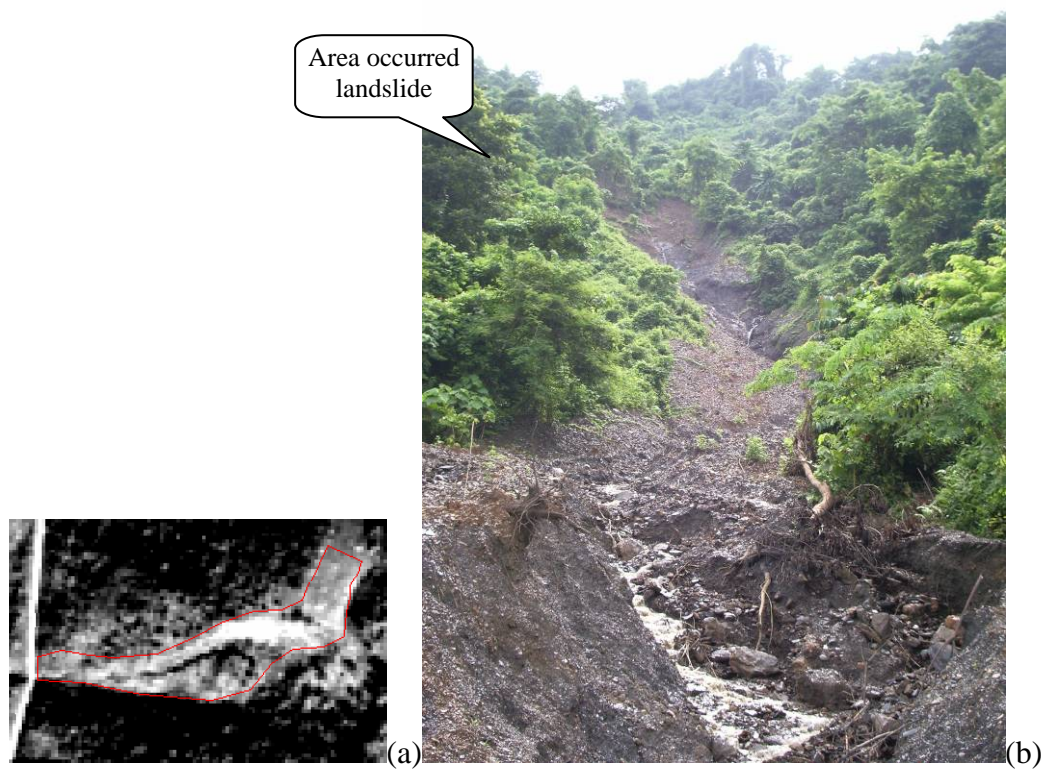


Figure 4-3. Examples of a landslide event in Ban Moi, Muong Tung, Muong Lay. a) Signs of landslide concern on aerial photograph; b) Photo-landslide observed outside in the field

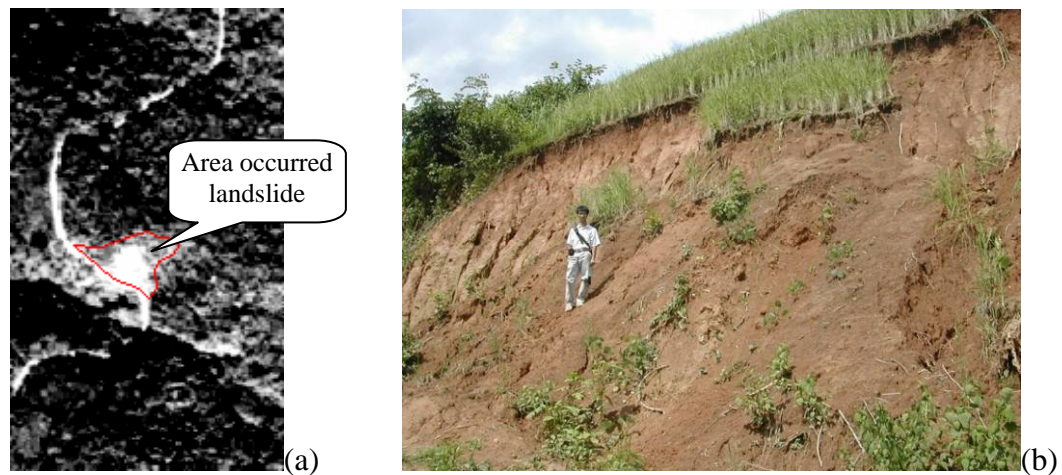


Figure 4-4. Examples of a landslide event in Ma Lu Thang, Muong Lay. (a) Signs of landslide concern on aerial photograph; (b) Photo-landslide observed outside in the field

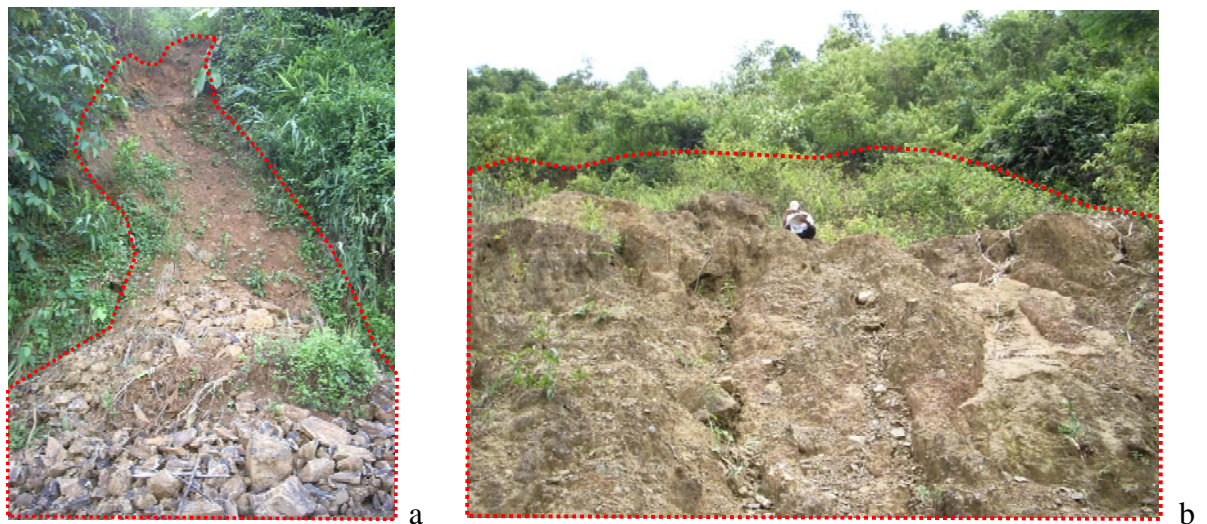


Figure 4-5. Some pictures of landslide occurrences in Muong Lay. a) Landslide in Ho Muc, Pa Ham, Muong Cha; b) Landslide in Xa Long, Huoi Leng, Muong Cha

4.1.2. Landslide occurrence map of Muong Lay

Landslide occurrences are usually determined through the interpretation of aerial photographs and field surveys, and then digitized directly into an instability map using a GIS. The analysis of landslide inventories attempts to predict future patterns of instability directly from the past distribution of landslide deposits. A landslide inventory map provides spatial information on instability directly from the mapping of previous landslides. The analysis of this distribution can lead to the extrapolation to other areas of possible future instabilities and classification into a final instability map (*Guzzetti, et al., 1999*).

There are 88 landslides in this research area. (According to Lai Chau province's documents, VIGMR's additive survey data combination with data of aerial photogrammetric). Quantitative landslides are classified from small to extremely large

(Table 4-1). The average density of landslide is 8 landslides/10km². Exclusively the road from Ma Thi Ho (belonging to rural district Muong Cha) come to Da River ward (Muong Lay), about 1.5 km wide and 50km long has more than 30 landslides. Road 12 from Muong Lay to Dien Bien, about 100km long, has 110 landslides (*Tuyet, 1999*). The landslides here range from moderately large to extremely large. Especially, the landslide locate in Huoi Lo (called Huoi Lo landslide) is with 1,500m long, 60m wide, 90,000 m² large and has 1,350,000 m³ unit of mass ; the Le Loi landslide has 100,000 m³ unit of mass (*Tuyet, 1999*).

Landslide types here mostly consist of complex-slides between translational slide and rotational slide. Most landslides are active in crust of weathering of metamorphic rocks and many aluminosilicate recipient polymetamorphic rocks, much clay in the slope of 25-35°, and almost no vegetation cover. Especially in the annual rain season, most landslides recur (*Tuyet, 1999*).

Huoi Lo landslide has been active since 1990, most powerful during the monsoon in 1996. Landslides locate in Deo Hoa and LeLoi have been active since 1994. Some ancient landslides such as SuoiHe landslide, Deo Cong Troi landslide... have been inactive but can still return (*Tuyet, 1999*).

Especially during the rainy season, landslides occur frequently, when the rainfall is concentrated in a short time, which is usually the case with the monsoon in August. On the other hand, rains that last for longer periods (e.g., days or weeks) in January and August can also cause landslides in the research area (*Tuyet, 1999*).

The average area of a landslide in the research area is approximately 4 ha. Some pictures of landslide are shown in Figure 4-3 to 4-6. The observed landslides are divided into 5 types depending on their volumes as proposed by Lomtatze (1997). The landslide classification of Muong Lay is given in Table 4-1.

Table 4-1. Quantitative landslide classification (Lomtatze, 1997) with corresponding number of slides in Muong Lay

Classification	Size	Volume (m ³)	Number of slides
I	Small	< 200	6
II	Moderately large	200 -1000	60
III	Large	1000 -100000	19
IV	Very large	100000 -1000000	2
V	Extremely large	> 1000000	1

(supplemented by *Tuyet, 1999*)

Table 4-2. List of landslide occurrences in Muong Lay

No	NAME	X	Y	SURVEY	SIZE
1	TL_101	306369.74	2444220.75	N	Moderately large
2	TL_102	304661.85	2444159.75	AF	large
3	TL_106	310727.8	2443722.67	N	Moderately large
4	TL_108	306810.82	2443394.69	N	Moderately large
5	TL_109	303443.94	2442941.83	PS	Very large
6	TL_112	307329.02	2442497.47	N	Moderately large
7	TL_113	308276.39	2442087.24	N	Moderately large
8	TL_115	305945.39	2441128.21	AF	Moderately large
9	TL_117	303654.00	2440393.15	AF	Moderately large
10	TL_118	306744.09	2437913.02	AF	large
11	TL_120	301054.88	2436888.45	AF	Moderately large
12	TL_121	305879.77	2436655.82	AF	large
13	TL_122	299829.49	2436616.53	AF	large
14	TL_123	311183.57	2436027.21	PS	Very large
15	TL_124	298726.19	2435882.89	AF	Moderately large
16	TL_125	304504.72	2435752.2	AF	large
17	TL_127	304936.87	2434927.17	AF	large
18	TL_128	303066.17	2434844.8	AF	Moderately large
19	TL_129	303483.23	2434828.95	PS	Small
20	TL_130	301270.91	2434818.79	AF	Moderately large
21	TL_132	303534.52	2434428.52	AF	Moderately large
22	TL_133	301505.07	2434376.47	AF	Moderately large
23	TL_134	303014.14	2434298.42	AF	Moderately large
24	TL_135	309276.9	2433985.4	N	Moderately large
25	TL_136	305761.91	2433944.98	AF	large
26	TL_137	303768.69	2433908.13	AF	Moderately large
27	TL_138	299891.92	2433856.11	AF	Moderately large
28	TL_139	304184.99	2433830.08	AF	Moderately large
29	TL_140	300772.4	2433827.11	PS	Small
30	TL_141	307058.39	2433748.54	AF	large
31	TL_143	303248.31	2433699.99	AF	Moderately large
32	TL_144	301505.07	2433673.97	AF	Moderately large
33	TL_147	300698.5	2433309.72	AF	Moderately large
34	TL_148	303534.52	2433127.58	AF	Moderately large
35	TL_150	310358.58	2433041.36	AF	large
36	TL_152	303856.47	2432962.79	PS	Small
37	TL_155	301244.88	2432711.29	AF	Moderately large
38	TL_156	297498.22	2432685.26	AF	Moderately large
39	TL_157	304679.33	2432659.25	AF	Moderately large
40	TL_158	304288.62	2432648.49	PS	Small
41	TL_159	306194.1	2432530.63	AF	large
42	TL_160	303950.81	2432529.16	AF	Moderately large
43	TL_162	305303.78	2432347.02	AF	Moderately large
44	TL_166	302108.18	2431469.86	AF	large
45	TL_169	300752.75	2431037.7	PS	Small
46	TL_170	310830.01	2430959.13	AF	Extremely large
47	TL_172	299683.78	2430603.79	AF	Moderately large
48	TL_174	300281.31	2430585.89	PS	Small
49	TL_175	302304.6	2430526.96	AF	large
50	TL_178	310044.25	2429937.64	AF	large
51	TL_181	306390.51	2429505.48	AF	large
52	TL_182	305054.73	2429466.2	AF	large
53	TL_183	310793.7	2429120.73	AF	Moderately large
54	TL_185	309414.7	2428834.53	AF	Moderately large
55	TL_186	304627.29	2428678.41	AF	Moderately large
56	TL_188	306626.24	2428562.58	AF	large
57	TL_189	310169.24	2428522.3	AF	Moderately large

58	TL_191	305303.78	2428314.15	AF	Moderately large
59	TL_192	311053.86	2427923.87	AF	Moderately large
60	TL_194	308111.16	2427812.42	AF	Moderately large
61	TL_195	311834.41	2427559.62	AF	Moderately large
62	TL_197	309808.55	2426676.78	AF	large
63	TL_199	311444.15	2426440.81	AF	Moderately large
64	TL_201	305121.65	2426310.72	AF	Moderately large
65	TL_203	303898.77	2426076.56	AF	Moderately large
66	TL_205	310923.77	2425712.29	AF	Moderately large
67	TL_207	307267.21	2425619.15	N	Moderately large
68	TL_208	305017.57	2425296.00	AF	Moderately large
69	TL_209	309376.36	2425223.14	AF	large
70	TL_210	307165.16	2425157.12	AF	Moderately large
71	TL_214	304426.15	2424555.25	AF	large
72	TL_217	308712.19	2424203.22	AF	Moderately large
73	TL_219	308998.41	2423604.79	AF	Moderately large
74	TL_224	300542.38	2422485.99	AF	Moderately large
75	TL_225	308139.8	2422407.94	AF	Moderately large
76	TL_226	305017.57	2422355.9	AF	Moderately large
77	TL_253	305797.9	2418665.17	N	Moderately large
78	TL_254	305660.91	2418434.15	N	Moderately large
79	TL_266	305559.27	2417604.37	N	Moderately large
80	TL_281	298538.96	2414316.17	AF	Moderately large
81	TL_282	301140.82	2414264.14	AF	Moderately large
82	TL_288	301088.77	2413171.36	AF	Moderately large
83	TL_289	304558.19	2413116.86	PS	Moderately large
84	TL_290	304551.25	2413033.22	N	Moderately large
85	TL_295	304159.74	2412352.93	PS	Moderately large
86	TL_301	296075.38	2410835.79	N	Moderately large
87	TL_307	296128.29	2409915.14	N	Moderately large
88	TL_308	296266.68	2409257.94	N	Moderately large

(N: New; AF: Airphotos+Fieldcheck; PS: Previous studies;
X, Y: coordinate system of UTM, Zone 48)

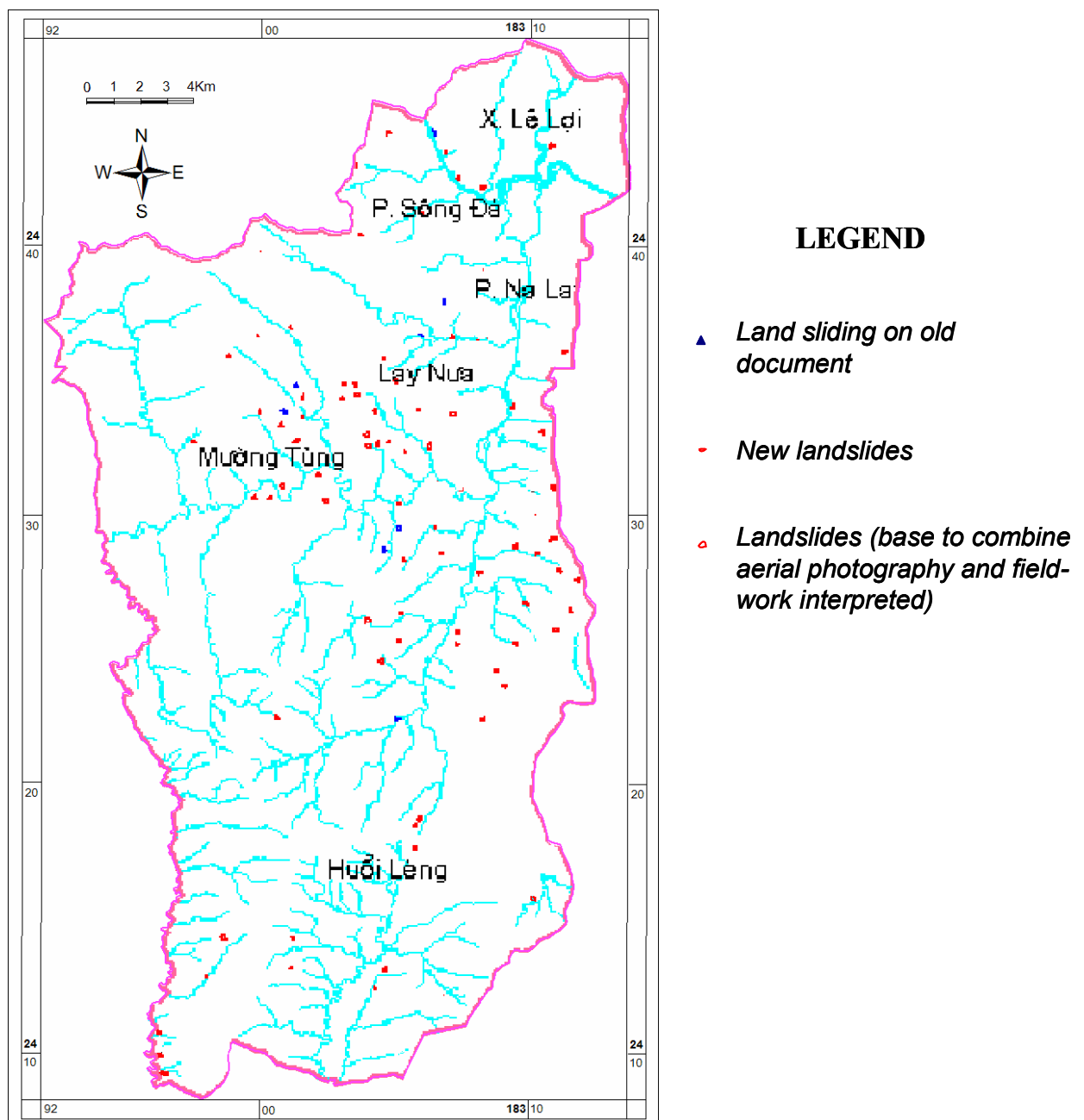


Figure 4-7. Landslide occurrence map of Muong Lay

All 88 landslides identified by VIGMR's additive survey data combined with data of aerial photogrammetric are located in Muong Lay.

4.2. DATA LAYER PREPARATIONS

Landslide can have several causes, including bed rock geology, morphology, physical, hydrologic conditions and anthropogenic activities. These causes can be broadly grouped into two categories: internal causes which make the slope susceptible to movement and the external causes such as triggering event or human.

The triggering factors such as earthquakes and human activities whose magnitude and temporal behavior are difficult to gauge and misfit in model with scale map 1:50'000.

Therefore, they could not be considered here due to the non-availability of past records regarding landslide occurrences.

The factors considered in our study are essentially the internal causes for which pertinent data can be collected from available resources as well as from the field. These seven factors which present for strength of soil and rock, morphological features, hydrology and landcover in the research area, were geotechnical features, weathered crust, lineament, elevation, slope degree, density drainage and landcover.

Each factor was then divided in to corresponding classes by its unit or values depending on the type of factor map. The selection of these factors and theirs and their classes was primarily based on the field observations of existing landslides and their associated terrain factors. The different types of datasets used to generate these factors were as follows:

- Topographic maps of Survey of Vietnam at scale 1:50.000 to form the base map.
- Geological map representing lithology and weathering types at scale 1:200.000 (compiled by Bureau of Geology and Mineral of Vietnam, 2000).
- LandSat TM (dated 20th February 1999) in seven bands with 30m ground resolution.
- Field data involving observations on landslides, geology, structure and landcover.

As mentioned in the section III.2, for the landslide hazard zonation objectives in this study, nine factors were prepared:

- Geotechnical, geomorphological, weathering crust and lineament density features
- Slope degree and elevation map
- landcover classes
- Drainage density map
- Rainfall

The details of these layers are described as follows:

4.2.1. Geological factor

Geology strongly influences slope stability (*Sarkar, et al., 1995*). Because most slope failures are shallow, involving deposits near the surface, particular attention must be given to the geology of an area. The close relationship between geological and landslide occurrences was also discussed in the literature review. At present, weathering crust, geological and faults density are by far the most commonly used information sources for landslide hazard analysis in Vietnam. Hence, the geology is considered as a fundamentally causative factor in this research.

The geological features in the research area (Figure 4-8) can be divided into four main groups:

- **Group 1: Quaternary deposits** primarily in river valleys and plains, characterized by

incoherent textures, diversified components, abundant material sizes, and essential alluvium faces: (aQ).

• **Group 2: Aluminosilicate sediments rocks** consisting of pebbles, cobble, gravels, gritstones, sandstones, siltstones, claystones, carbonates, alternated rhyolites, dacites and andesite sediments, and tuffs. This group includes the Cam Thuy ($P_3\ ct$), Nam Cuoi formation ($S_2-D_1\ nc$), Ban Pap Formation ($D_{1-2}\ bp$), and Nam Pia Formation ($D_1\ np$). Nam Po Formation ($J_{1-2}\ np$), Suoi Bang Formation ($T_{3n-r}\ sb$), Lai Chau Formation ($T_{2-3}\ lc$), and Song Da Formation ($P_{1-2}\ sd$).

Table 4-3: Some remarkable features of geological

	Stratigraphic units	Symbol	Petrographic constituent	Thick (m)	Location
Quaternary deposits	Quaternary deposits	aQ, apQ, adQ	pebbles, cobble, gravels, sand, silt, clay and organic materials	0.5-5	located at coastal plain area and to long streams
Aluminosilicate sediments rocks	Nam Po Formation	$J_{1-2}\ np$	light-grey sandstones, interbeds of chocolate siltstones, claystones, some bed conglomerates	700	Si pa phin, Muong toong
	Suoi Bang Formation	$T_{3n-r}\ sb$	conglomerate, gritstones, sandstones, siltstones, clay shales, marl	550	Si pa phin, Nam Cang
	Lai Chau Formation	$T_{2-3}\ lc$	black clay shale, silty sandstones	700	Muong Lay, Chan Nua
	Cam Thuy Formation	$P_3\ ct$	limestones, cherty limestones, cherts, sandstones, siltstones, claystones, a few tuffs	200	Lao Xa Phinh, Ca Nang
	Song Da Formation	$P_{1-2}\ sd$		1800-2050	Muong Cha, Muong Tung, Muong Mo, Chan Nua, Nam Hang
	Ban Pap Formation	$D_{2-3}\ bp$	black-grey bedded to massive limestone, marl	1150	Muong Cha, Xa Tong, Muong Lay
	Nam Cuoi Formation	$S_2-D_1\ nc$	sandstones, black-grey lustrous clay-sericite shales, calcareous sandstones, marl	400	Muong Lay
Metamorphic rocks	Nam Co Formation	$NP\ nc$		1050	Muong Cha, Nam Muc
Acid-neutral magma	Phia Bioc Complex	$\gamma T_{3n}\ pb$	granit aplites, lamprophyre		Muong Lay, Muong Tung, Nam Hang
	Complex system of Dien Bien (phase 1)	$\gamma\delta P_3-T_1\ db$	granit aplites, pegmatite, lamprophyre		Muong Lay, Lay Nua, Muong Tung, Nam Hang

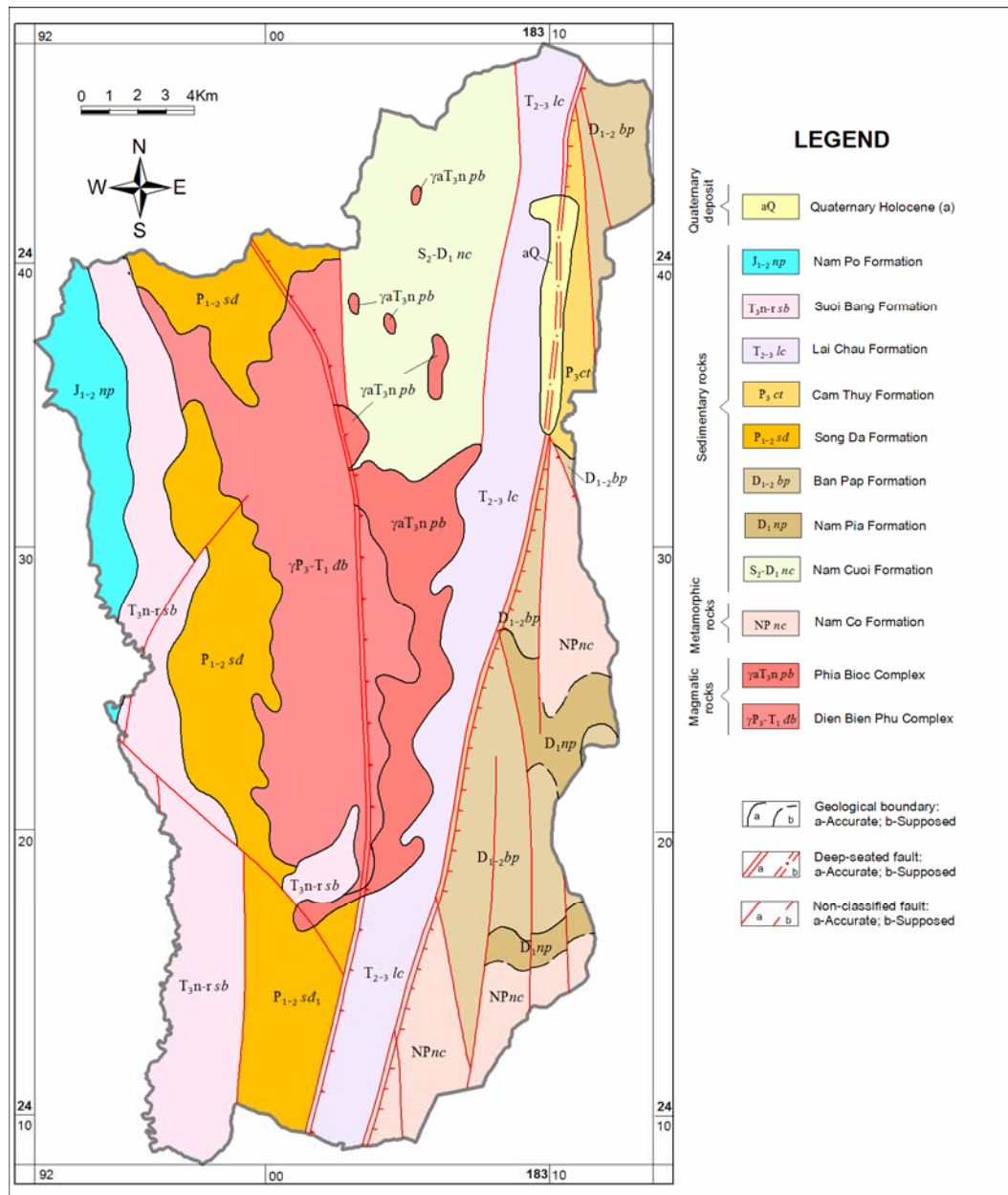


Figure 4-8. The Geological map of Muong Lay (Source: Tuyet, 1999)

- Group 3: Metamorphic rocks.** Metamorphic rocks with rich aluminosilicate components. The metamorphic rocks consist of green schist, chlorite schist, sericite schist, quartz-sericite schist, gneiss-biotite-granite, plagiogneiss-amphibole-biotite, amphibolite-biotite, plagiomigmatite, quartz-biotite schist, biotite schist, schist-feldspar-biotite, etc. This group includes Nam Co formation (NPnc).
- Group 4: Magmatic rocks.** The extrusive magmas consist of rhyolite, dacite, felsite, and andesite rocks. The intrusive granite magmas consist of plagiogranite, granophyre, granosyenite, granodiorite, diorite, and diorite-quartz. This group includes Triassic - Phia Bioc Complex (γaT_{3n} pb), and Dien Bien Phu Complex (γP₃-T₁ db).

4.2.2. Weathering crust factor

Weathering strongly influences landslide occurrences in a tropical region as Muong Lay, as discussed in the literature review. Hence, weathering is an indispensable causative factor for landslide susceptibility analysis in the study.

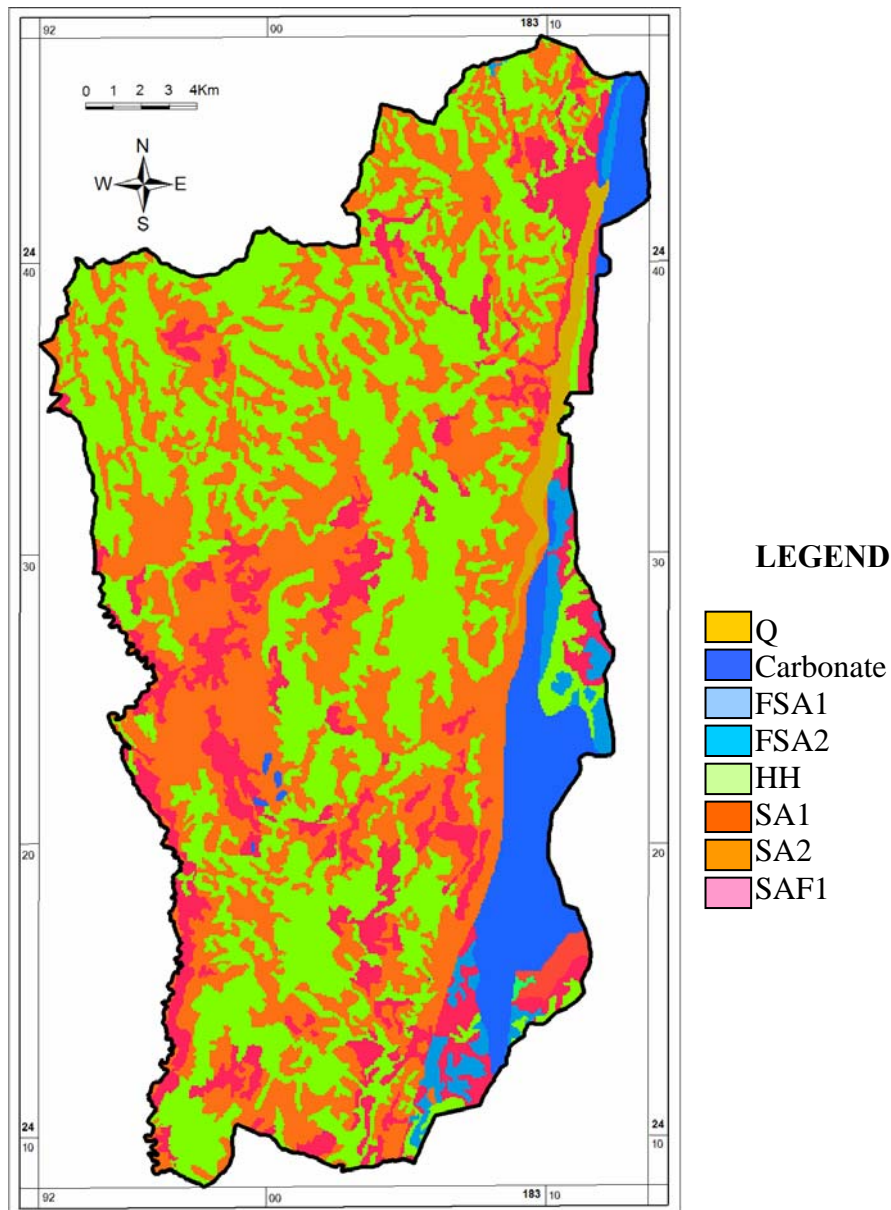


Figure 4-9. The Weathering crust map of Muong Lay area (*Source: Tuyet, 1999*)

Tropical climate in region with warm and wet climate influences the materials involved in land sliding and serves as the most common mechanism for their initiation. The rapid weathering of bedrocks under humid conditions creates a regolith generally weaker than the parent rocks. The presence of clay either inherited from parent sedimentary bedrocks or derived from weathering of metamorphic contributes to the tendency of soil masses to fail. The seasonal pattern of rainfall punctuated with intense storms serves as an efficient means for triggering landslide in this regional.

Some researches about weathering features in the province are subsequently briefly described:

Weathering phenomenon in Muong Lay province is controlled strongly by weathering elements. The most important elements are bedrock and terrain. At relief which elevation is lower than 800 m and has a slope degree less than or equal to 30° weathering process is almost continuously developed with high thickness, normally more than 5m (Tuyet, 1999).

Weathered crusts in research area are classified to weathered zones based on its chemical and mineral component of each zone (Figure 4-9). Based on the quantitative relation among three products of weathering process: SiO_2 , Al_2O_3 , Fe_2O_3 , five weathered zones were classified in to Feralit, Ferosialit, Sialferit, Sialit and Silixit. Furthermore, based on the quantitative relation among new mineral products of weathering process, five weathered zones were recognized: Gibbsite - Kaolinite, Kaolinite – gibbsite – hydromica or Kaolinite – gibbsite -hydromica (montmorilonite), Kaolinite–hydromica-gibbsite or Kaolinite - hydromica (montmorilonite) - gibbsite, Kaolinite-hydromica and Quartzite (Kaolinite, gibbsite). Nine major weathered crusts in the research area have been found in related to both weathered zones mentioned above

- Gibbsite – Kaolinite weathered zone corresponds to Feralit (FA)
- Kaolinite – gibbsite – hydromica weathered zone corresponds to Ferosialit (FSA1) while Kaolinite – gibbsite – hydromica (montmorilonit) corresponds to Ferosialit (FSA2).
- Similarly, Kaolinite-hydromica - gibbsite or Kaolinite - hydromica (montmorilonite) - gibbsite correspond to Sialferit (SAF1/SAF2).
- Kaolinite – hydromica corresponds to Sialit (SA).
- Kaolinite-hydromica relates to Silixit (SL).
- The mixing of Silixit with other weathering crusts as above is signed as HH.
- Quaternary weathering crust (Q)

Weathering process was observed mostly at weathered crusts which had thick and rich amount of clay content such as ferosialit (FSA) and sialferit (SAF1). These weathered crusts were created by the weathering products of metamorphic rock and magma. In particularly, weathering process is strongly developed at complicated weathered crust (HH) which is made from the mixing of Silixit with other weathered crusts. These types of weathered crust enhanced the intensive occurrence of landslide, which distributed at terrain lower than 800 m, with slope degree from 16° to 30° (Tuyet, 1999).

4.2.3. Geomorphological factor

Geomorphology is considered as an important factor related to landslide occurrence in the research area. Based on the analyses of the topological characteristics, geological structures, Neotectonic movements, and morphometries, eight geomorphologic units can be identified in the research area (*Tuyet, 1999*) (Figure 4-10).

Tectonic landforms (TD)

This type of landforms originates under the direct impact of faults. They are usually created on the wall with slope $>30^\circ$, oriented in a certain way, on the surface where sliding usually occurs closely related with the fault movements, depending on the amplitude of the movements between the blocks that create the corresponding surface. In the area of research this type has developed in the town of Muong Lay, the HuoiLeng, LuThang, develop along the faults. The identification of these landforms is very clear by straight dips or vertical slopes and prolonging slopes formed by fault. Quaternary age (Q) and the rock fall or topple usually develop.

Karst landforms (KD)

Karst landforms develop in a large area of approximately 100 km², distributed in Muong Lay town, developing along the south, southeast, along the NamMuc streams, following directions of sub meridian and from Mo villa to HongThu.

Karst landforms mainly from under :

- Peak cluster - depression karst with limestone base slopes, thin regolith cover at some places, Neogene-Quaternary age (N-Q).
- Tower karst with limestone base slope thin regolith cover at some places, Neogene-Quaternary age (N-Q).
- Doline, closed depression, valley in the peak cluster- depression area with changing regolith, formed in Quater (Q)
- Dolines, closed closed, valleys in tower karst area with regolith on the bottom, formed in Quaternary (Q).
- Collapsed dolines with breakdown rocks on the bottom, formed in Quaternary (Q)

Karst landforms often formed high topography in fields and development of the system of cave, hole, valley, systems carren, and microcarren. These landforms have vertical slopes, scarps and steeps. Here often topple and rock fall type is found.

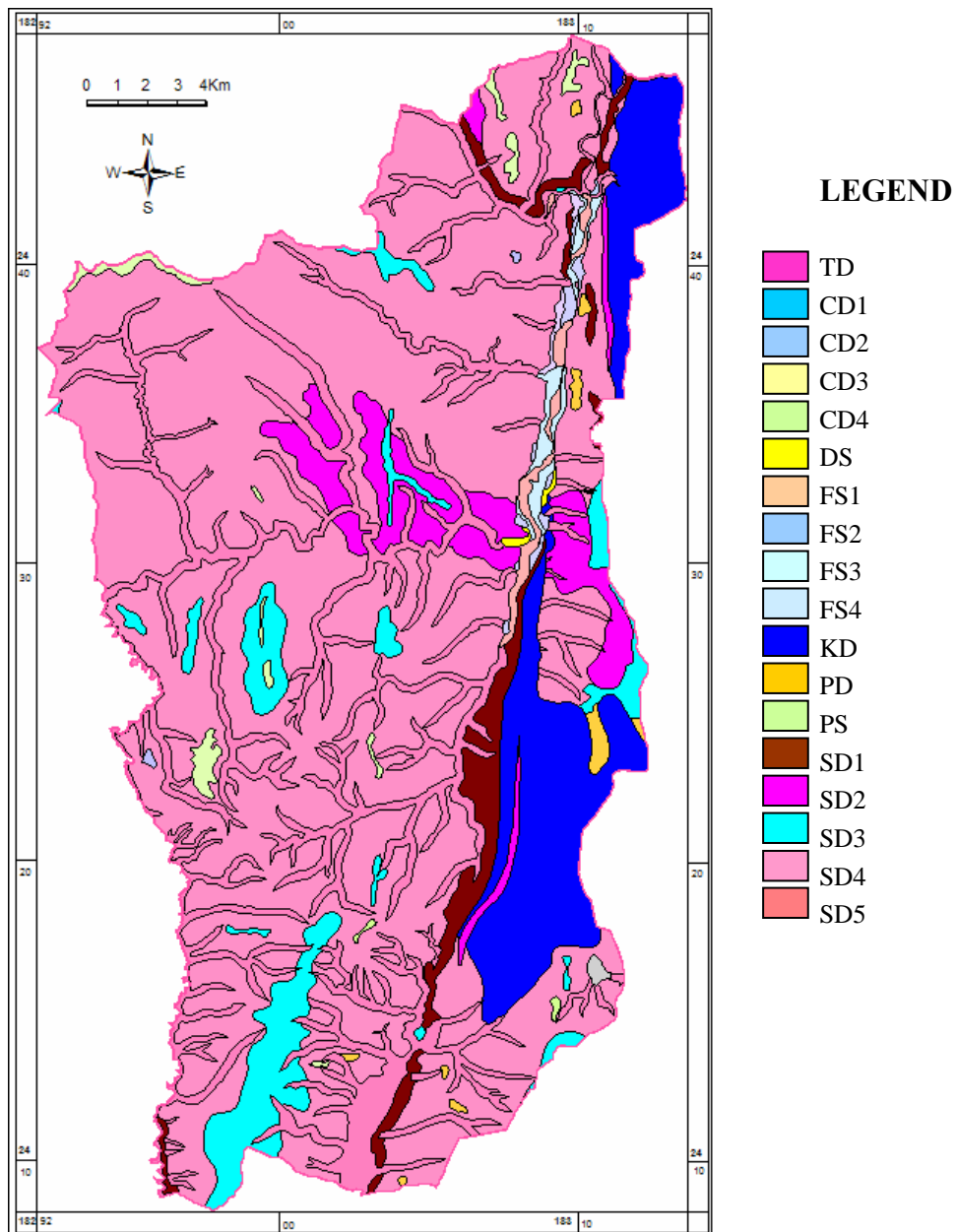


Figure 4-10. The Geomorphologic map of Muong Lay area (*Source: Tuyet, 1999*)

Denudation landforms

a- Plateau Surfaces

In the research area exist 4 levels surface (CD1, CD2, CD3 and CD4). The surface area available in the research is under exploitation style origin of denudation, distributed in several different levels, with small area, and distributed on the high-level is very fluctuation:

- CD1: Plateau Surfaces in high-level 400-600m.
- CD2: Plateau Surfaces in high-level 700-1000m
- CD3: Plateau Surfaces in high-level 1000-1600m.
- CD4: Plateau Surfaces in high-level > 1600m.

b- Denudation slopes

- SD1: Denudation slopes developed on terrigenous rocks, Neogene-Quaternary age (N-Q), with dip: $>30^\circ$, $30^\circ-20^\circ$, $< 30^\circ$
- SD2: Denudation slopes developed on horizontal or gentle lying terrigenous rocks, Neogene-Quaternary age (N-Q), with dip: $>30^\circ$, $30^\circ-20^\circ$, $< 30^\circ$
- SD3: Denudation slopes developed on metamorphic rocks, Neogene-Quaternary age (N-Q), with dip: $>30^\circ$, $30^\circ-20^\circ$, $< 30^\circ$
- SD4: Denudation slopes developed on volcanic rocks, Neogene-Quaternary age (N-Q), with dip: $>30^\circ$, $30^\circ-20^\circ$, $< 30^\circ$
- SD5: Quaternary pediment (Q). This landform developed on permanent runoffs, material transfer and build along the flow, they often change their shape and size following the seasons.

Agglomeration landforms

Agglomeration landforms are related to the activities of runoffs. With permanent runoffs, they are the product of terraces different in height. With the impermanent runoffs, they are the product of the mix agglomerates, with lower of option, they distributed in the low local as the middle valley between the mountains, or agglomerates in the hill-foot. In the area of research are present the above types of landforms with different scales typical along the valley MuongLay from MuongTung to ChanNua.

- Owing to permanent runoffs

- FS1: Holocene floodplain (Q_2). They are low-ground of alluvial in riverside. This landform met in big rivers, distributed strings of discontinuous, 0.5-2m high. The materials of this landform often change by season. This landform is very fluctuant, only after a rainy season they have been disappeared, and the mainly material is cobble, gravel, sand, clay and powdered clay.
- FS2: Pleistocene terrace (Q_1). They are high-ground of alluvial in riverside, distributed along the big rivers where the effect of the water enough strength to transport materials and re-sediment. This landform is higher (about 4 - 6m) and less fluctuant than FS1. The powdered clay is usually higher. People often farm on this landform.
- FS3: Agglomeration terrace, level I, with a high from 4m to 15m, main material is cobble, gravel, sand, clay and powdered clay, the component is multi-mineral.
- FS4: Agglomeration terrace, level II, with a high from 20m to 30m, main material is cobble, gravel, sand, clay and powdered clay. The components with the same level and more often in laterit. This landform is affected strongly by the human activity.

- Owing to impermanent runoffs

- PS: Proluvi terrace. Products are sand foundation-stones, hogging clod cobbles, crushed stones with thickness 5-10m. This terrace is continuing to be eroded by new runoffs, floods, sand, pebbles, and gravel covering.

- DS: Deluvi terrace is encountered in the valley, in plats of agglomeration form foot and slope of hill. Different from proluvi terrace, materials of this type of topographical arrangement are more chaotic, with lower degree of roundish-grind. Its components are crushed stones, hoggins, sand, clay with thickness 0.5 - 7m.

4.2.4. Lineament density factor

Lineaments are the linear morpho-tectonic features of the terrain which include faults, fractures, ridges, major discontinuities etc (*Sarkar, et al., 1995*). In this work, lineaments were interpreted from Landsat 7 images during 1999-2000. The lineament density for each 20m by 20 m cell was computed using the line density analysis extension of the Lineament analysis software which created by Hung (2001) and was classified density in table 3-5 above.

Radbruch-Hall (1982) noted that highly faulted zones were areas of particularly high incidence of unstable slopes. Varnes (1984) concluded that the degree of fracturing and shearing played an important role in determining slope stability. Especially, neotectonics contributes to slope instability by fracturing, faulting, jointing and deforming foliation structures. The close relationship between tectonically zones and landslides in the central part of Vietnam was discussed in a previous work (*Văn, 2001*). Hence, fault density is taken into account as a causative factor for landslides in the research area.

Faults and lineament can be extracted from satellite imagery (Landsat TM) and the Muong Lay geological map, scale 1:50.000 (*Long, Khanh, 2008*).

The fault density is defined as the total length of faults per 1 km². Hence, the fault density map of Muong Lay is derived as follows:

- The total length of faults in each polygon is determined. Then the value of total fault length per surface area in each polygon is calculated and assigned to the attribute of each polygon.
- The map is converted into a raster map, and is resample and smoothly filtered into a raster map with the same pixel size of 20x20m as shown in Figure 4-11.

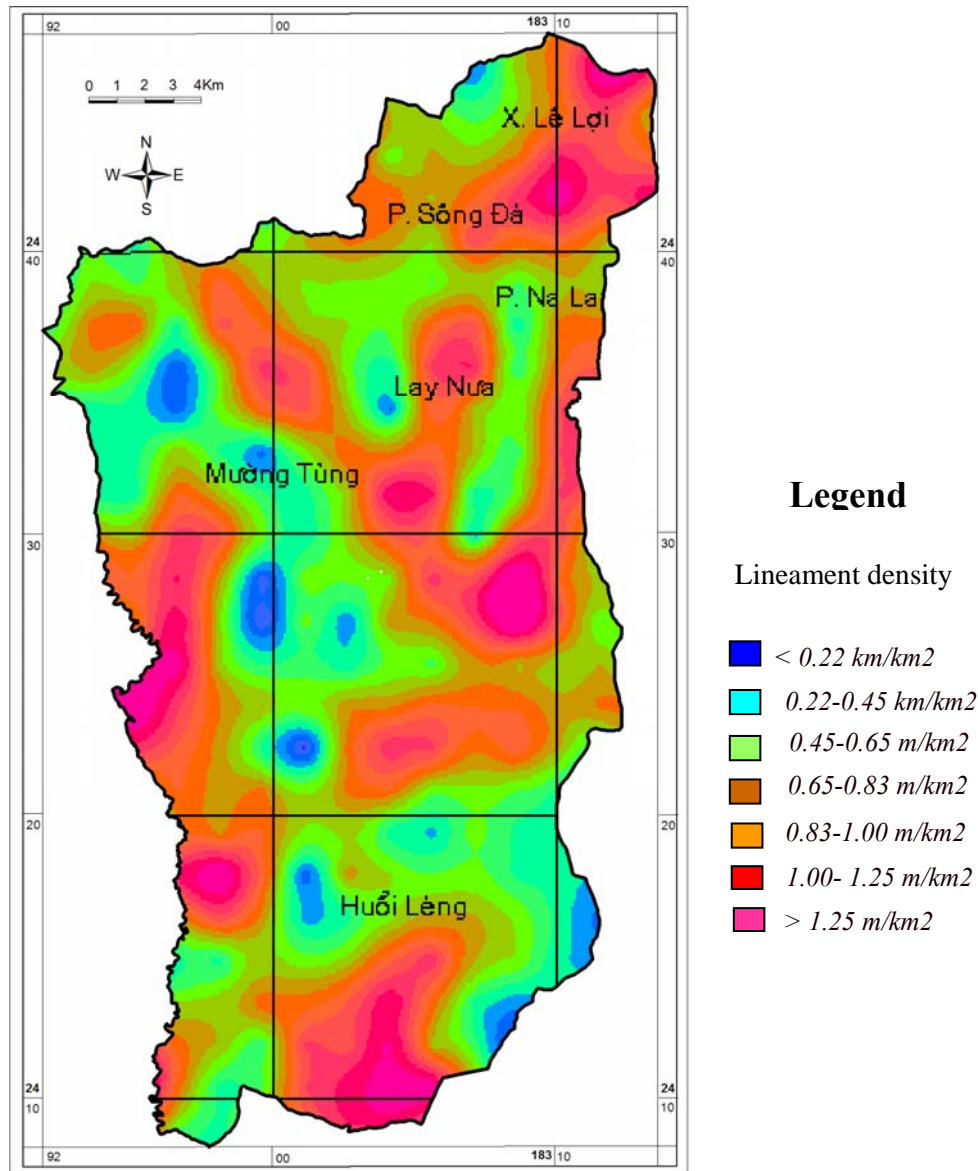


Figure 4-11. Lineament density map of Muong Lay

4.2.5. Elevation factor

Elevation's influences on landslides are often displayed as indirect relationships or by means of other factors. In the research area, the weathering factor plays an important role in land sliding in combination with deviation. Fridland (1973) used iron content to identify the depth of the weathering crust. At higher altitudes, strong hydrate reactions are present because of the higher humidity and consequently increase the amount of iron oxides. However, at high altitudes, more erosion occur leading to lesser weathering depth. Because the region has a tropical monsoon climate, where erosion and weathering processes are intense, they strongly affect the influence of elevation on landslides (Văn, 2001). Văn (2001) represented a close relationship between weathering crusts and altitude in the research area as follows:

- At an altitude range of 0 to 100 m the terraces that have developed contain Ferralite zones. The terraces can be rigid laterite rocks or dark brown ferriferrous soils.

- At an altitude range of 100 to 300 m there are mostly plain wave denudation terraces with low slope inclination. There are two common types of weathering crusts: (1) Sialferite on acid-neutral magma rocks, or (2) Ferosialite on other rocks.
- At an altitude range of 300 to 800 m there are medium dissected terraces, with abundant Ferosialite, Sialferite and less Sialite weathering crusts.

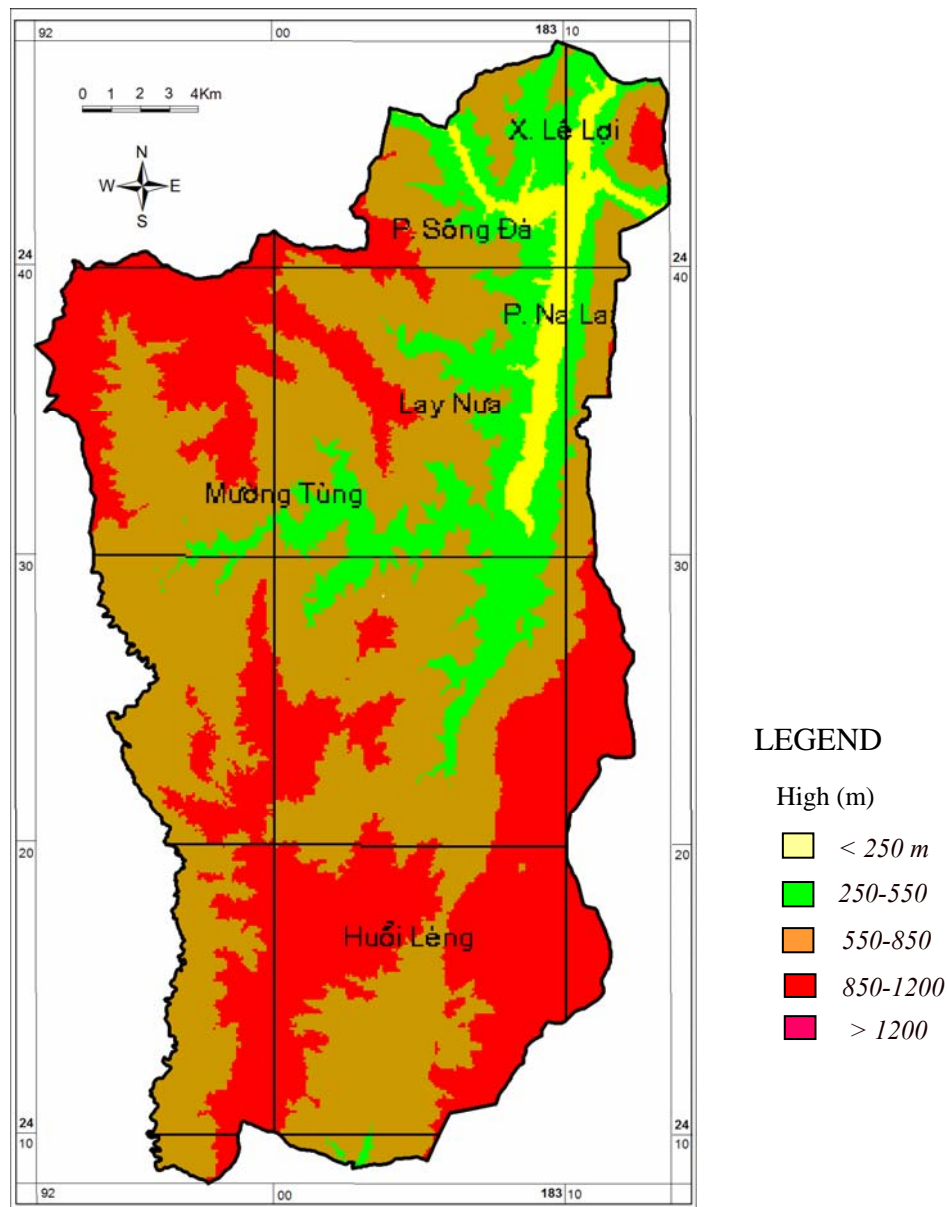


Figure 4-12. The elevation map of Muong Lay

- At an altitude range of 800 to 1800 m the topography is mountainous with fairly high dissections, and abundant weathering crusts of Sialite, Sialferite, and weak weathering zones. Sometimes, Ferosialite crusts exist on supermafic and mafic rocks. The weak weathering crusts usually exit on the steep and upper slopes. Sialite is always present on the surfaces of mountain tops, flat mountain shoulders, or acid-neutral magma rocks.

Therefore, the elevation factor is related to weathering and should be put into the model for landslide susceptibility mapping in Muong Lay.

In order to build a DEM of the research area, the topographic map with scale 1:50.000, from the Cartographic Publishing House, Vietnamese Ministry of Natural Resources and Environment of Vietnam, was digitized.

On the basis of polyline contours with intervals of 20m and altitudes ranging from 160 to 1980m, the DEM with a pixel size of 20 m by 20 m was derived by “Inverse distance” interpolation using the ILWIS3.0 software (Figure 4-12)

4.2.6. Slope degree factor

It is apparent that slope is the principle factor affecting landslide occurrence. The higher the slope, the greater the risk of landslide due to the higher shears induced by gravity. The slope map of Muong Lay is derived from the DEM using the slope function of ILWIS 3.0. The slope map is in the form of a raster map with the same pixel size as the DEM.

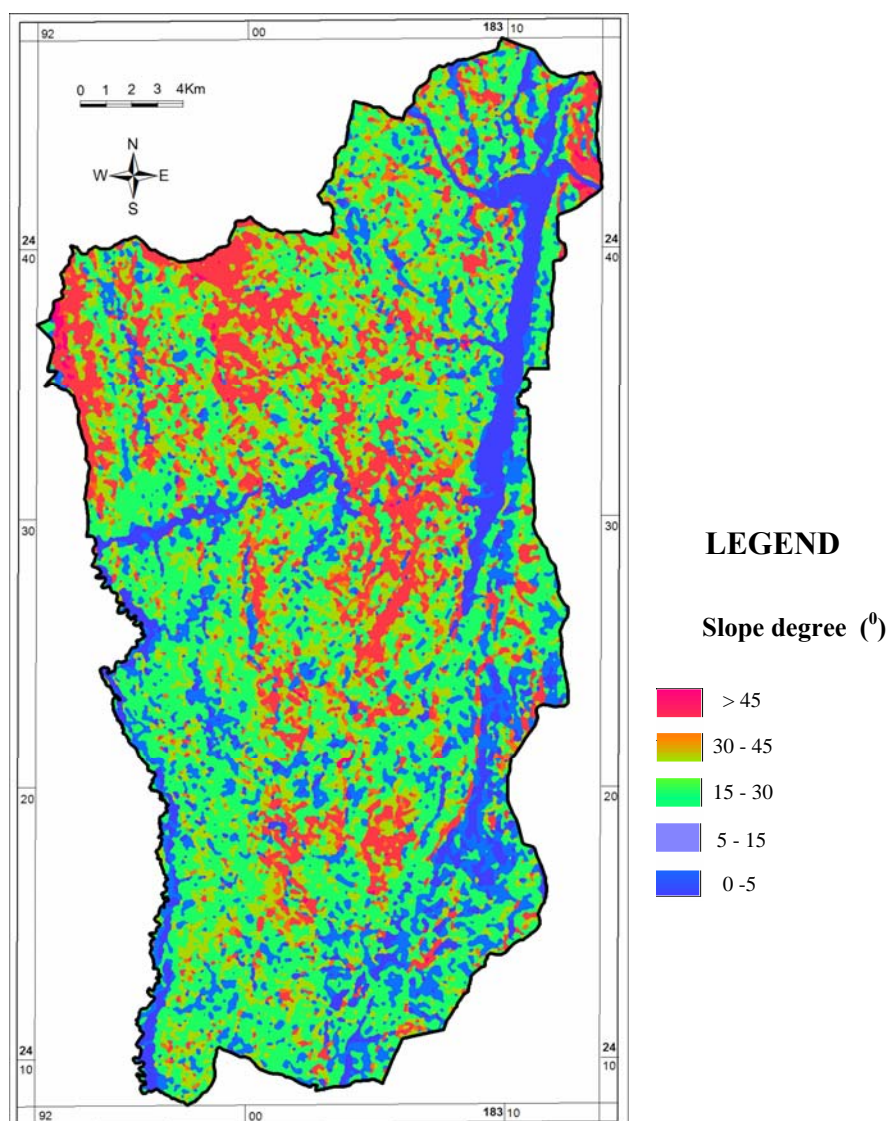


Figure 4-13. The map of slope classes in the study area

A map of slope classes is generated by separating the slope angles into six different classes (Figure 4-13): (1) flat-gentle slope ($<5^{\circ}$), (2) fair slope ($5-15^{\circ}$), (3) moderate slope ($15-30^{\circ}$), (4) fairly moderate slope ($30-45^{\circ}$), (5) very steep slope ($>45^{\circ}$).

Statistical analysis indicates that moderate slopes and fairly moderate slope are dominant (44.5%), and represent 65.2% of the landslide occurrence in the area. Very steep slopes occupy only 14.4%, and the landslide occurrence in this range of slopes is 21.3%. The area of flatgentle slopes is 21.5%, and landslides occurrence is only 2.1%. Fair slopes occur in 19.4% of the total area and the landslide occurrence reaches 11.2%. Figure 4-13 shows the percentage of different slope classes and the percentage of landslide occurrence in these classes.

4.2.7. Drainage density factor

Drainage density is defined as the ratio of sum of the drainage lengths in the cell and the area of the corresponding cell. Or Drainage density defined as the total length L of channels per unit area A (Long, Khanh, 2008).

$$D_d = \frac{L}{A} \quad (7)$$

Where: D - Drainage density (km/km²)
 L - The total length of rivers and streams (km)
 A - Unit area (km²)

The under-cutting action of the river may induce instability of slopes. Hence, some of the major drainage segments were digitized to include the effect of this causative factor and converted into raster format. The drainage density was computed considering a 20x20m by cell and classified with intervals as show in figure 4-14.

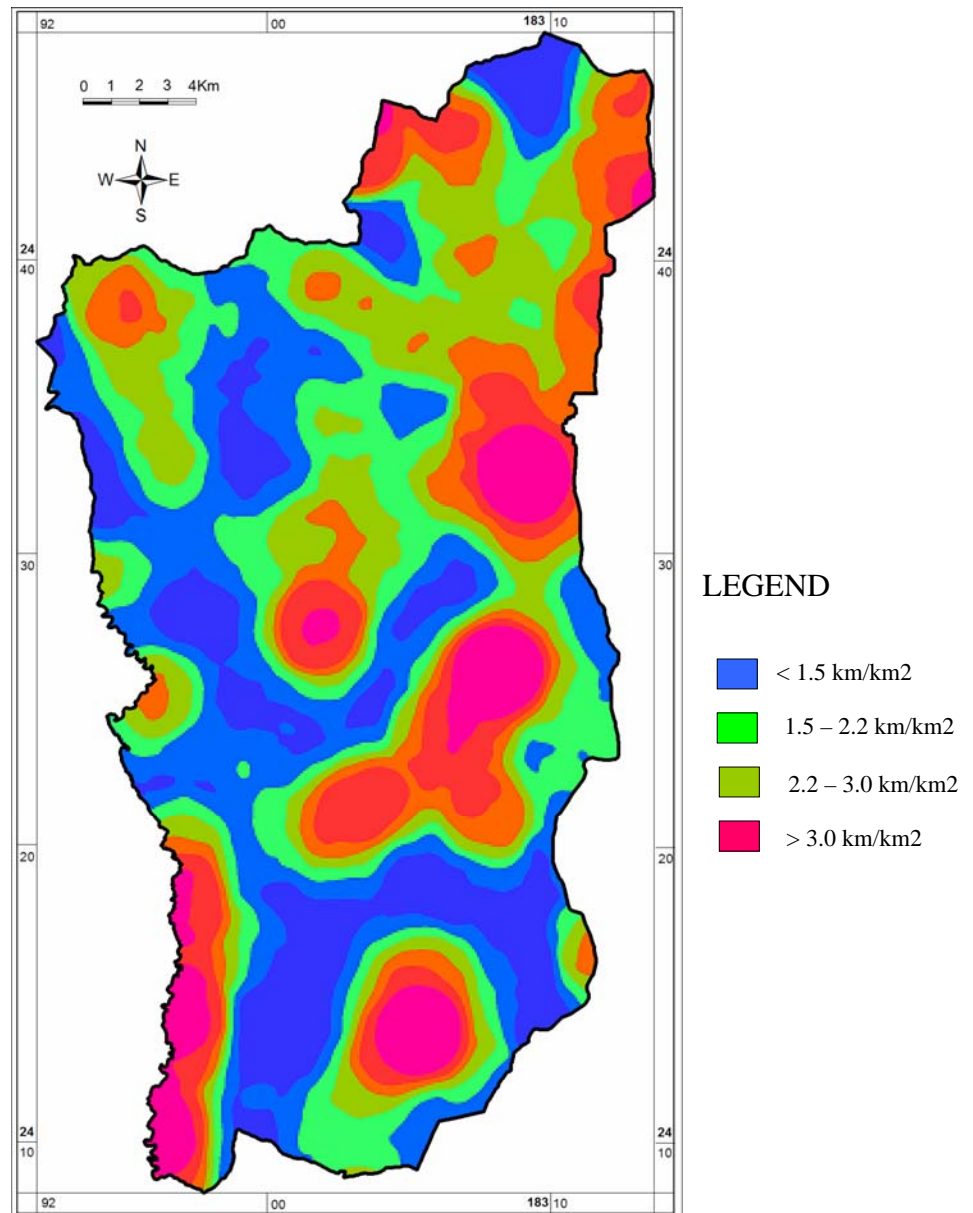


Figure 4-14. Drainage density map of Muong Lay

4.2.8. Landcover factor

In this study, a landuse map was derived from a LandSat TM image dated 20th February 1999 (Path/row: 125/48) covering the research area (Figure 1-3).

The landuse map is processed with the supervised classification method. The take samples and field check samples were taken by Long, Khanh (2008). The classification and image interpretation indicate that there are seven major landuse patterns in the region as shown in Figure 3-9, 3-10. The six types of landuse are: (1) water, (2) shrubs and bare hills, (3) agriculture area, (4) Young forests, and (5) Mixed forests, (6) Sustained forests. Afforested area is 27.2% of the forest total area, and mainly consists of *Acacia mangium* and *Acacia eucoliformic* trees. Paddy rice fields are dominantly in agriculture area. Shrubs and bare hills are dominant with 17.1% of the area. The natural vegetation has been

strongly altered by man-made activities as agriculture and timber production in recent years.

The large areas of shrubs and bare hills in the study region are very favorable for land sliding.

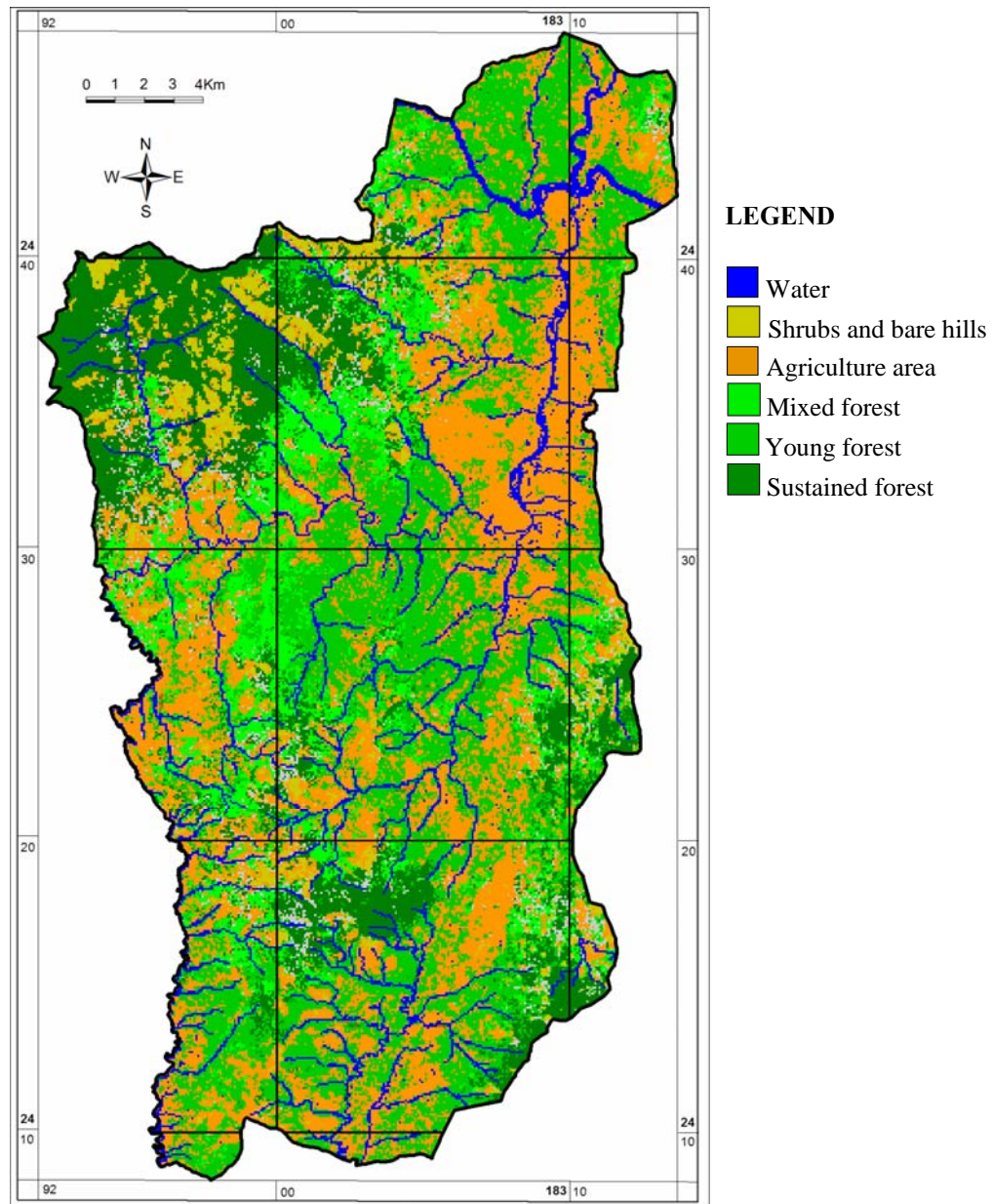


Figure 4-15. Landcover map of Muong Lay

4.2.9. Rainfall factor

The research area has been strongly incurred and affected by tropical monsoon climate and long rainy season. Therefore, it is very necessary to take rainfall into account as a factor input for the model of landslide susceptibility mapping. The data which used to calculated for rainfall map is average values of rainfall parameters around 10 years from hydrometeorology stations in Muong Lay, Lai Chau province and surroundings (Figure 4-16)

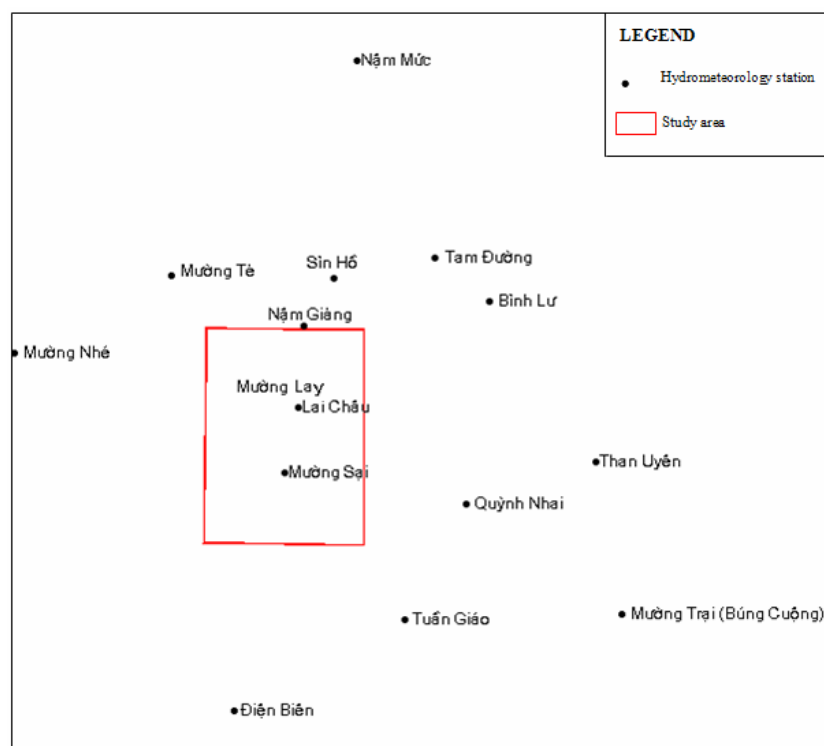


Figure 4-16. Location sketch of hydrometeorology stations in Muong Lay, Lai Chau province and surroundings

Table 4-4. The average annual rainfall of 14 hydrometeorology stations from 1996 to 2005 (10 years).

Stations	Province	X	Y	The average annual rainfall from 1996 to 2005 (mm)
Bình Lư	Lai Châu	103°37'	22°19'	2512.19
Mường Tè	Lai Châu	102°50'	22°22'	2540.75
Muong Lay (Lai Châu)	Lai Châu	103°09'	22°04'	2225.81
Tam Đường	Lai Châu	103°29'	22°25'	2441.70
Sin Hồ	Lai Châu	103°14'	22°22'	2856.68
Quỳnh Nhai	Sơn La	103°34'	21°51'	1744.06
Thân Uyên	Lào Cai	103°53'	21°57'	1893.32
Nậm Múc	Lai Châu	103°17'	22°52'	1634.23
Nậm Giàng	Lai Châu	103°09'34"	22°15'17"	2211.38
Mường Sại	Sơn La	103°07'	21°55'	1482.40
Mường Nhé	Lai Châu	102°27'	22°11'	2154.25
Mường Trại (Búng Cuộng)	Sơn La	103°57'	21°36'	2118.46
Điện Biên	Điện Biên	103°00'	21°22'	2076.23
Tuần Giáo	Điện Biên	103°25'	21°35'	2061.27

(X,Y: coordinate system of Longitude/Latitude)

Applied statistical method for rainfall mapping of study area

In this study area, the average year of rainfall map is established based on average martinet interpolation altered with the average weight calculation by inverse distance interpolation. This method is represented by mathematical formula follow:

$$Z_p = \frac{\sum_{i=1}^n Z_i W_i}{\sum_{i=1}^n W_i} \quad (4-1)$$

Where:

Z_p is value interpolated

Z_i is measurable value at position (x_i, y_i)

W_i is weight function

n is sampling points

Weight number of input points is calculated by weight function that gets defined according to inverse distance method. Where: the exponent selected of weight is 2. The resulting of interpolated map will inform raster with size of pixel is 20x20m.

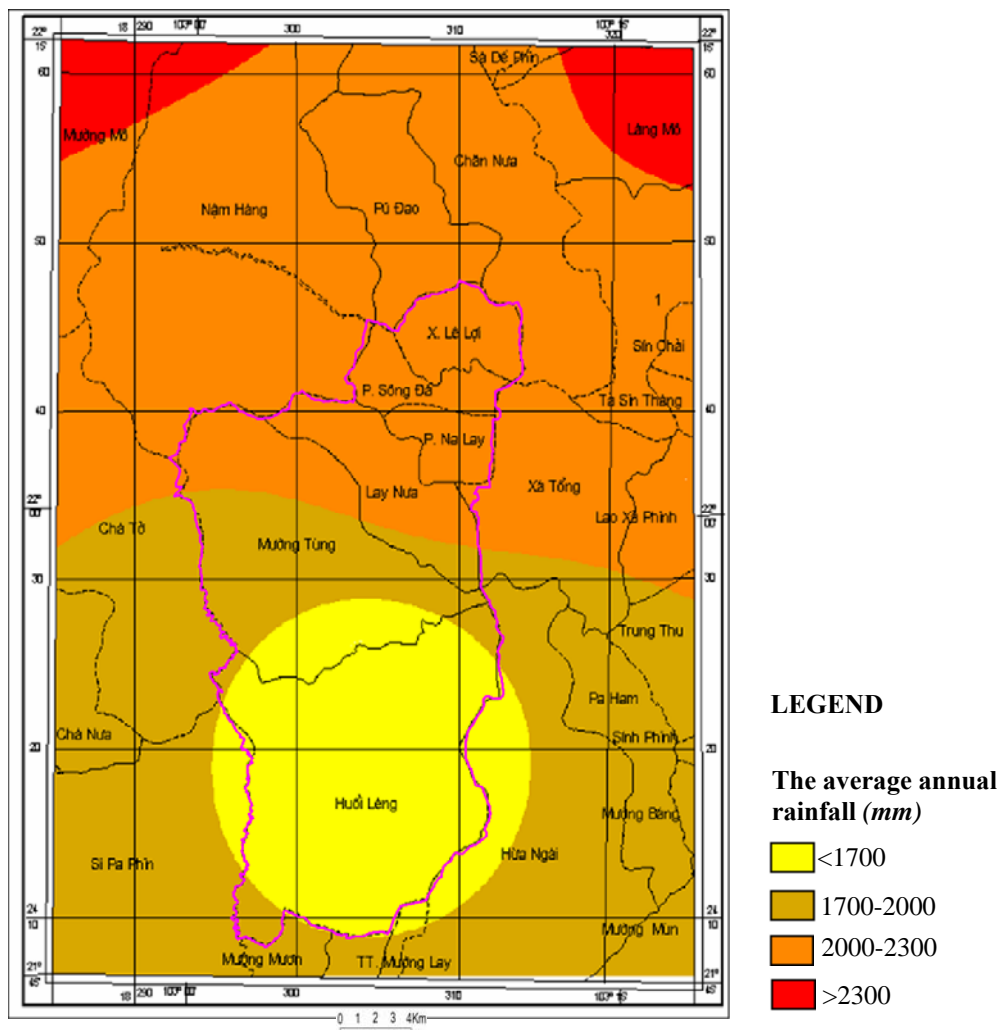


Figure 4-17. The map distributed rainfall average year of Muong Lay with monitoring period of 9 years (from 1996 to 2005)

For achieve the map distributed rainfall average year with monitoring period of 9 years (from 1996 to 2005) for research area, then map result of interpolated will remove the non-inbuilt component in the research area.

The distribution map of annual average rainfall is very important in landslide study and it will be the data input for important model classification for landslides of the research area.

The research area is in the tropical monsoon mountainous region and the distribution of rainfall is divided into some areas relatively clear. Therefore, in this study the total annual rainfall is divided into 4 classes based on reflecting the differences in terms of rainfall and climate of the research area. Figure 4-17 shows diagrams of the classes with total average rainfall in different time monitoring from 1996 to 2005 in the research area. The values of 4 classes: < 1700 mm/year, 1700-2000 mm/year, 2000-2300 mm/year, and > 2300 mm/year as shown in Figure 4-17

4.3. APPLICATION OF STATISTICAL ANALYSIS APPROACHES FOR LANDSLIDE HAZARD MAPPING IN MUONG LAY

4.3.1. Bivariate statistical and multivariate statistical approaches

Many different types of landslide hazard zonation techniques have been developed over the last decades (*Hansen, 1984; Varnes, 1984; Soeters, Van Westen, 1996; Aleotti, Chowdhury, 1999*). But generally speaking, landslide hazard zonation techniques can be subdivided into *direct* and *indirect* methods (Figure 4-18). In direct mapping the geomorphologies, based on his experience and knowledge of terrain conditions directly determines the degree of susceptibility directly. Indirect mapping uses either statistical models or deterministic models to predict landslide prone areas, based on information obtained from the interrelations between landslide conditioning factors and the landslide distribution. The increasing popularity of Geographic Information Systems over the last decades has lead to a majority of studies, mainly using indirect susceptibility mapping approaches (*Aleotti, Chowdhury, 1999*). GIS is very suitable for indirect susceptibility mapping, in which all possible landslide contributing terrain factors are combined with landslide inventory map, using data-integration techniques (*Chung, et al., 1995*). And Carrara (1983) introduced the so-called statistical approach for landslide hazard assessment, in which spatial factors can be successfully used for predicting landslide prone areas. This technique has been widely employed and has become one of the most popular approaches for landslide hazard assessment all over the world. The prominent features of the statistical analysis approach is its high efficiency, low costs, and better and more precise understanding of the relationships between the spatial factors used to identify the landslide-prone areas.

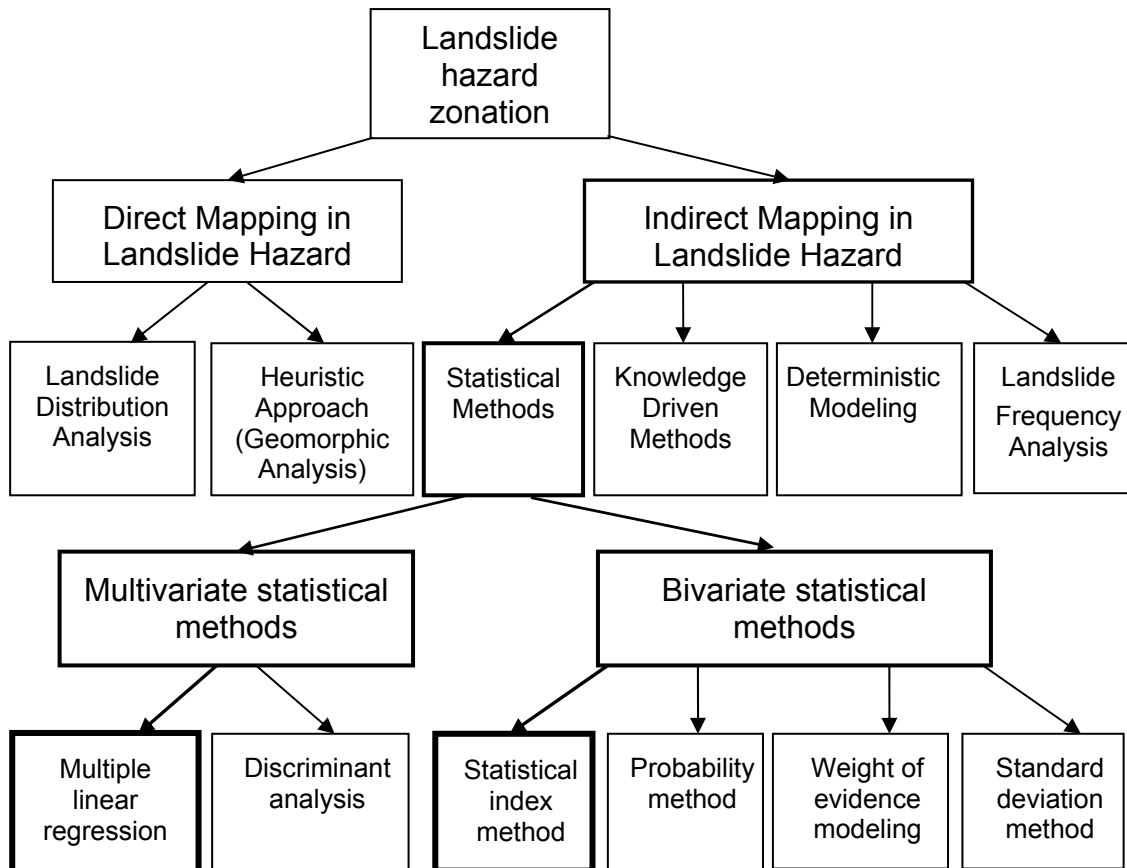


Figure 4-18. Flowchart of landslide hazard zonation techniques

The bivariate methods, as termed by Van Westen, Soeters, Rengers (1994), are a modified form of the qualitative map combined with the exception that weights are assigned based upon statistical relationships between past landslides and various factor maps; alternatively, these statistics can be used to develop decision rules (*Van Westen, et al., 1994*). Individual factor maps (independent variables) or combinations of factor maps (e.g. unique condition units) are overlaid with a landslide map (dependent variable) to develop cross tabulations for each factor and subclass. From this data, weights or decision rules are developed to be applied to each factor subclass. To use weights, normalized values are calculated and summed for a relative instability score that can then be classified. To use decision rules, specific combinations of factors are classified using a matrix of instability classes.

Recently, multivariate methods have been used for slope instability zonation. The prominent techniques used in multivariate methods are: multiple linear regression analysis (*Carrara, 1983*), discriminate analysis (*Carrara, 1983; Guzzetti, et al., 2005*), and logistic regression analysis (*Dai, et al., 2001; Süzen, Doyuran, 2004; Lee, et al., 2004*). When many factors are available, to reduce the number of variables and to limit their interdependence, principal component analysis (PCA) is an option (*Carrara, et al., 1991*).

In statistical landslide hazard analysis, the combinations of factors that have led to landslides in the past are determined statistically, and quantitative predictions are made

for areas which are currently free of landslides but exist similar conditions exist. Later on, many other statistical approaches have been derived and used in landslide analyses, which can be classified in two groups, i.e. *bivariate statistical method* and *multivariate statistical method* approaches

Bivariate statistical methods

In bivariate approaches, the core of the analysis is to determine the densities of landslide occurrences within each parameter map and its parameter map classes, and to derive data driven weights based on the class distribution and the landslide density (Süzen, Doyuran, 2004). With these weights parameter maps can be combined to obtain a landslide hazard map. In order to apply bivariate analyses, continuous parameter maps have to be converted into discrete (categorical) maps, in order to compute the corresponding weight of each class. However, such conversions still remain always unclear in the literature as most of the author uses their expert opinion for dividing them into classes (Van Westen, 1993; Soeters, Van Westen, 1996).

Moreover, the result of bivariate analysis methods also depends on the selection of parameters or causative factors for landslide instability. This is also an important subjective element in the method. For a bivariate statistical approach, maps of medium scale are most appropriate, in the range of 1:25000 to 1:500000, because the technique is not detailed enough to be applied on a larger scale.

In bivariate statistical analysis the dependent variable (in this case the occurrence of mass movements) is compared to each causal factor separately and the importance of each factor is determined independently from the other factors. Specific combinations of factors can also be tested by using a combination map as a new variable. Hence, the technique is based on the assumption that the important factors leading to mass movement can be quantified by calculating the density of mass movements for each variable class, or by combining various parameter maps into a new map, which is then overlaid by the landslide map to give a density per each unique combination of input parameters. There are several ways by which such analyses can be performed as discussed in Figure 4-19.

In the first phase of landslide susceptibility analysis, the statistical index method proposed by Van Westen et al. (1997) was employed under a GIS environment. This method is exactly a bivariate statistical analysis for landslide susceptibility analysis. Other researchers (Cevik, Topal, 2003; Oztekin, Topal, 2005) also applied this technique and termed it statistical index method.

BIVARIATE STATISTICAL ANALYSIS

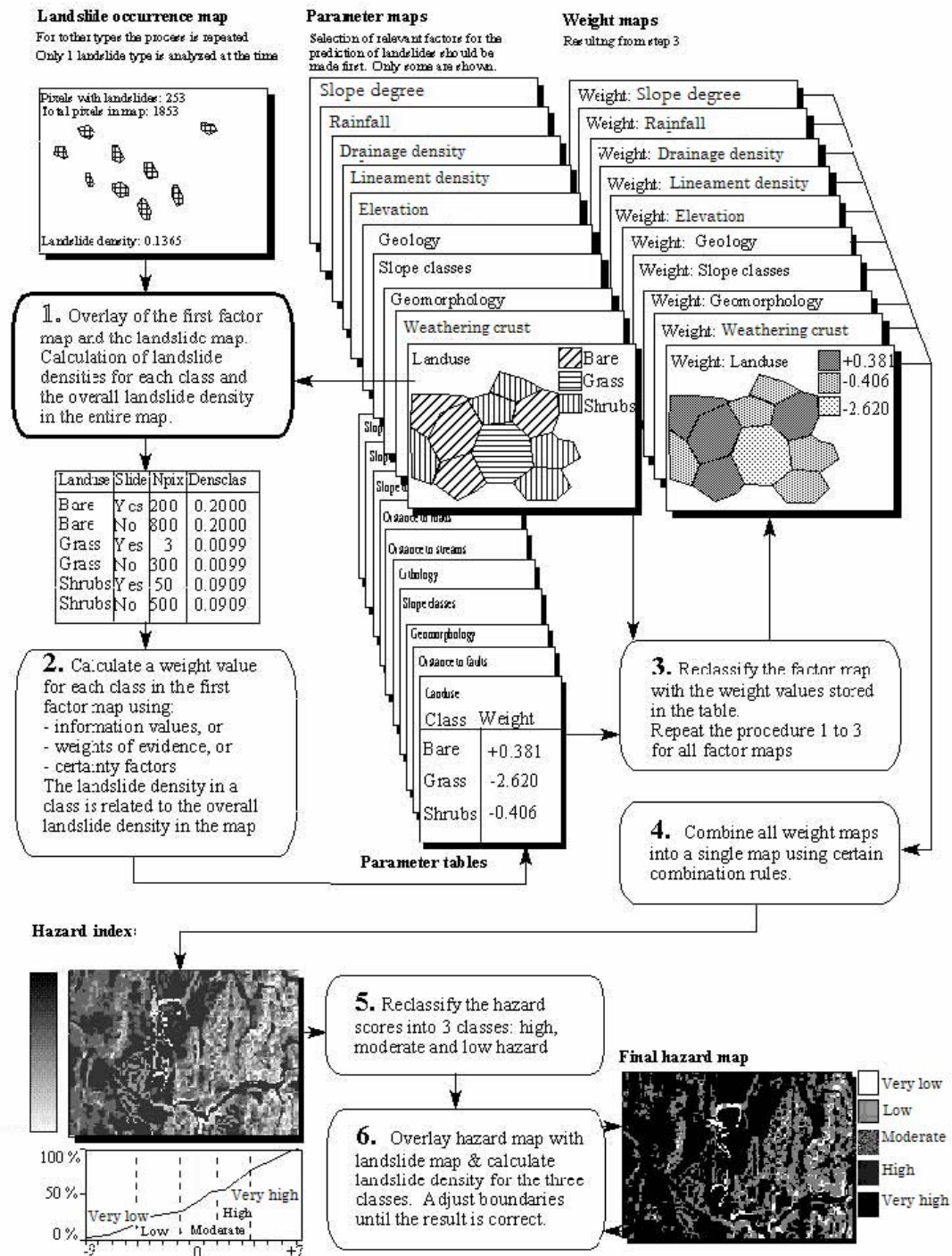


Figure 4-19. Simplified flowchart for bivariate statistical analysis (adopted from Westen 2003)

Multivariate statistical methods

Multivariate statistical analyses of causal factors controlling landslide occurrence may indicate the relative contribution of each of these factors to the degree of hazard within a defined land unit. These analyses are based on the presence or absence of stability phenomena within the units (*Van Westen, 1993*).

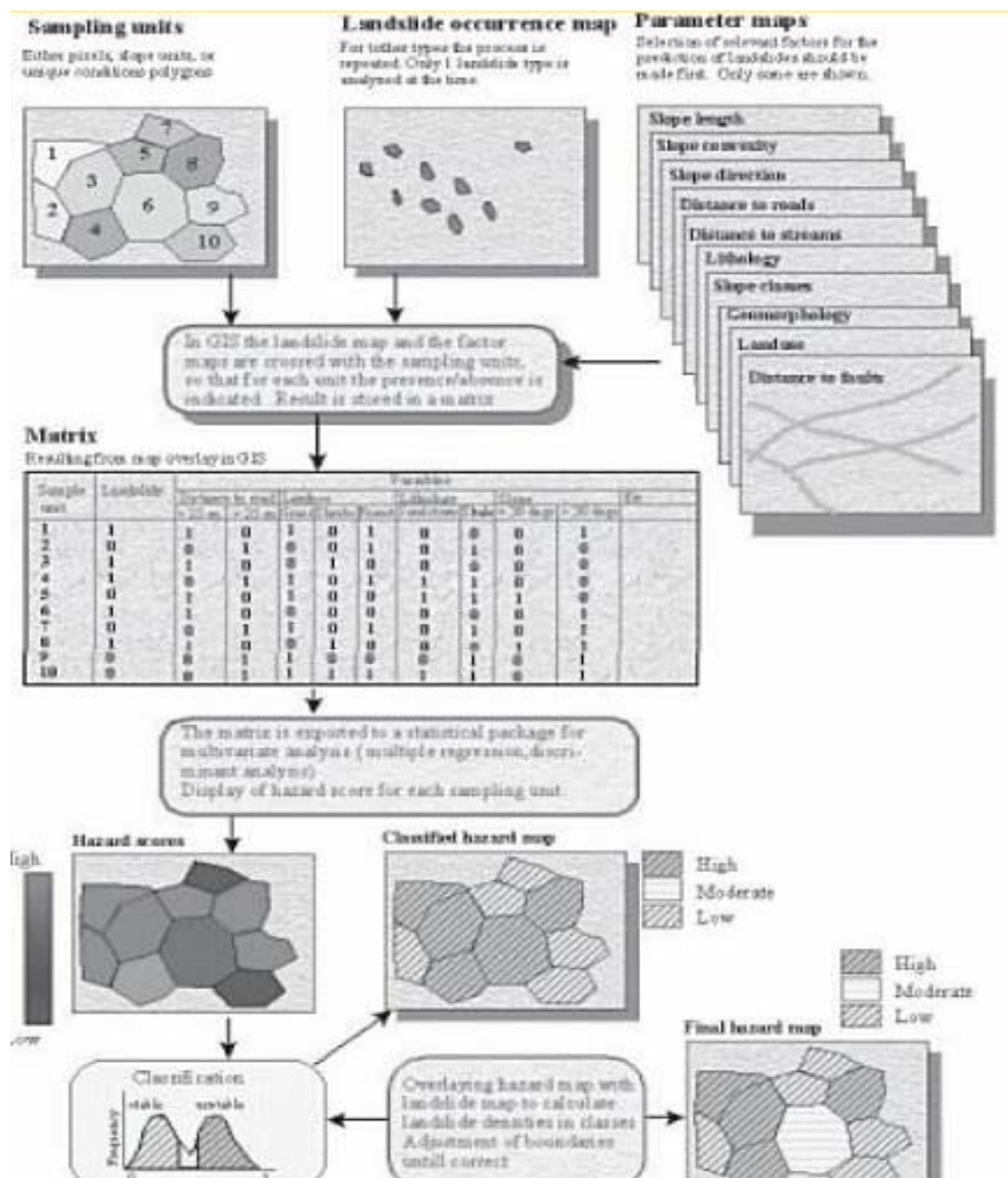


Figure 4-20. Multivariate statistical analysis Flowchart (adopted from Van Westen 2003)

Multivariate statistical analysis models for landslide hazard zonation were developed in Italy, mainly by Carrara (1983) and his colleagues (*Carrara, et al., 1991*). In their applications, all relevant factors are sampled either on a large-grid basis or in morphometric units. For each of the sampling units, the presence or absence of landslides is also determined. The resulting matrix is then analyzed using multiple regression or

discriminate analysis. With these techniques good results can be expected in homogenous zones or areas with only a few types of slope instability processes. When complex statistics are applied, as was done by Carrara (1983) and his colleagues (Carrara, *et al.*, 1991) subdivision of the data depending on the type of the landslide should be also made as well. Therefore, large data sets are needed to obtain enough cases to produce reliable results. The use of complex statistics implies laborious efforts in collecting large amounts of data, because these methods do not use selective criteria based on professional experience. Multivariate statistical analyses of important factors related to landslide occurrence give the relative contribution of each of these factors to the total hazard within a defined land unit. The analyses are based on the presence or absence of mass movement phenomena within these land units, which may be catchment areas, interpreted geomorphic units, or other kinds of terrain units.

The following GIS procedures are commonly used in multivariate statistics for landslide hazard zonation:

1. Determination of the list of factors that will be included in the analysis. As many input maps are of alphanumeric type, they should be normally converted into numerical maps. These maps can be converted into several maps with presence/absence values for each land unit, or one map with values as the percentage cover of each parameter class or expert values according to increasing observed landslide density.
2. Conversion of the observed landslide map into a numerical map by attributing the value 1 to observed landslide areas and the value zero to the other areas.
3. Export for each pixel of the map the different numerical values to a statistical package for subsequent analysis.
4. Import of the estimated results into a raster map.
5. Classification of the map into hazard classes.

Two types of multivariate analyses with names are: *multiple linear regression* and *discriminate analysis*.

In this study, the author mainly used statistical analysis methods for landslide susceptibility mapping in Muong Lay. There are many similar methods in upper methodologies. Thus, the author selected two methods to predict the landslide hazard for the research area: Multivariate statistical method and Bivariate statistical method (Statistical index method and Multiple linear regression method). Therefore, only the **Statistical index** method and **Multiple linear regression** method are described in this section.

4.3.2. Statistical index method for landslide susceptibility

In the statistical index method, a weight value for a parameter class, such as a certain geological unit or a certain slope class is defined as the natural logarithm of the landslide density in the class divided by the landslide density in the entire map (Van Westen, et al., 1997). The formula given below forms the basis of this approach:

$$w_{ij} = \ln \left(\frac{\text{Densclass}}{\text{Densmap}} \right) = \ln \left(\frac{D_{ij}}{D} \right) = \ln \left(\frac{\frac{Npix(Si)}{Npix(Ni)}}{\frac{\sum_{i=1}^n Npix(Si)}{\sum_{i=1}^n Npix(Ni)}} \right) \quad (4-1)$$

Where,

W_{ij} - The weight given to a certain class i of parameter j .

D_{ij} - Densclass - The landslide density within the class i of parameter j .

D - Densmap - The landslide density within the entire map.

$Npix(Si)$ - Number of pixels that contain landslide in a certain parameter class.

$Npix(Ni)$ - Total number of pixels in a certain parameter class.

$\sum Npix(Si)$ - Total number of landslide pixels.

$\sum Npix(Ni)$ - Total number of studied parameter pixels.

Hence, the statistical index method is based on the statistical correlation of the landslide inventory map with attributes of different parameter maps. The W_{ij} value in equation 4-1 is only calculated for classes that have landslide occurrences. In the case of no landslide occurrences in a parameter class ($\ln 0 = -\infty$). Therefore, the W_{ij} will be the arbitrary value -2.000 as filler (Ashis, 2004; Yalcin, 2007). This also means that the parameter class with no landslide occurrences will have no correlations with the landslide inventory. Hence, it has no influence on the calculation of the landslide susceptibility index.

In this study, every parameter map is crossed with the landslide inventory map, and the density of the landslide in each class is calculated.

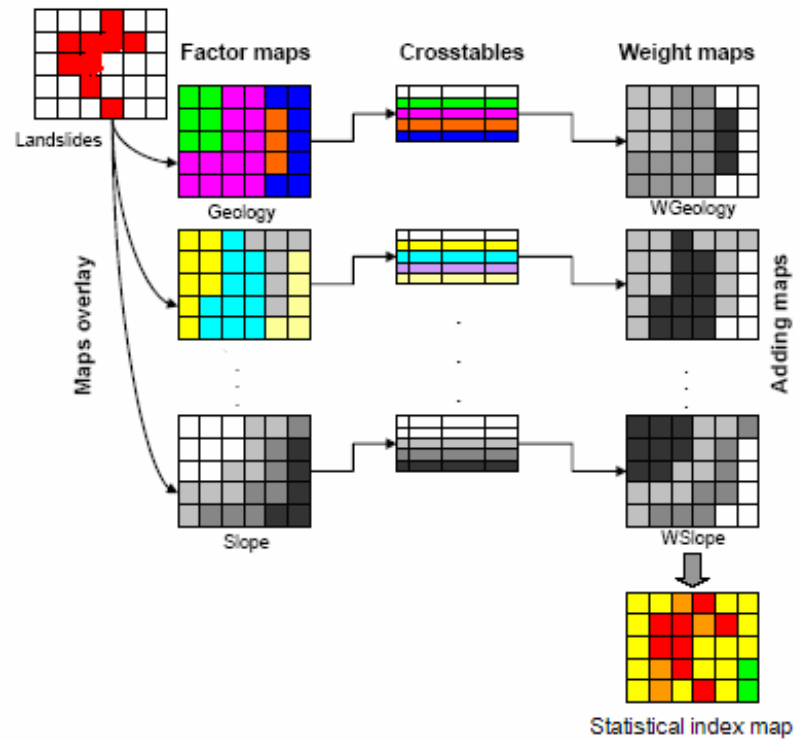


Figure 4-21. Schematic representation of statistical index method implemented in GIS.

4.3.3. Multiple linear regression method for landslide susceptibility

One of the most common and well-known multivariate statistical methods used in landslide zonation is multiple linear regression. It is used to correlate landslide causative factors with mass movements, usually according to a linear equation. Hence, the multiple linear regression model is given by:

$$Y = b_0 + b_1X_1 + b_2X_2 + \dots + b_nX_n \quad (4.3.3)$$

Where the dependent variable Y represents the presence (1) or absence (0) of observed landslides and the variables X_j are the causative factors. It can also be expressed as the percentage of a terrain unit covered by landslides. The variables X_1 - X_n are the independent variables, such as slope class, geological units, etc. the symbols b_0 - b_n are the partial regression coefficients. The standardized partial regression coefficients, which are the partial regression coefficients expressed in units of standard deviation, indicate the relative contribution of the independent variables to the occurrence of landslides (Davis, 1986). The following statistics are used to evaluate the result of a calculation. The details of the regression analysis are given in Figure 4-21, 4-22.

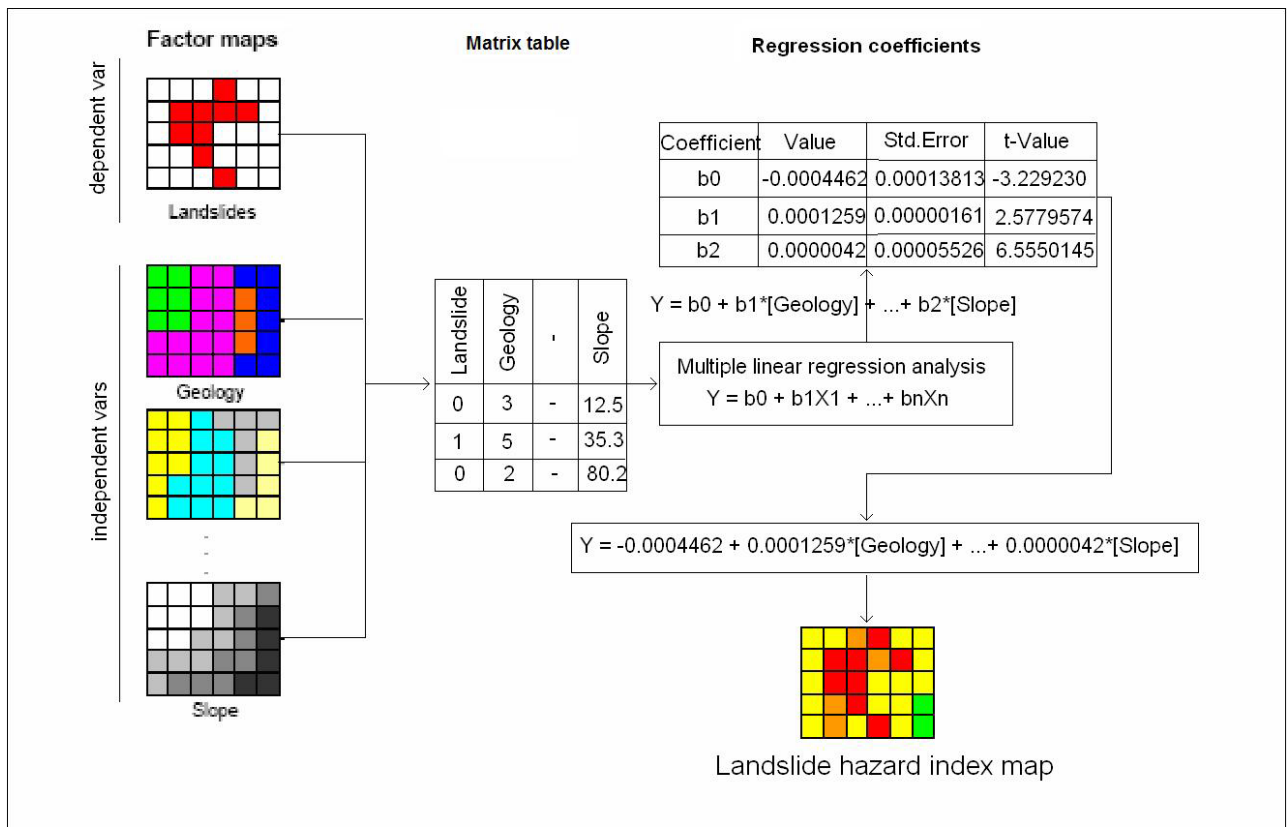


Figure 4-22. Schematic representation of multiple linear regression method implemented in GIS.

The standardized regression coefficients or t-values, which are the regression coefficients expressed in units of their standard deviation, indicate the relative contribution of each causative factor to the occurrence of landslides (*Davis, 1986*) and allow deciding whether a certain factor has a significant contribution in the equation.

CHAPTER 5.

RESULTS AND DISCUSSTION

In statistical analysis of landslide hazard, the combination of factors that have led to landslides in the past are statistically determined and quantitative prediction is made for current zones of landslide areas where similar conditions to landslide factors exist. In our model, each landslide occurrence is converted to raster cells, one pixel which has size: 20m × 20m.

5.1. ANALYSIS RESULTS OF STATISTICAL INDEX METHOD

5.1.1. Weighted factors

5.1.1.1. *Weighted factors of slope degree*

Slope is a very important factor for landslide study. If the slope is higher then there is a chance of landslide occurrence. The slope degree cumulative curve demonstrates that landslides are found mostly at slopes ranging from 5° to 45° within the research area (Figure 5-1)

The five-slope interval ranking distinguished in the Muong Lay, no landslide occurrences were found to originate on DEM derived slopes under 5° which are located on the valleys of area (figure 5-1). Thus the susceptible level to landslides of this ranging slope is >5%. The slope interval ranging from 5° to 15° also facilitates the frequency of landslide with the susceptibility level of 10.39 %. The slope interval ranging from 15° to 30° which covers 37.76 % of the research area has the susceptibility level to the occurrence of landslides of -0.0395. The slope (>45°) within this factor has the highest susceptibility level to landslide (0.1532), occupying only 12.24% of the total landslides occurred in the province. The second highest susceptibility level (34.61 %) which belongs to the slope interval ranging from 30° to 45° has the dangerous susceptibility level of 0.0522 to the occurrence of landslides.

Statistical Index value of this factor, ranging from -0.7369 to 0.1532, is computed in table 5-1. This high weight value of slope reveals that the occurrences of landslides are quite concentrated in some specific slope degree ranges.

Table 5-1. Distribution of landslide and susceptibility classes of slope degree

Slope degree class (°)	Nclass (pixel)	Nslide (pixel)	Dij (%)	D (%)	Wij
0-5	60	68952	2.40	5.01	-0.7369
5-15	265	143201	10.58	10.39	0.0186
15-30	909	520576	36.30	37.77	-0.0395
30-45	913	477124	36.46	34.61	0.0522
> 45	357	168672	14.26	12.23	0.1532
Sum	2504	1378525	100	100	

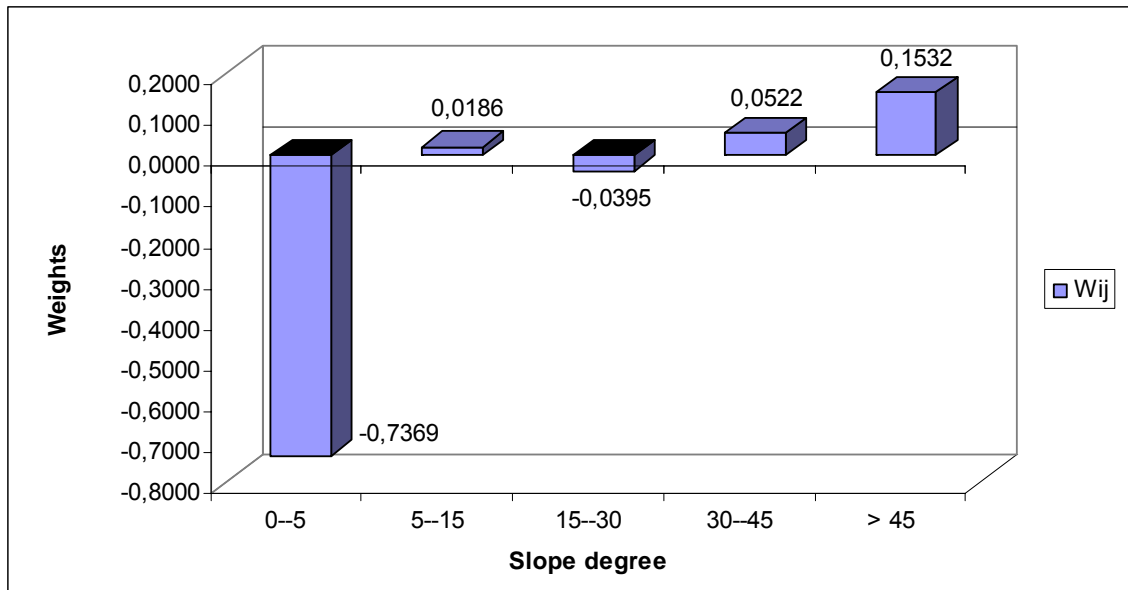


Figure 5-1. The weight index of each class of slope factor

5.1.1.2. Weighted factors of weathering crust

Weathering process is considered one of the important factors that impact the strength of soil and rocks. Among seven weathering crusts, HH, FSA1 and SA1 are found to be the most susceptible crusts which are significantly related to the occurrence of landslide in Muong Lay. These relationships can be recognized by the weathering cumulative curve between weathered crust factors and the landslide frequency (Figure 5-2).

This curve is very low at FSA2 and Q. It then strongly and creates a peak at HH. Beyond FSA1, this curve gradually increases again until SA2. The second significant remark on this cumulative curve is the peak that corresponds to SA1.

Table 5-2. Distribution of landslides and susceptibility classes of weathering crust

Weathering crust class	Nclass (pixel)	Nslide (pixel)	Dij (%)	D (%)	Wij
Limestone	145080	99	3.95	10.52	-0.9790
FSA1	39000	96	3.83	2.83	0.3039
FSA2	611	0	0.00	0.04	-2.0000 ^a
HH	507221	1042	41.61	36.79	0.1231
Q	19787	0	0.00	1.44	-2.0000 ^a
SA1	465483	898	35.86	33.77	0.0602
SA2	192839	369	14.74	13.99	0.0521
SAF1	8504	0	0.00	0.62	-2.0000 ^a
Sum	1378525	2504	100	100	

^a Arbitrary value as filler

The distribution of landslides and weathering classes is given in table 5-2. The susceptibility level weights of each class are then directly converted to weight values, representing for weighted class.

The clearest relationship between the landslide frequency and the susceptibility level of weathering crusts is illustrated in figure 5-2. Weathered kaolinite – gibbsite – hydromica and the mixing of silixit with other weathering crusts (FSA1 and HH) show the highest susceptibility level (0.3039 and 0.1231), covering 3.83 % and 41.61 % of the total area among the seven crusts. This is a reliable result as the more inhomogeneous the constituent is and the more instable the structure is, the easier the weathering process becomes. It is supported by the fact that HH is a complicated weathered crust which is created from the mixed weathering of morphologic rocks and clay sediments which are intermixed with rich quartzite sediments. Besides, most of the landslides are observed at this type of weathered crust. The SA1 area is presented by the second highest susceptibility value (35.86 %) which belongs to Kaolinite – hydromica corresponding to Sialit (SA1 and SA2). The remaining area (3.83 %) is distributed for three weathered crusts: Gibbsite – Kaolinite (FA), Quaternary (q), Kaolinite-hydromica-montmorilonit (SAF1) showing the highest frequency of landslides to these crusts, thus their susceptibility values are. Statistical Index value of weathered crust factor shows value from -2.0000 to 0.3039. The values -2.0000 of table are the arbitrary value as filler.

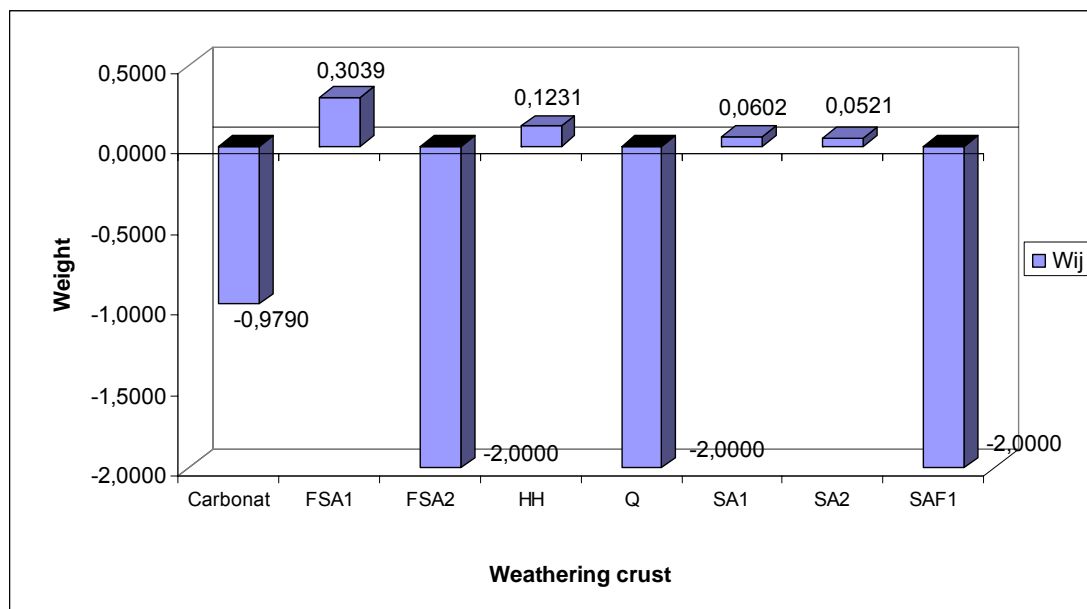


Figure 5-2. The weight index of each class of weathering factor

5.1.1.3. Weighted factors of geology

Likewise, an overview of the susceptibility level of each unit of geological factor and landslide frequency in the research area is illustrated through geological cumulative curve (figure 5-3). No landslide frequency is found at Quaternary units on this curve. This

cumulative curve strongly varies at two last geological units: PZ and AR-PR, showing the significant remark within geological factors. It also means that in this factor, landslide frequency is only concentrated in a few units of geological factors and does not occur in all units.

The relationship between the landslide frequency and the susceptibility level of geological units can be recognized by figure 5-3. Landslides are not observed at three geological Quaternary units: River – deposit Q(a). Hence, these units are zero (0%) and -2.000 in susceptibility level with the occurrence of landslide in research area. The highest susceptibility value (21.41%) is found on weathered products of Aluminosilicate sediments rocks (S_2-D_1nc) that consist of pebbles, cobbles, gravels, gritstones, sandstones, siltstones, claystones, carbonates, alternated rhyolites, dacites and andesite sediments, and tuffs. Almost of the three over fourths of all landslides happened in this unit, which indicates a certain reactivation and confirms the former landslide susceptibility. The remaining mass movements 0.7940 occurred in the weathered products of the *intrusive magma rocks* group: Granites, granosyenites, syenitdiorit, gabbro, gabbro-norite and dunite ($\gamma aT_3n pb$).

Table 5-3. Distribution of landslide and susceptibility units of geological factors.

Geological	Nclass	Nslide	Dij (%)	D (%)	Wij
aQ	18086	0	0.00	1.31	-2.0000 ^a
S_2-D_1nc	162020	536	21.41	11.74	0.5995
P_3ct	20371	37	1.48	1.48	-0.0001
D_1np	34414	62	2.48	2.50	-0.0082
$T_{2-3}lc$	180848	422	16.85	13.11	0.2505
$NPnc_2$	97040	304	12.14	7.03	0.5450
$\gamma aT_3n pb$	81623	328	13.10	5.91	0.7940
$P_{1-2}sd$	203135	176	7.03	14.75	-0.7403
$D_{1-2}bp$	135681	95	3.79	9.85	-0.9533
$T_3n-r sb$	179016	182	7.27	13.00	-0.5803
$J_{1-2}np$	51305	26	1.04	3.73	-1.2766
$\gamma \delta P_3-T_1 db$	214986	336	13.42	15.60	-0.1503
Sum	1378525	2504	100	100	

^a Arbitrary value as filler

Statistical Index values of geological factors show values from -2.000 to 0.7940. High values can be expected as only four units of geological factors that have significant impact on the occurrence of landslide among 12 units found in the research area (table 5-3)

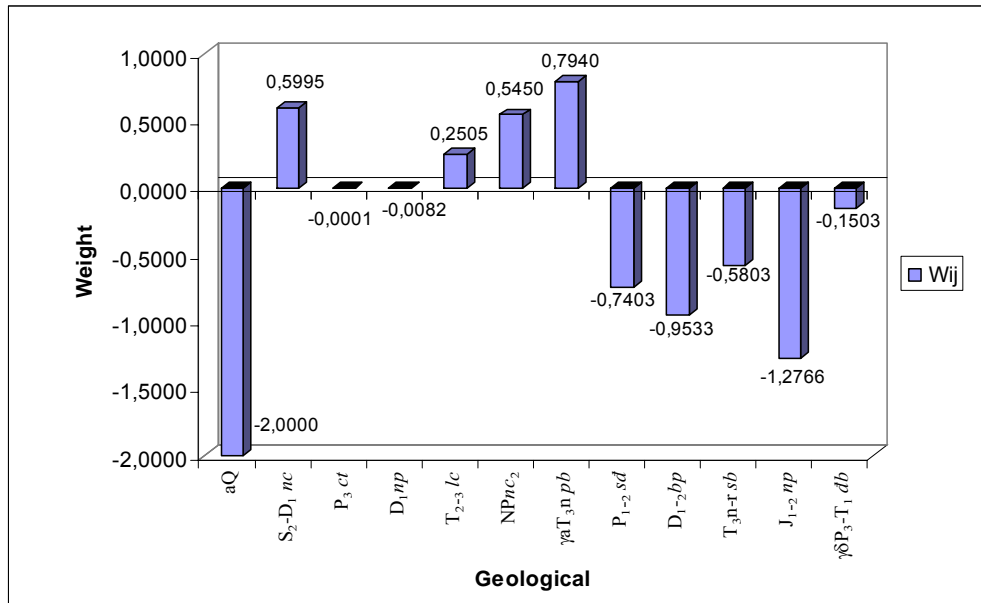


Figure 5-3. The weight index of each class of engineering geology factors

5.1.1.4. Weighted factors of geomorphology

Geomorphologic process is considered one of the important factors that impact the strength of soil and rock.

The distribution of landslides and geomorphologic classes is given in table 5-4. The susceptibility level percentage of each class is then directly converted to percentage value, representing the weighted class.

Table 5-4. Distribution of landslides and susceptibility classes of geomorphology

Geomorphology	Nclass	Nslide	Dij (%)	D (%)	Wij
TD	6788	0	0.00	0.49	-2.0000 ^a
CD1	3648	0	0.00	0.26	-2.0000 ^a
CD2	669	0	0.00	0.05	-2.0000 ^a
DS	1199	0	0.00	0.09	-2.0000 ^a
CD3	9225	6	0.24	0.67	-1.0270
CD4	794	0	0.00	0.06	-2.0000 ^a
FS1	8866	0	0.00	0.64	-2.0000 ^a
FS2	8719	0	0.00	0.63	-2.0000 ^a
FS3	4021	0	0.00	0.29	-2.0000 ^a
FS4	1882	15	0.60	0.14	1.4788
FS	182	0	0.00	0.01	-2.0000 ^a
KD	131740	109	4.35	9.56	-0.7864
PD	6253	0	0.00	0.45	-2.0000 ^a
PS	1208	0	0.00	0.09	-2.0000 ^a
SD1	39757	406	16.21	2.88	1.7267
SD2	60664	400	15.97	4.40	1.2892
SD3	72876	154	6.15	5.29	0.1513
SD4	799588	998	39.86	58.00	-0.3752
SD5	220446	416	16.61	15.99	0.0382
Sum	1378525	2504	100	100	

A clearest relationship between the landslide frequency and the geomorphologic susceptibility level is illustrated in figure 5-4. Denudation landforms (SD4) show the highest susceptibility level (39.86 %), covering 58.00 % of the total area among seven crusts. This is a reliable result as the more inhomogeneous the constituent is and the more instable structure is, the easier the geomorphologic process is. It is supported by the fact that SD1, SD2, SD3, SD4 are complicated weathered crust which is created from the mixture geomorphologic of morphologic rocks and clay sediments which are intermixed with rich quartzite sediment. Besides, most of landslides are observed at this type of weathered crust. About one tenth (9.56 %) of the area is presented by the second highest susceptibility value (1.4788) which belongs to FS4: agglomeration terrace, level II, with a height of 20m to 30m, main material are cobble, gravel, sand, clay and powdered clay.

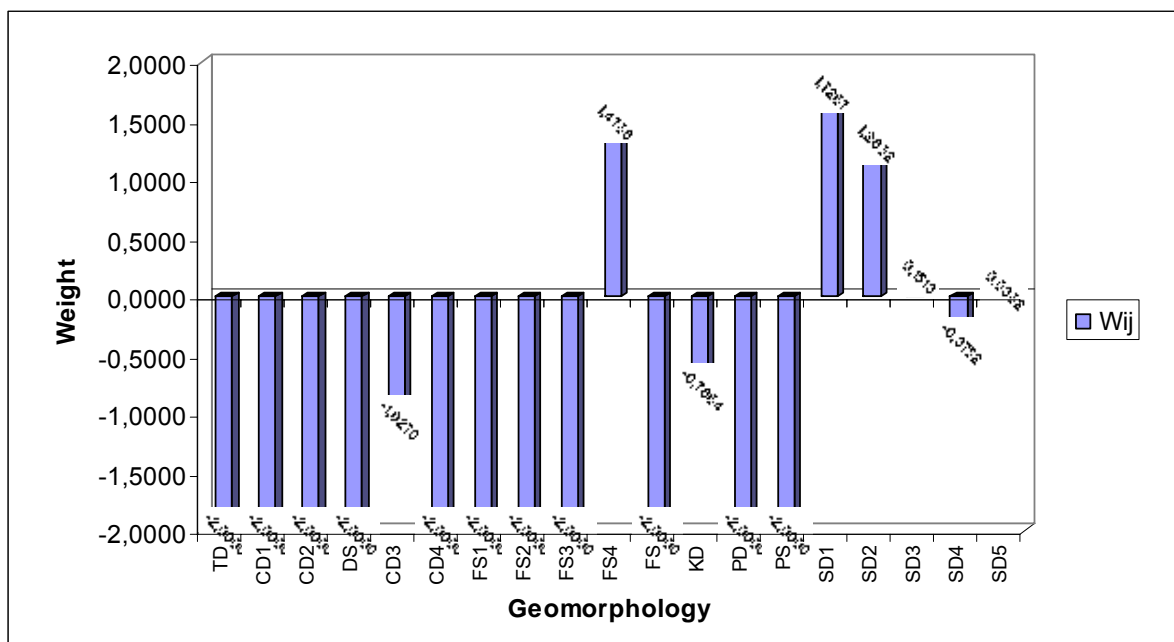


Figure 5-4. The weight index of each class of Geomorphological factors

Statistical Index values of weathered crust factors vary from -2.0000 to 1.7267. This value will be then discussed at the end of this section after comparing Statistical Index values of geological factors and the lineament density within factors related to strength of soil and rocks.

5.1.1.5. Weighted factors of lineament density

This is the last factor which represents for strength factors in this model. The cumulative curve (figure 5-5) demonstrates the relationship between the lineament density class and the landslide frequency as well as the susceptibility level of each class to landslides.

Results show that the highest susceptibility level (26.08%) was found at low lineament density class (0.65-0.83 km/km²) while the lowest susceptibility level (0.00 %) is presented by very low lineament density class (< 0.25 km/km²). Very strong lineament

density class (1.00–1.25 km/km²) is the second highest susceptibility level (0.0587) of landslide in the Muong Lay area. These irregular frequencies of landslide show that they were not much dependent on the tectonic activities in the research area. The sum of susceptibility levels from very low, low to moderate lineament density classes reveal that more than two thirds of total landslide frequencies occurred on these low ranks of lineament density classes. Since most of the lineament may represent fractures which might not move, this result is possible. However, the results also show that some tectonics may be still active in the research area. Their activities directly enhance the occurrence of landslide which is proved by the second highest value (20.09 %) corresponding to the very strong lineament density class.

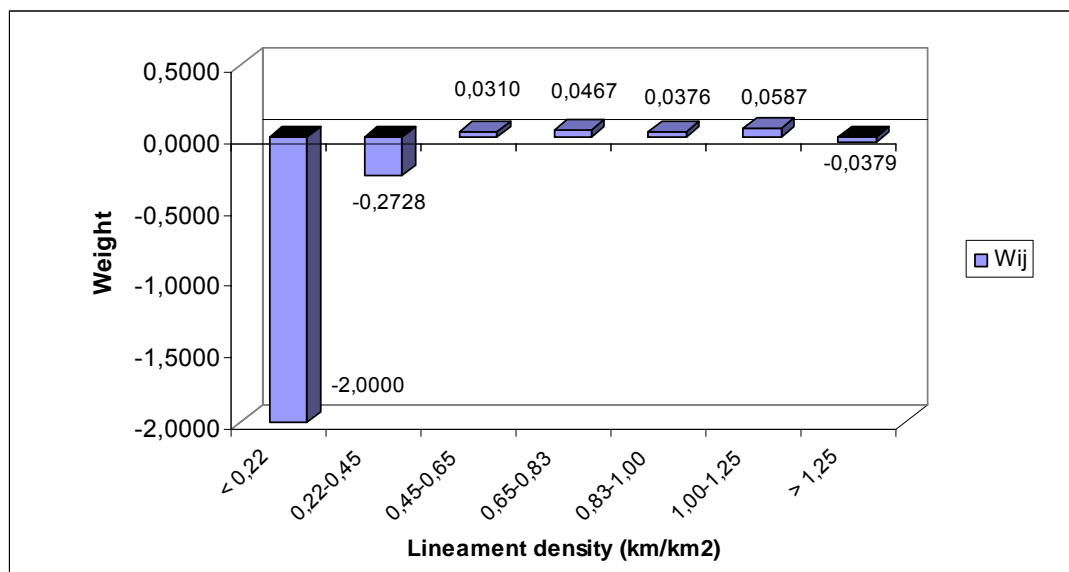


Figure 5-5. The weight index of each class of lineament density factors

Table 5-5. Distribution of landslide and susceptibility classes of lineament factors

Lineament density	Nclass	Nslide	Dij (%)	D (%)	Wij
< 0.22	9648	0	0.00	0.70	-2.0000
0.22-0.45	152588	211	8.43	11.07	-0.2728
0.45-0.65	309552	580	23.16	22.46	0.0310
0.65-0.83	343096	653	26.08	24.89	0.0467
0.83-1.00	266688	503	20.09	19.35	0.0376
1.00-1.25	212330	409	16.33	15.40	0.0587
> 1.25	84623	148	5.91	6.14	-0.0379
Sum	1378525	2504	100	100	

^a Arbitrary value as filler

Statistical Index values of this factor ranges from -2.000 to 0.0587 (Table 5-5). In comparison with standard deviation values of weathering crusts and geological factors, these standard deviation values show to be the lowest values among factors in strength factors group. It also reveals that the occurrence of landslide only concentrates on some

specific geological units in the research area. Therefore it has a significant role in the occurrence of landslides in general speaking.

5.1.1.6. Weighted factors of elevation

Similarly, the relationship between the elevation and landslide frequency is shown by the elevation cumulative curve (Figure 5-6). Landslide frequency is mostly found at mountainous and hilly regions where forests have been severely destroyed due to the deforestation of ethnic people. These regions are dominated by elevations ranging from <250m, 250-550m, 550-850m, 850-1200m and >1200m. This observation of landslide could be possible as forest still exists at high elevations and steep slopes where inhabitants have been prevented from logging as well as cultivating.

The highest susceptibility level (0.3865) of elevation factors belongs to the relief ranging from 250-550m (Figure 5-6). This elevation presents for the denotative topography which has the slope degrees ranging from gentle sloping ($5-15^{\circ}$) to moderate sloping ($15-30^{\circ}$). At lower elevations (less than 250 m) where the slope is less than 5° , no landslides occur therefore susceptibility level is the lowest among six terrain classes (2.84%). The susceptibility level to landslide is also high at elevation ranging from 550-850m, covering 33.83% of the total landslides. Very few landslides are found at elevations higher than 850m, only -0.3096.

Table 5-6. Distribution of landslide and susceptibility classes of elevation factors

Elevation	Nclass	Nslide	F (%)	F* (%)	Wij
<250	44797	71	2.84	3.25	-0.1363
250-550	236391	632	25.24	17.15	0.3865
550-850	407555	847	33.83	29.56	0.1346
850-1200	464691	654	26.12	33.71	-0.2551
>1200	225091	300	11.98	16.33	-0.3096
Sum	1378525	2504	100	100	

Table 5-6 gives statistical index values of elevation factors ranging from -0.3096 to 0.3865. It will be then compared with slope factors and discussed at the end of this section.

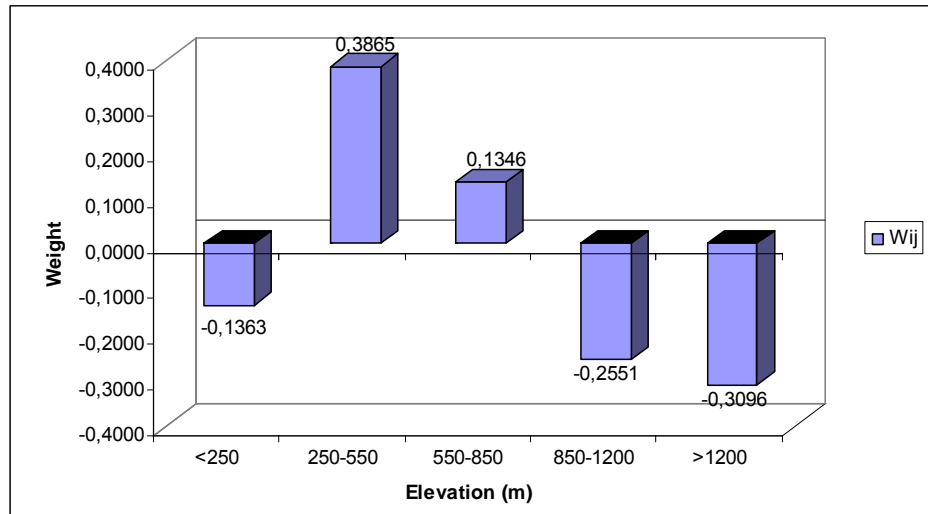


Figure 5-6. The weight index of each class of elevation factors

5.1.1.7. Weighted factors of drainage density

In our model, drainage density is chosen among hydrogeologic factors related to the occurrence of landslides. An overview of the relationship between landslides and the susceptibility level of each drainage density interval class is illustrated by the drainage density cumulative curve (Figure 5-7). As shown from this curve, landslides occurred in nearly all of its classes with different impact to each class. This occurrence of landslides was observed from low drainage density to high drainage density; especially no landslides occurred at the very high drainage density. The comparison of the relative coverage of every drainage density interval reveals that high susceptibility levels such as very low, low and moderate drainage density correspond to mountainous and hilly terrains while low susceptibility level (high drainage density) is related to coastal plains.

Among five drainage density levels, no landslides occurred in the very high drainage density interval ($>3.0 \text{ km/km}^2$). Thus this class has -0.0216 susceptibility level value. The drainage density interval ($<1.5 \text{ km/km}^2$) is given the lowest susceptibility level of -0.1065 while the moderate interval ($2.2 - 3.0 \text{ km/km}^2$) has the highest susceptibility level to landslides, getting 0.0796 of the total landslide occurrence (Figure 5-7). These results were contrary to the usual trend in common practice that the higher the drainage density is, the greater the landslide possibility is.

Table 5-7. Distribution of landslides and susceptibility classes of density drainage.

Drainage density	Nclass	Nslide	Dij (%)	D (%)	Wij
< 1.5	184939	302	12.06	13.42	-0.1065
1.5-2.2	547528	973	38.86	39.72	-0.0219
2.2-3.0	425538	837	33.43	30.87	0.0796
> 3.0	220520	392	15.65	16.00	-0.0216
Sum	1378525	2504	100	100	

However, these results reflect the true reality because landslides only occurred in mountains in study area. Besides, drainage systems in the province are concentrated at coastal plains which are abundant in river system. For those reasons, this drainage density interval does not cause much instability as compared to the moderate drainage density interval at mountainous regions where most of the water infiltrations cause instability. This statement can be supported by the fact that the terrain corresponding to the moderate level is dominated by morphologic rocks such as shale, silica schist, quartzite schist, sericit schist, and gneiss. The weathered products of such rocks allow water to easily infiltrate causing landslide occurrences.

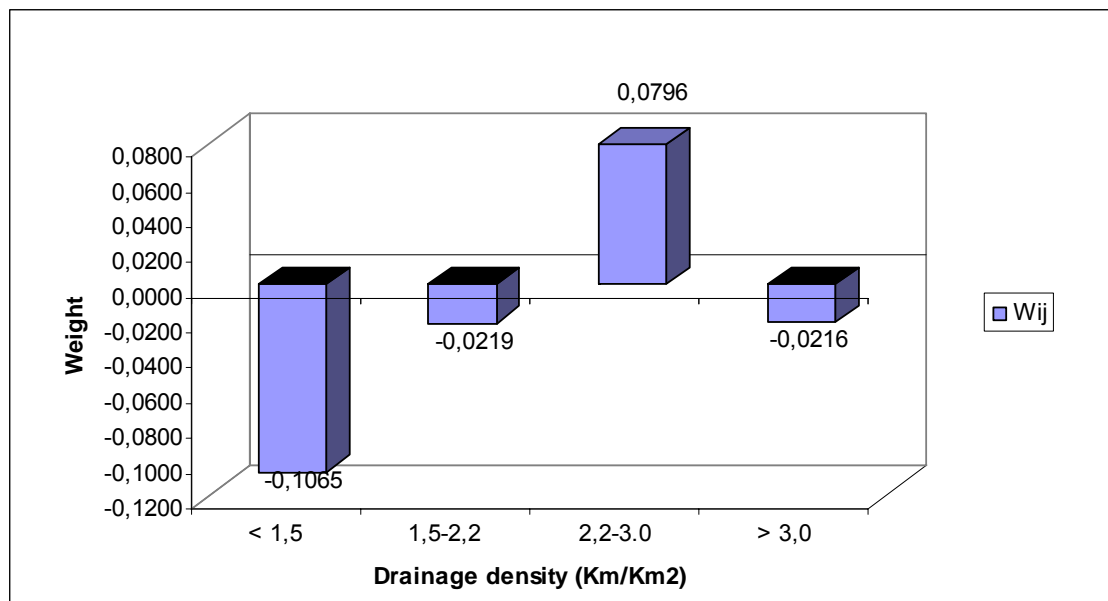


Figure 5-7. The weight index of each class of the drainage density factor

Statistical index value of this factor ranges from -0.1065 to 0.0796, (computed by table 5-7). This is the third highest statistical index value in comparison with all previous statistical indexes. Therefore, in general, its role in the occurrence of landslide among these factors is important. This value also reveals that the frequency of landslides is concentrated at some specific density ranges, and not distributed at all of its ranges.

5.1.1.8. Weighted factors of land cover

Since 1980, the natural forests in the research area have been drastically changed by uncontrolled deforestation. That deforestation has severely caused the land cover pattern in the area. However, a small primeval forest area still exists mostly distributed at high mountains with steep slope. More than a half of the area within this province is now dominated by low density vegetation such as shrubs and bare hills which once were the forest area.

Most of the present research areas are now covered by shrubs, bushes, grasses and bare hills, occupying more than 20% of the total area while approximately 70 % of the area is

forests (including sustained forests, light forests and young forests). About 10 % of the remaining areas are water bodies, agriculture and mixed plantation. Agriculture, particularly paddy rice, is the predominant economic activity in the province's flat coastal plain.

Table 5-8. Distribution of landslides and land cover classes

Landcover	Nclass	Nslide	Dij (%)	D (%)	Wij
Water	3014	0	0.00	0.22	-2.0000
Rice	13418	0	0.00	0.97	-2.0000
Forage crops	114696	148	5.91	8.32	-0.3419
Grass and bare hills	99572	348	13.90	7.22	0.6544
Shrub and bush	70744	278	11.10	5.13	0.7717
Young forest	314551	580	23.16	22.82	0.0150
Sustained forest	369601	592	23.64	26.81	-0.1258
Mixed forest	392929	558	22.28	28.50	-0.1100
Sum	1378525	2504	100	100	

The results from table 5-8 and figure 5-8 by crossing the landslide occurrence map with the land cover map shows that >25% of the landslides were found in shrubs - bare hills class. Statistical index values of this factor are range from -2.000 to 0.7717, computed in table 5-8.

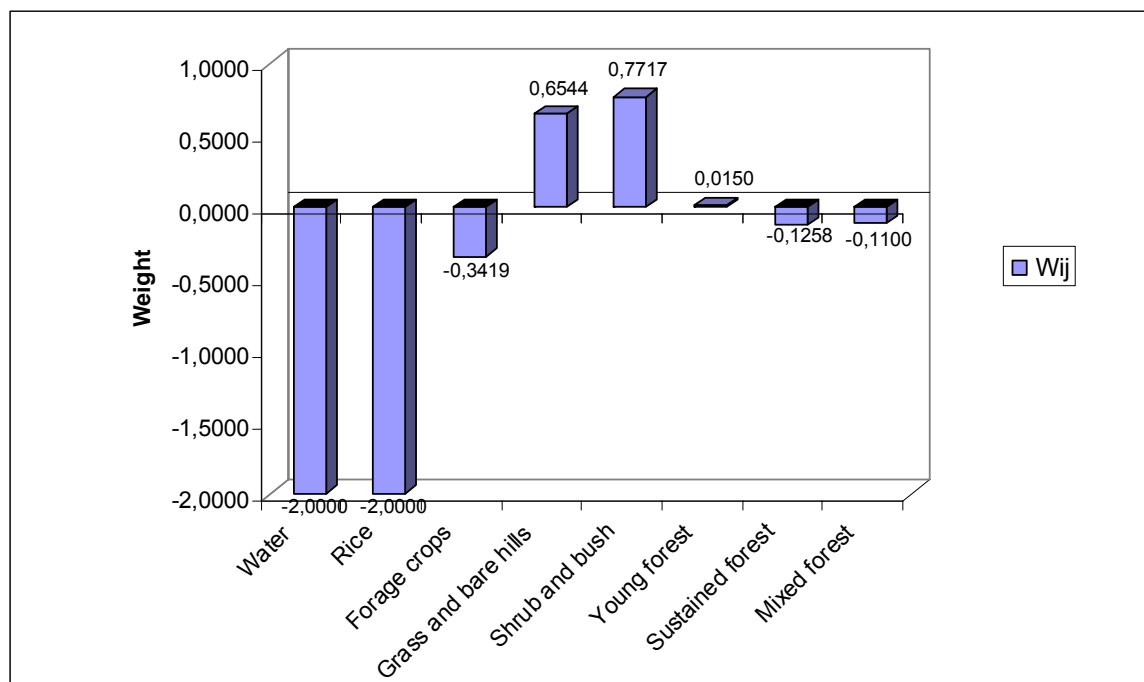


Figure 5-8. The weight index of each class of land cover factor

5.1.1.9. Weighted factors of rainfall

Rainfall is commonly considered as the triggering factor for land sliding. The research area has been strongly incurred and affected by the tropical monsoon climate and the long rainy season. Therefore, it is very necessary to take rainfall into account as a factor input for the model of landslide susceptibility mapping.

Table 5-9. Distribution of landslides and rainfall classes

	Nclass	Nslide	Dij (%)	D (%)	Wij
<1700	627927	858	34.27	45.55	-0.2847
1700-2000	349129	763	30.47	25.33	0.1849
200-2300	401469	883	35.26	29.12	0.1913
	1378525	2504	100	100	

The result from table 5-9 and figure 5-9 by crossing the landslide occurrence map with the rainfall map shows that >29% landslides were found in 2000-2300 mm/year class. The weight index values of this factor range from 0.1913, computed in table 5-8. In table 5-8, >25% landslides were found in >1700-2000 mm/year class. The weight index values of this factor are the same as 2000-2300 class.

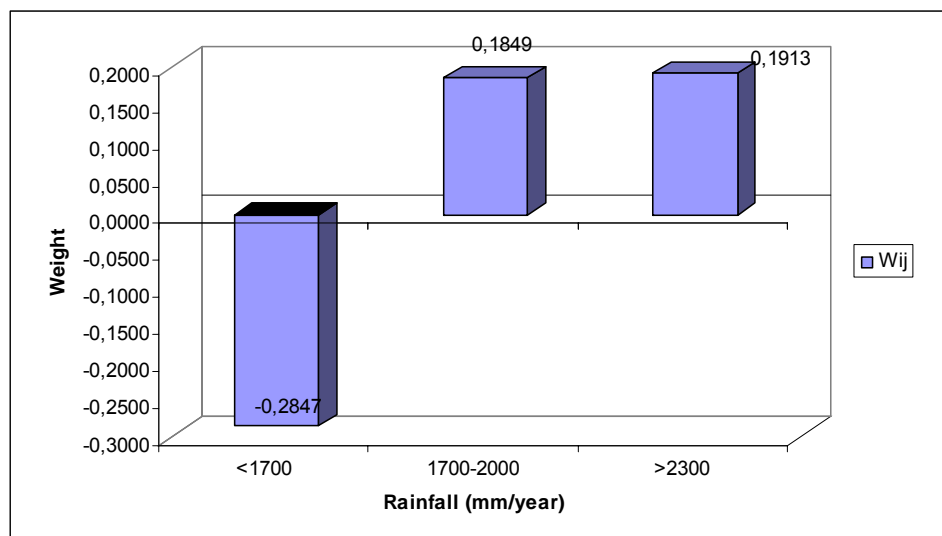


Figure 5-9. The weight index of each class of rainfall factor

In table 5-8, >45% landslides fall in <1700-2000 mm/year class. The weight index value of this factor is -0.2847. This factor is equated with the two factors above. Therefore, in general, its role in the occurrence of landslide among all factors is not important. This value also reveals that the frequencies of landslides are concentrated at two factors above, and not distributed at this factor.

5.1.2. Landslide hazard zonation map of statistical index method

The author used the weights calculated for the individual factor map to assess which maps are important for the prediction. Therefore, it is necessary to make sure that the output tables with the weights can be linked to the factor maps. That is the reason why the weight calculation is done in the attribute tables, and not in the cross tables. Table 5-10 shows that in the statistical index method of landslide susceptibility mapping only nine remaining factors: slope degree, weathering, geological, geomorphological, lineament density, drainage density, land cover, elevation and rainfall. Weights can be added to each map of the individual factor. The statistical index map is created by the overlay method of GIS function. The landslide susceptibility index (LSI) in the research area is calculated and summed up by the contrast of the factors. The higher the values are in this map, the higher the susceptibility for landslides is, and vice versa.

Table 5-10. List of weighted values of nine factors

Slope degree (degree)	Nslide (pixel)	Nclass (pixel)	Dij (%)	D (%)	Wij
0-5	60	68952	2.40	5.01	-0.7369
5-15	265	143201	10.58	10.39	0.0186
15-30	909	520576	36.30	37.77	-0.0395
30-45	913	477124	36.46	34.61	0.0522
> 45	357	168672	14.26	12.23	0.1532
Weathering crust (class)					
Limestone	99	145080	3.95	10.52	-0.9790
FSA1	96	39000	3.83	2.83	0.3039
FSA2	0	611	0.00	0.04	-2.0000
HH	1042	507221	41.61	36.79	0.1231
Q	0	19787	0.00	1.44	-2.0000
SA1	898	465483	35.86	33.77	0.0602
SA2	369	192839	14.74	13.99	0.0521
SAF1	0	8504	0.00	0.62	-2.0000
Geological (class)					
aQ	0	18086	0.00	1.31	-2.0000
S ₂ -D ₁ <i>nc</i>	536	162020	21.41	11.74	0.5995
P ₃ <i>ct</i>	37	20371	1.48	1.48	-0.0001
D ₁ <i>np</i>	62	34414	2.48	2.50	-0.0082
T ₂₋₃ <i>lc</i>	422	180848	16.85	13.11	0.2505
T ₂₋₃ <i>lc</i>	304	97040	12.14	7.03	0.5450
γaT _{3n} <i>pb</i>	328	81623	13.10	5.91	0.7940
P ₁₋₂ <i>sd</i>	176	203135	7.03	14.75	-0.7403
T ₂₋₃ <i>lc</i>	95	135681	3.79	9.85	-0.9533
T _{3n-r} <i>sb</i>	182	179016	7.27	13.00	-0.5803
J ₁₋₂ <i>np</i>	26	51305	1.04	3.73	-1.2766
γδP ₃ -T ₁ <i>db</i>	336	214986	13.42	15.60	-0.1503

Geomorphological (class)					
TD	0	6788	0.00	0.49	-2.0000
CD1	0	3648	0.00	0.26	-2.0000
CD2	0	669	0.00	0.05	-2.0000
DS	0	1199	0.00	0.09	-2.0000
CD3	6	9225	0.24	0.67	-1.0270
CD4	0	794	0.00	0.06	-2.0000
FS1	0	8866	0.00	0.64	-2.0000
FS2	0	8719	0.00	0.63	-2.0000
FS3	0	4021	0.00	0.29	-2.0000
FS4	15	1882	0.60	0.14	1.4788
FS	0	182	0.00	0.01	-2.0000
KD	109	131740	4.35	9.56	-0.7864
PD	0	6253	0.00	0.45	-2.0000
PS	0	1208	0.00	0.09	-2.0000
SD1	406	39757	16.21	2.88	1.7267
SD2	400	60664	15.97	4.40	1.2892
SD3	154	72876	6.15	5.29	0.1513
SD4	998	799588	39.86	58.00	-0.3752
SD5	416	220446	16.61	15.99	0.0382
Lineament density (km/km2)					
< 0.22	0	9648	0.00	0.70	-2.0000
0.22-0.45	211	152588	8.43	11.07	-0.2728
0.45-0.65	580	309552	23.16	22.46	0.0310
0.65-0.83	653	343096	26.08	24.89	0.0467
0.83-1.00	503	266688	20.09	19.35	0.0376
1.00-1.25	409	212330	16.33	15.40	0.0587
> 1.25	148	84623	5.91	6.14	-0.0379
Drainage density (km/km2)					
< 1.5	302	184939	12.06	13.42	-0.1065
1.5-2.2	973	547528	38.86	39.72	-0.0219
2.2-3.0	837	425538	33.43	30.87	0.0796
> 3.0	392	220520	15.65	16.00	-0.0216
Landcover (class)					
Water	0	3014	0.00	0.22	-2.0000
Rice	0	13418	0.00	0.97	-2.0000
Forage crops	148	114696	5.91	8.32	-0.3419
Grass. bare hills	348	99572	13.90	7.22	0.6544
Shrub and bush	278	70744	11.10	5.13	0.7717
Young forest	580	314551	23.16	22.82	0.0150
Sustained forest	592	369601	23.64	26.81	-0.1258
Mixed forest	558	392929	22.28	28.50	-0.1100
Elevation (m)					
<250	71	44797	2.84	3.25	-0.1363
250-550	632	236391	25.24	17.15	0.3865
550-850	847	407555	33.83	29.56	0.1346
850-1200	654	464691	26.12	33.71	-0.2551
>1200	300	225091	11.98	16.33	-0.3096
Rainfall (mm/year)					
<1700	627927	858	34.27	45.55	-0.2847
1700-2000	349129	763	30.47	25.33	0.1849
200-2300	401469	883	35.26	29.12	0.1913

The resulting LSI map is shown in Figure 5-11. The LSI map is re-classified into different landslide susceptibility zones by the natural break method in ILWIS 3.0 software) as shown in Figure 5-10. The cut-off percentage of the observed landslide occurrence and the LSI value points between very low, low, moderate, high and very high landslide susceptibility zones are shown in Figure 5-12. The areas and percentages of various landslide susceptibility zones are shown in Figure 5-12. The areas and percentages of various landslide susceptibility zones are displayed in Table 5-11.

In the LSI map, the hazard values range from -10 to 6. In order to classify the hazard value into Landslide Hazard Index (LHI) classes the distribution of all hazard values is taken into account. The *hazard* levels were categorized into very low, low, moderate, high and very high hazard using the *natural break* method in ILWIS 3.0 software. The final hazard map displays five different degrees of landslide hazards: very low, low, moderate, high and very high hazard.

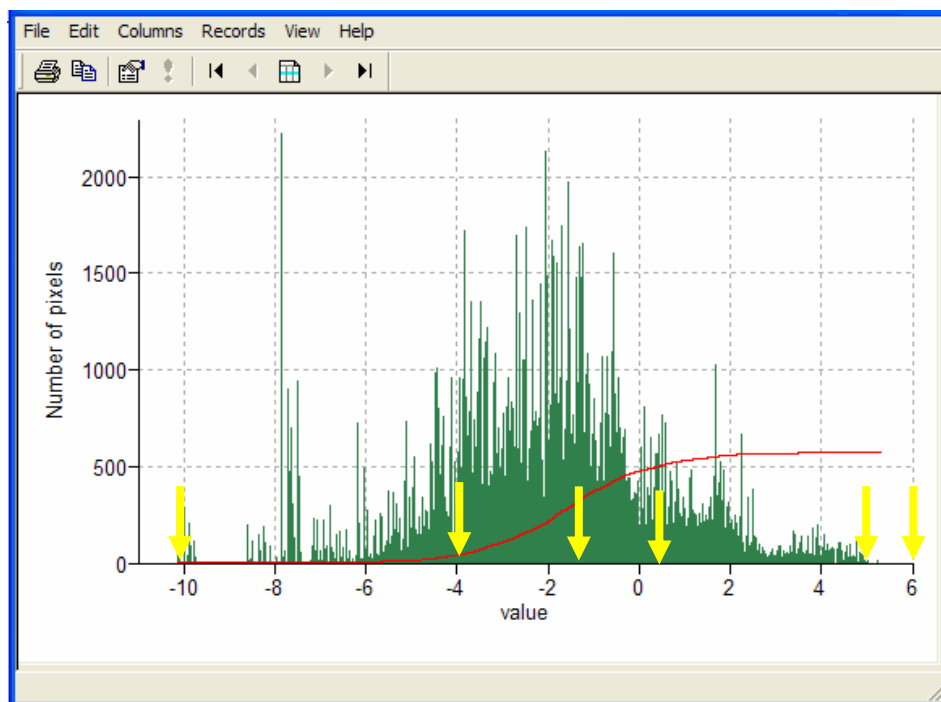


Figure 5-10. The frequency histogram in *natural break* method (ILWIS3.0)

As the very high hazard zone is the most interesting one in term of hazard, its threshold boundary for this zone will be discussed first beyond the highest break from 5 to 6. Besides, the maximum hazard value is reaches at 6, therefore the value of 5 is chosen as the threshold boundary which indicates the very high hazard zone. The second break in the frequency diagram from the right to the left is observed at the value from 0.3 to 5. Hence, this 0.3 is the threshold boundary that indicates the starting of the high hazard zone and the ending of moderate hazard zone. Likewise, the following LHI threshold boundaries were used according to the change in both the frequency diagram and the cumulative curve: -1.5; -4.0; -10.0. These threshold boundaries correspond to very low hazard, low hazard and moderate hazard zones.

In this map, there are small areas consisting of a few pixels of a class surrounded by another class. Therefore, a 3×3 'majority filter' has been applied to the map as a post-classification filter to reduce the high frequency variation. Figure 5-12 shows the Landslide Hazard Zonation map prepared for the research area.

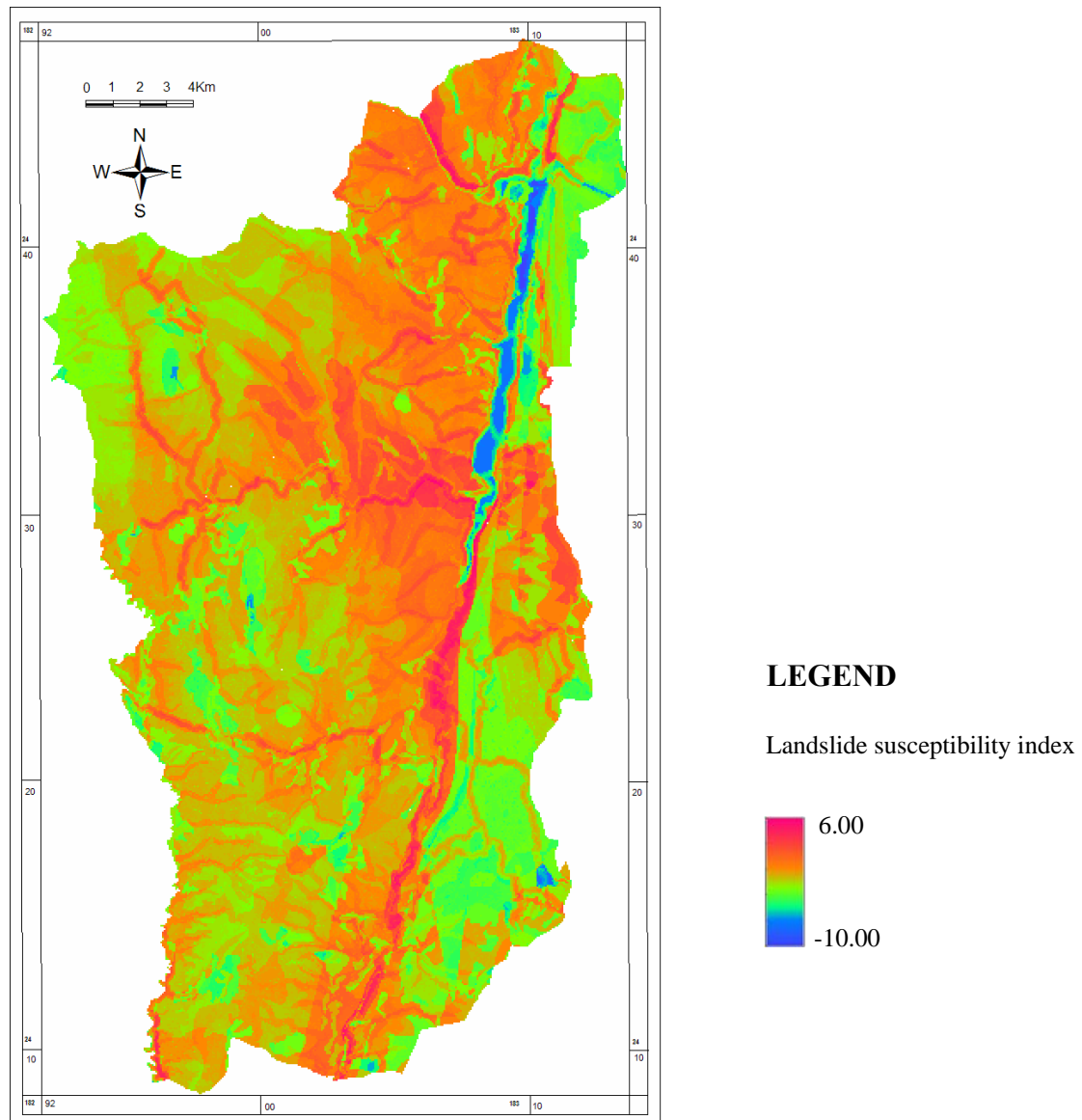


Figure 5-11. The map of landslide susceptibility index of Muong Lay

Table 5-11. The areas of different landslide hazard zones based on the statistical index method

Landslide hazard zones	Area	
	(km ²)	(%)
Very low landslide hazard	16.0132	2.91
Low landslide hazard	182.638	33.14
Moderate landslide hazard	225.25	40.87
High landslide hazard	108.0552	19.61
Very landslide hazard	19.122	3.47

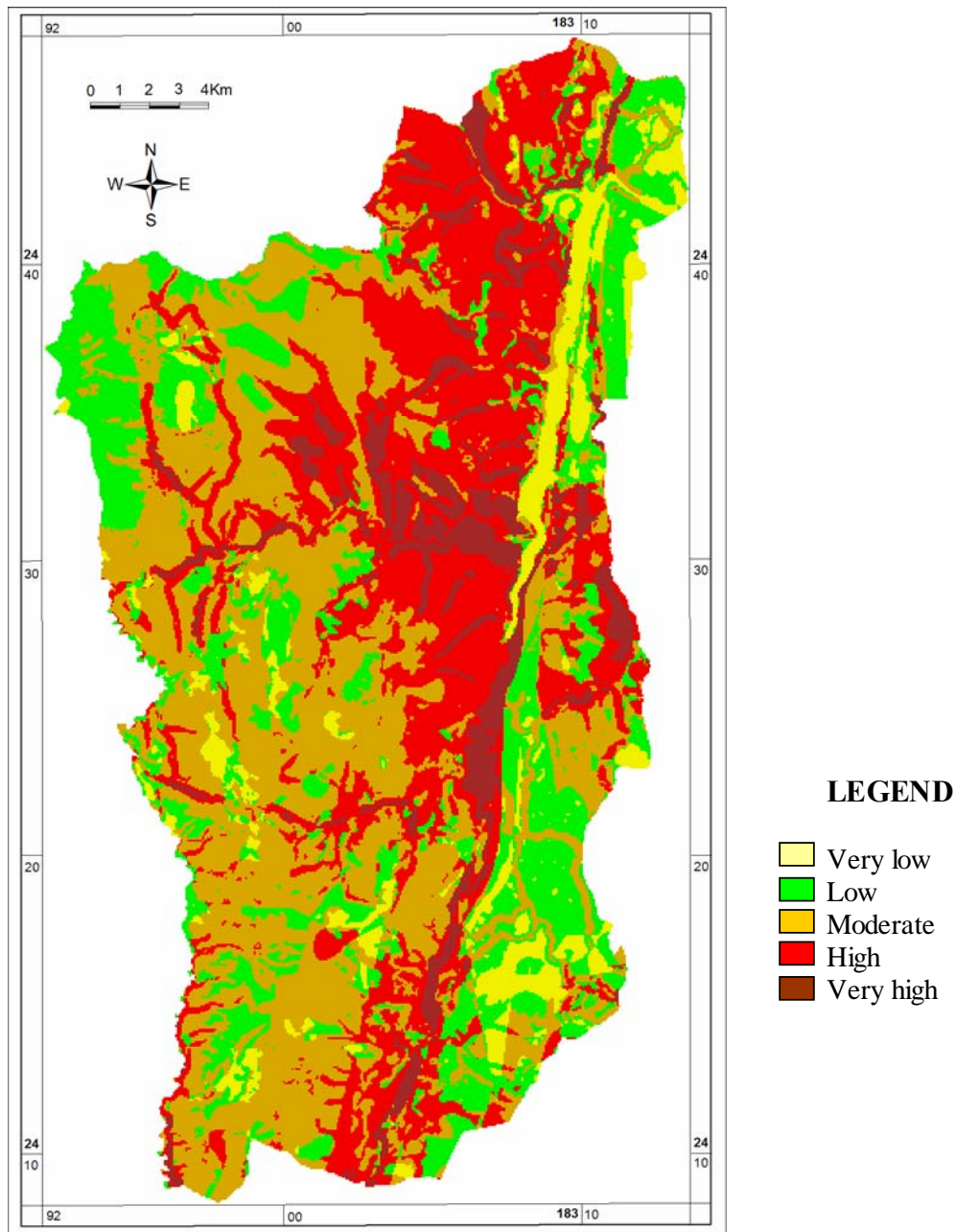


Figure 5-12. Landslide hazard zonation map from the Statistical index method

The statistical index values of the landslide hazard zonation map for the saturated scenario show that:

- The very high landslide susceptibility classes in the research area cover 3.47%, equivalent to 19.122 km².
- The high landslide susceptibility classes in the research area cover 19.61%, equivalent to 108.0552 km²
- The moderate landslide susceptibility classes in the research area cover 40.87%, equivalent to 225.25 km²

- The low landslide susceptibility classes in the research area covers 33.14%, equivalent to 182.638 km²
- The very low landslide susceptibility classes occupy only 2.91% (16.0132 km²) of the total area.

5.2. ANALYSIS RESULTS OF MULTIPLE LINEAR REGRESSION METHOD

5.2.1. Variables description

In this study, there are nine causative factors for the multiple linear regression model of landslide susceptibility as independent variables, but not all variables are numerical. Only five variables, including slope degree, drainage density, lineament density, elevation, and rainfall are numerical; the others, including weathering crust, geological formation, geomorphologic units and land cover are alphanumeric types or categories that cannot be processed immediately. According Lee, Pradhan (2006), these categorical types are assigned in the form of frequency ratio values. This frequency ratio expresses the relationship between the observed landslide occurrences in an area and the landslide-related factors. The frequency ratio is defined as following:

$$W_{ij} = \frac{F_{ij}}{F_{ij}^*} \quad (5.1)$$

Where:

W_{ij} is the frequency ratio of class *i* of parameter *j*.

F_{ij} is the frequency of observed landslides in class *i* of parameter *j*.

*F_{ij}** is the frequency of non-observed landslides in class *i* of parameter *j*.

Therefore, the greater the ratio above unity, the stronger the relationship between the landslide occurrences and the given factors attributes, and the lower the ratio below unity, the lesser the relationship between the landslide occurrences and the given factors attributes (Lee, Pradhan, 2006).

The calculated frequency ratios are given in Table 5-12. Rating layers for the different causative factors is constructed based on the obtained frequency ratios. The frequency ratio values of weathering, geological, and geomorphologic factors are given in Table 5-12.

Table 5-12. Frequency ratios of all classes of weathering crust, geological, and geomorphologic factors

Geological \ factors	Nslide (pixel)	Nclass (pixel)	Fij (%)	Fij* (%)	Frequency ratio
aQ	0	18086	0.0000	1.3144	0.0000
S ₂ -D ₁ <i>nc</i>	536	162020	21.4058	11.7356	1.8240
P ₃ <i>ct</i>	37	20371	1.4776	1.4777	0.9999
D ₁ <i>np</i>	62	34414	2.4760	2.4965	0.9918
T ₂₋₃ <i>lc</i>	422	180848	16.8530	13.1122	1.2853
T ₂₋₃ <i>lc</i>	304	97040	12.1406	7.0301	1.7269
γaT _{3n} <i>pb</i>	328	81623	13.0990	5.9080	2.2172
P ₁₋₂ <i>sd</i>	176	203135	7.0288	14.7497	0.4765
T ₂₋₃ <i>lc</i>	95	135681	3.7939	9.8535	0.3850
T _{3n-r} <i>sb</i>	182	179016	7.2684	12.9965	0.5593
J ₁₋₂ <i>np</i>	26	51305	1.0383	3.7266	0.2786
γδP ₃ -T ₁ <i>db</i>	336	214986	13.4185	15.5993	0.8602
Weathering crust					
TD	6788	0	0.0000	0.4933	0.0000
CD1	3648	0	0.0000	0.2651	0.0000
CD2	669	0	0.0000	0.0486	0.0000
DS	1199	0	0.0000	0.0871	0.0000
CD3	9225	6	0.2396	0.6700	0.3576
CD4	794	0	0.0000	0.0577	0.0000
FS1	8866	0	0.0000	0.6443	0.0000
FS2	8719	0	0.0000	0.6336	0.0000
FS3	4021	0	0.0000	0.2922	0.0000
FS4	1882	15	0.5990	0.1357	4.4151
FS	182	0	0.0000	0.0132	0.0000
KD	131740	109	4.3530	9.5661	0.4550
PD	6253	0	0.0000	0.4544	0.0000
PS	1208	0	0.0000	0.0878	0.0000
SD1	39757	406	16.2141	2.8598	5.6697
SD2	60664	400	15.9744	4.3796	3.6475
SD3	72876	154	6.1502	5.2849	1.1637
SD4	799588	998	39.8562	58.0362	0.6867
SD5	220446	416	16.6134	15.9903	1.0390
Geomorphological					
Carbonat	145080	99	3.9537	10.5362	0.3752
FSA1	39000	96	3.8339	2.8273	1.3560
FSA2	611	0	0.0000	0.0444	0.0000
HH	507221	1042	41.6134	36.7857	1.1312
Q	19787	0	0.0000	1.4380	0.0000
SA1	465483	898	35.8626	33.7629	1.0622
SA2	192839	369	14.7364	13.9874	1.0535
SAF1	8504	0	0.0000	0.6180	0.0000
Landcover					
Water	33014	0	0.0000	2.3992	0.0000
Rice	33418	0	0.0000	2.4286	0.0000
Forage crops	114696	148	5.9105	8.3246	0.7100
Grass and bare hills	99572	348	13.8978	7.2109	1.9273
Shrub and bush	70744	278	11.1022	5.1210	2.1680
Young forest	314551	580	23.1629	22.8173	1.0151
Sustained forest	369601	592	23.6422	26.8171	0.8816
Mixed forest	342929	558	22.2843	24.8812	0.8956

After frequency ratios of weathering crust, geological, and geomorphologic factors have been calculated, all variables are integrated into the matrix table of number data. Table 5-13 is statistical characterization description of all variables. Details of the matrix table are given in the appendix.

Table 5-13. Statistical characterizations description of all variables

	Cell	Mean	Minimum	Maximum	Avg.	St. Dev
[Slope_degree]	1378525	29.03	0	80.2	40.10	13.08
[Rainfall]	1378525	0.89	1700	2200	1950	0.52
[Landcover]	1378525	0.57	0.00	2.1680	1.08	0.46
[Weathering_crust]	1378525	0.96	0.00	1.3560	0.68	0.27
[Geomorphological]	1378525	0.84	0.00	5.6697	2.83	0.65
[Geological]	1378525	0.87	0.00	2.2172	1.11	0.51
[Lineament_density]	1378525	3.79	0.12	1.50	0.81	1.26
[Elevation]	1378525	2.61	199	1640	919.5	0.92
[Drainage_density]	1378525	3.07	1.2	3.5	2.35	1.51

Regression Model:

$$Y[\text{landslide_ocurrent}] = B_0 + B_1[\text{Slope_degree}] + B_2[\text{Rainfall}] + B_3[\text{Landcover}] + B_4[\text{Weathering_crust}] + B_5[\text{Geomorphological}] + B_6[\text{Geological}] + B_7[\text{Lineament_density}] + B_8[\text{Elevation}] + B_9[\text{Drainage_density}]$$

- Dependent variable is observed landslides [landslide_ocurrent]. The presence of observed landslide is (1) or absence of observed landslide is (0)
- Independent variables are 9 factors such as: Geological, Geomorphological, Weathering_crust, Slope_degree, Lineament_density, Drainage_density, Elevation, Landcover, and Rainfall.

5.2.2. Regression coefficients

In order to process the multiple linear regression model of landslide susceptibility with the current data, the SPSS Statistical 17.0 software (SPSS Inc, copyright 2009, www.spss.com) is used to process the data to estimate the regression. Details of the regression analyses are given in Figure 4-22.

Table 5-14. Results of multiple linear regression model

Var	B - Coefficient	Std. Error	t-Value
[Constant]	-0.0039041	0.0004245	5.7581698280
[Slope_degree]	0.0000077	0.0000019	7.1274096033
[Rainfall]	0.0000012	0.0000002	6.7973047841
[Landcover]	0.0003911	0.0000561	-11.3197880107
[Weathering_crust]	-0.0002849	0.0001412	6.0145087570
[Geomorphological]	0.0017366	0.0000365	-2.3253588726
[Geological]	0.0014724	0.0000660	-2.8399139218
[Lineament_density]	-0.0001293	0.0000275	0.6912134855
[Elevation]	0.0000002	0.0000001	-7.3908588762
[Drainege_density]	0.0000003	0.0000001	1.9628305978

Regression Model = - 0.0039041 + 0.0000077 * [Slope_degree] + 0.0000012 * [Rainfall] + 0.0003911 * [Landcover] - 0.0002849 * [Weathering_crust] + 0.0017366 * [Geomorphological] + 0.0014724 * [Geological] - 0.0001293 * [Lineament_density] + 0.0000002 * [Elevation] + 0.0000003 * [Drainege_density]

The results of the regression analyses are given in Table 5-14. The standardized regression coefficients or t-values, which are the regression coefficients expressed in units of their standard deviation, indicate the relative contribution of each causative factor to the occurrence of landslides and enable to decide whether a certain factor has a significant contribution in the equation. If the absolute t-value is larger than 1.96 (*Davis, 1986*), the coefficient can be considered significant with 95% confidence. The values given in Table 5-14 indicate that causal factors such as slope degree, rainfall, weathering crust, and lineament density play a significant contribution in the regression model, and consequently have an important impact on land sliding. Land cover, elevation, geomorphological, and geological are less significant. Also the following statistics are used to evaluate the overall result of the model: Std. Error means standard error estimating, i.e. the square root of the residual mean square error which measures the unexplained variability in the dependent variable. In view of the fact that the model produces Y values between about > 0.1, the standard estimate error is rather high.

5.2.3. Landslide hazard zonation map of multiple linear regression method

The resulting LSI map is shown in Figure 5-13. The same classification procedure as before (see 5.1.2) is used for reclassifying the LSI map into different landslide susceptibility zones as shown in Figure 5-14. The cut-off percentage of the observed landslide occurrence and the LSI value points between very low, low, moderate, high and very high landslide susceptibility zones are shown in Figure 5-15. The areas and percentages of various landslide susceptibility zones are displayed in Table 5-15.

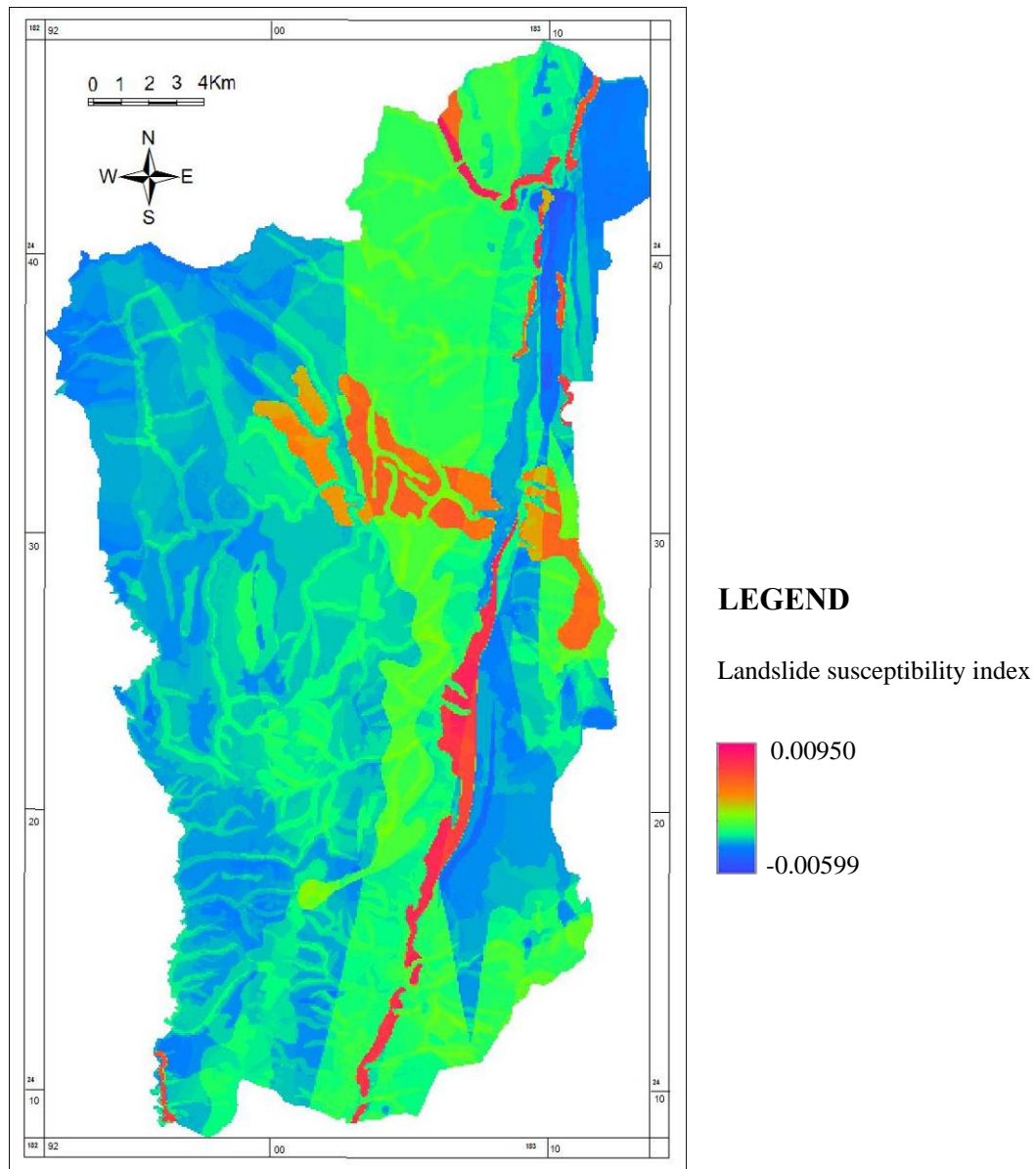


Figure 5-13. Map of landslide susceptibility index of Muong Lay

The resulting map of landslide susceptibility is shown in Figure 5-22. In the LSI map, the hazard values range from -0.00599 to 0.00950. In order to classify the hazard value into Landslide Hazard Index (LHI) classes the distribution of all hazard values is taken into account. The *hazard* levels were categorized into very low, low, moderate, high and very

high hazard using *natural break* method in ILWIS 3.0 software. The final hazard map displays five different degrees of landslide hazards: very low hazard, low, moderate, high and very high hazard.

Table 5-15. The areas of different landslide hazard zones based on the multiple linear regression method

Landslide hazard zones	Area	
	(km ²)	(%)
Very low landslide hazard	23.9652	4.35
Low landslide hazard	155.7808	28.28
Moderate landslide hazard	153.1144	27.79
High landslide hazard	176.7284	32.08
Very landslide hazard	41.3108	7.50

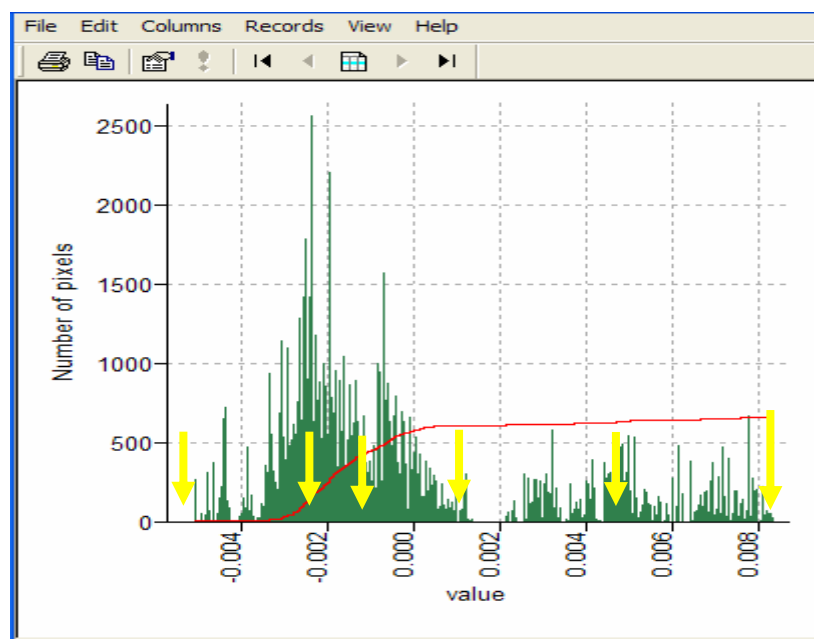


Figure 5-14. The frequency histogram in *natural break* method

As the very high hazard zone is the most interesting one in term of hazard, its threshold boundary for this zone will be discussed first beyond the highest break from 0.00563 to 0.00950. Besides, the maximum hazard value is reached at 0.00950, therefore value higher than 0.00563 is chosen as the threshold boundary that indicates the very high hazard zone. The second break in frequency diagram from the right to the left is observed at values from 0.00176 to 0.00563. Hence, 0.00176 is the threshold boundary that indicates the starting of high hazard zone until 0.00563 and the ending of moderate hazard zone. Likewise, the following LHI threshold boundaries were used according to the change in both frequency diagram and cumulative curve: -0.00212; -0.00135; -0.00599. These threshold boundaries correspond to very low hazard, low hazard and moderate hazard zones.

In this map, there are small areas consisting of a few pixels of a class surrounded by another class. Therefore, a 3×3 'majority filter' has been applied to the map as a post-classification filter to reduce the high frequency variation. Figure 5-15 shows the Landslide Hazard Zonation map prepared for the research area.

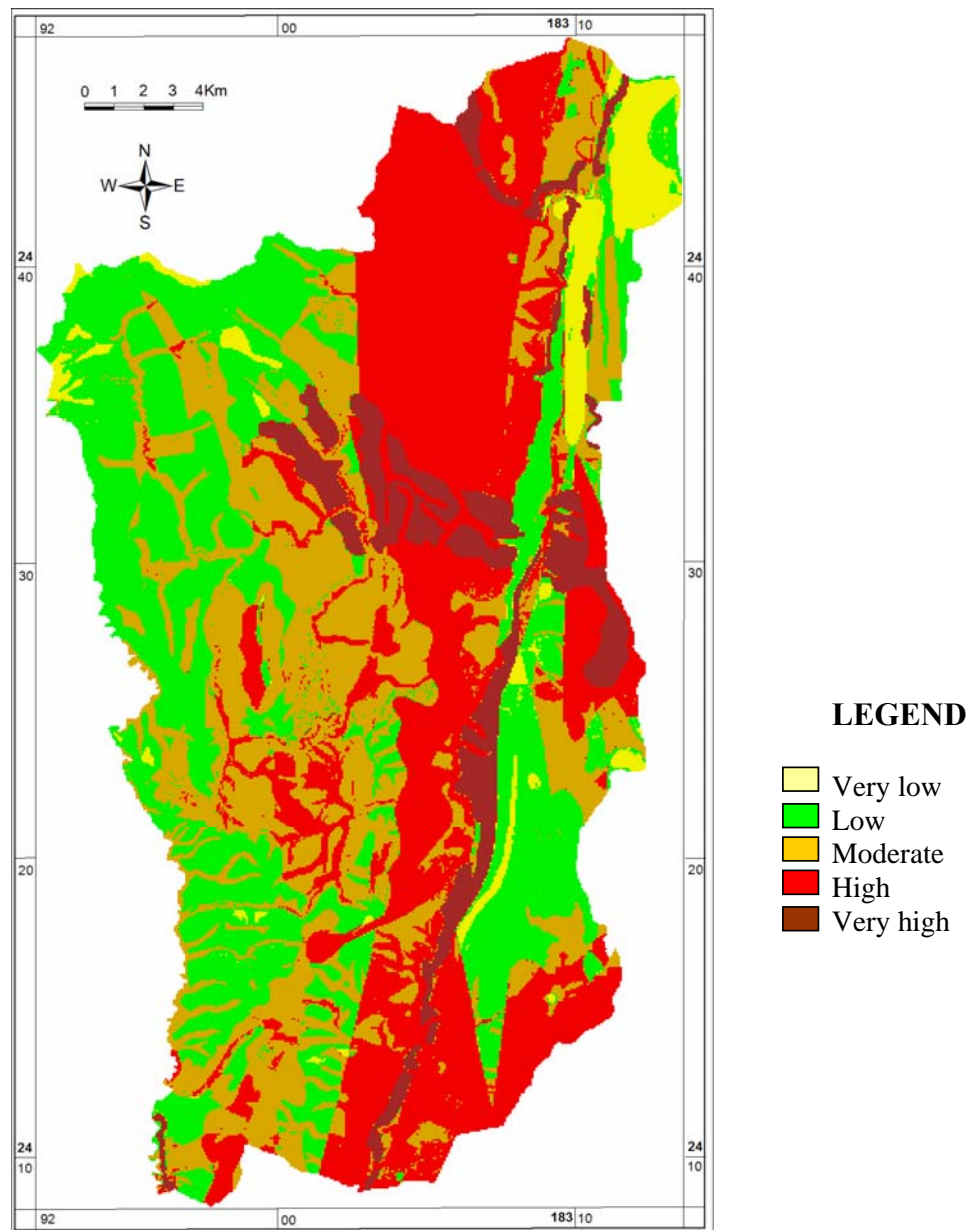


Figure 5-15. Landslide hazard zonation map from multiple linear regression method

The statistical index value of landslide hazard zonation map for the saturated scenario shows that:

- The very high landslide susceptibility classes in the research area cover 4.35%, equivalent to 23.9652 km².
- The high landslide susceptibility classes in the research area cover 28.28%, equivalent to 155.7808 km²

- The moderate landslide susceptibility classes in the research area cover 27.79%, equivalent to 153.1144 km²
- The low landslide susceptibility classes in the research area cover 32.08%, equivalent to 176.7284 km²
- The very low landslide susceptibility classes occupy only 7.50% (41.3108 km²) of the total area.

5.3. ACCURACY OF PREDICTION RESULTS

In estimating the accuracy of predicted results, there is a permanent problem: "What is the best method for landslide zonation mapping in the research area?". In order to answer this question, some criteria are considered for the evaluation of the results.

In most landslide studies, the observed landslides in different landslide susceptibility classes are always considered the key factor for result evaluation.

In this study, the author estimated the accuracy of landslide hazard mapping results base on three criteria:

- Considered of the area of landslide point (observed landslide) in the factor groups of landslide hazard classes
- Estimation of the accuracy of landslide prediction based on the number of landslide points (observed landslide) which are accurately or inaccurately predicted.
- Comparison of predicted results with other previous results of the research area

Based on the above criteria, the areas and landslide probability of the different landslide susceptibility classes are calculated as shown in Table 5-16.

Table 5-16. Comparison of different landslide mapping methods

	Area		Observed Landslide		Landslide probability
	(km2)	(%)	(m2)	(%)	
Statistical index method					
Very Low landslide hazard	16.0132	2.91	1200	0.12	0.0412
Low landslide hazard	182.638	33.14	198800	19.85	0.5984
Moderate landslide hazard	225.250	40.87	316000	31.55	0.7715
High landslide hazard	108.0552	19.61	329600	32.91	1.6803
Very high landslide hazard	19.122	3.47	156000	15.58	4.5173
Multiple linear regression method					
Very Low landslide hazard	23.9652	4.35	5200	0.5192	0.1193
Low landslide hazard	155.7808	28.28	134400	13.4185	0.4745
Moderate landslide hazard	153.1144	27.79	139200	13.8978	0.5001
High landslide hazard	176.7284	32.08	386800	38.6182	1.2038
Very high landslide hazard	41.3108	7.50	336000	33.5463	4.4728

Table 5-16 indicates that the statistical index method has the smallest predicted area of high and very high LHZ and consequently the highest posterior landslide probability for high and very high LHZ. Vice versa, the predicted area of low LHZ of the statistical index method is the largest, so it has the smallest posterior landslide susceptibility. This can also be noted from the graph that shows the accumulative percentage of observed landslide versus accumulative areal percentage of predicted increasing susceptibility, as shown in Figure 5-16. Figure 5-16 shows that the curve of the statistical index method has the nearest to perfect equality, and consequently is the best result for landslide susceptibility prediction based on the above criteria.

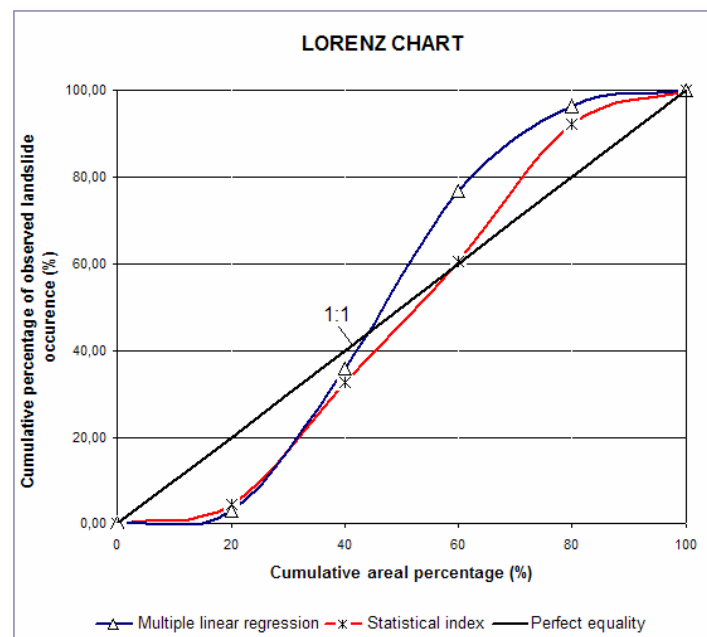


Figure 5-16. Curves of the observed landslide accumulation versus cumulative areal percentage of increased landslide susceptibility

On the other hand, based on the second criterion, the accuracy of the final LHZ map is evaluated based on the observed landslides. First, the final LHZ map is checked by overlaying with the observed landslide map. As shown in Figure 5-17, there are various possibilities of different LHZs coinciding with a landslide polygon.

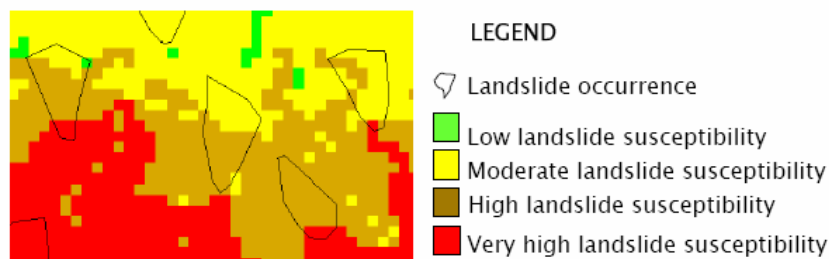


Figure 5-17. Example of some landslides overlaying the final LSZ map

The areas of different landslide susceptibility classes in each landslide polygon are the basis for evaluating whether the prediction is accurate or inaccurate. Some criteria are needed for the evaluation as follows:

- If the total area of an observed landslide is covered by only the low landslide susceptibility class of the final LSZ map, the prediction method is considered as “wrong” at this location. In other words, this landslide is not well predicted by the model.
- If more than 80% of the landslide area is covered moderate, high and very high landslide susceptibility classes, the prediction of the observed landslide can be considered “very good”.
- The other cases of various combinations between different landslide susceptibility overlaying a landslide polygon are concluded as "not decisive".

Based on the above criteria, the areas of the 88 landslides in the research area are classified into three groups with different levels of prediction accuracy as shown in table 5-17.

Table 5-17. Summary of the prediction accuracy of the LSZ map

Order	Accuracy of prediction	Observed landslide	
		Number of landslides	Percentage (%)
Statistical index method			
1	No evaluation	0	0
2	Very good	84	95
3	Wrong	4	5
Multiple linear regression			
1	No evaluation	0	0
2	Very good	77	91
3	Wrong	7	9

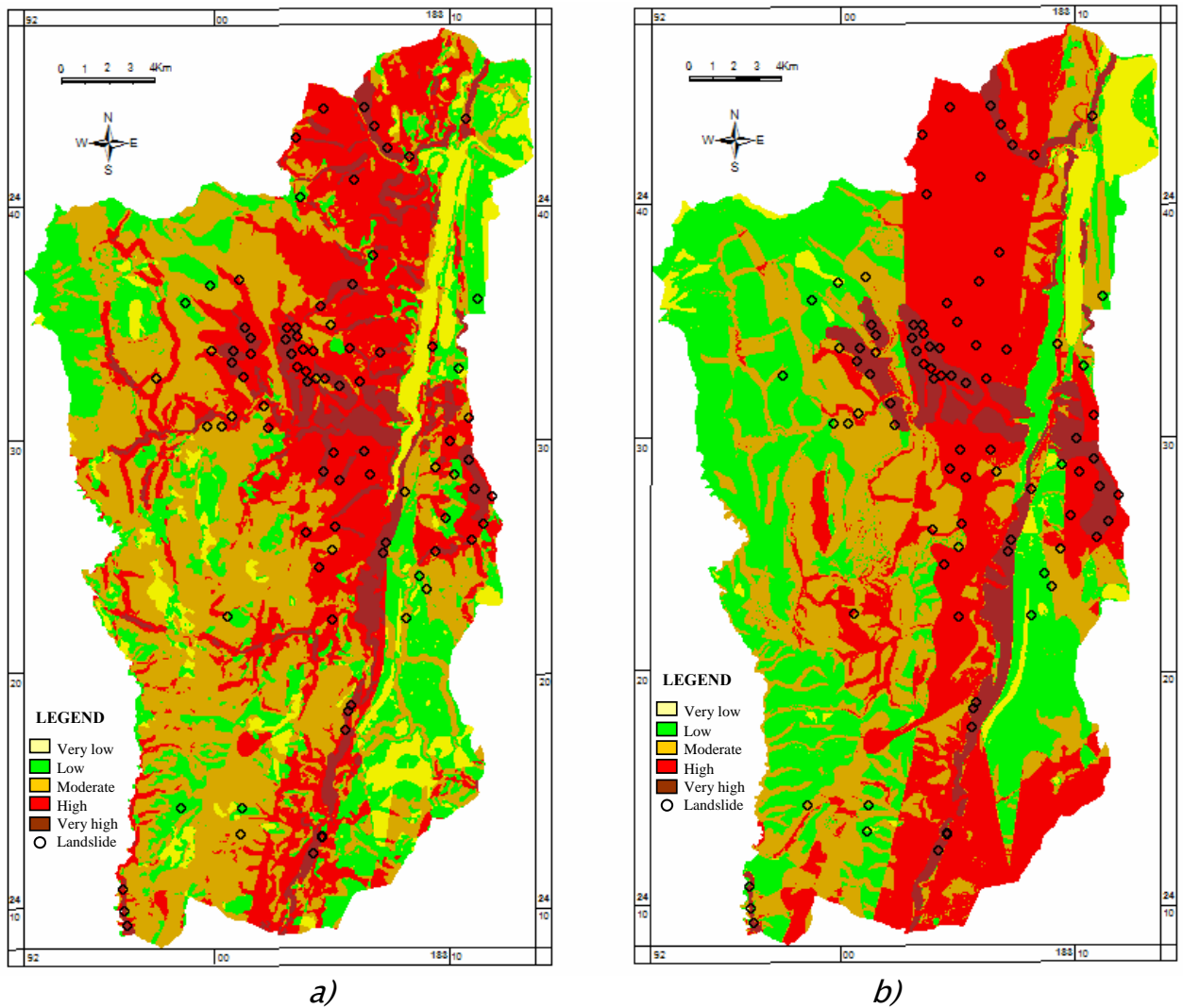


Figure 5-18. Landslide hazard zonation map with observed landslides. a) Landslide hazard map from statistical index model; b) Landslide hazard map from multiple linear regression model

Based on the evaluation of the prediction accuracy of the observed landslides on two LHZ maps, it can be remarked that as follows:

- The LHZ map of statistical index method with most of the observed landslide areas that are well predicted (95% of landslides), falls in moderate, high, and very high landslide susceptibility classes and 5% are wrongly predicted in this method. Hence, the high and very high landslide susceptibility classes in the LSZ map from the statistical index method can be considered as "highly believable".
- The LHZ map of multiple linear regression method with 91% of the observed landslide areas that are well predicted belongs to moderate, high, and very high landslide susceptibility classes. 9% are wrongly predicted in this method. Hence, the high and very

high landslide susceptibility classes in the LSZ map from Multiple linear regression can be considered "reliable".

□ Both of above methods are considered "reliable". However, the statistical index method is better than the multiple linear regression method with very high prediction percentage (95%).

Base on the result of above analyses, the statistical index method is considered as the best method for landslide susceptibility mapping in the research area, and the LHZ map resulting from the statistical index method is chosen as the final map of this study.

Moreover, the author compared predicted results with the "Landslide map of Northwest Vietnam, with map scale of 1:50'000, 1999". The areas of landslide probability of the different landslide susceptibility classes are accurate and very reliable.

5.4. DISCUSSION

A partition map predicting the landslide hazard in the research area based on the GIS system have been successfully built by the author with 5 levels of classification: 1. Very low; 2. Low; 3. Moderate; 4. High; and 5. Very high.

These results were compared with observed landslides as well as other studies conducted in of the research area, in particular the Landslide map of Northwest Vietnam (Figure 1-6). The predicted results were accurate and very reliable. The areas of landslide probability of the different landslide susceptibility classes were also accurate and very reliable.

An assessment of mapping prediction results indicated that at least 80% of landslides and 95% of the landslides in the research area have been accurately predicted. This result is relatively high with model predictions, so the partition results of disaster landslide risks are relatively accurate and can be applied to practical research areas in order to prevent and alleviate damages due to crashes landslide can cause.

The final map of landslide susceptibility zonation for the research area is shown in Figure 5-20, and the area percentages of landslide susceptibility classes in the final map of landslide susceptibility zonation for the research area are shown in Table 5-18.

Table 5-18. The hazard value ranges used for the classification of LHZ map

Landslide hazard zonation(LHZ) classes	Percentages (%)	Area (km2)
Very Low	2.91	16.0132
Low	33.14	182.638
Moderate	40.87	225.250
High	19.61	108.0552
Very high	3.47	19.122

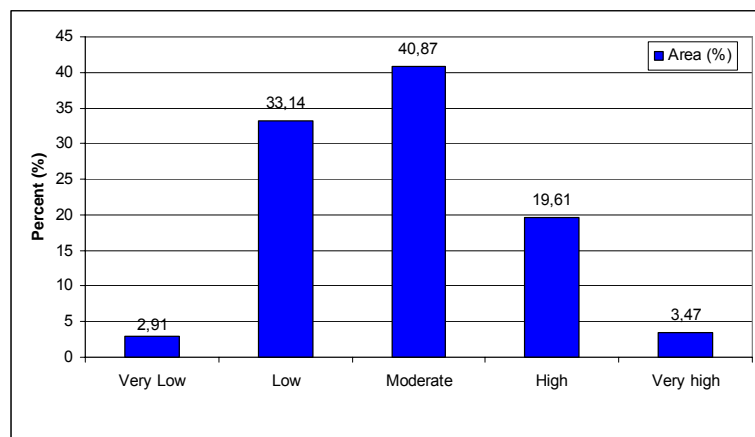


Figure 5-19. Bar chart showing the distribution of various hazard zones

slope degree, geological, geomorphological, weathering crust, land cover, lineament density, drainage density, and elevation. Among these variables, a number of critical factors were determined, including:

- A relatively high degree of slope, often $>15^{\circ}$ and frequently ranging $15-35^{\circ}$
- Distribution of land cover type (e.g., grass and bare hills, shrub and bush, and young forest)
- High average rainfall, in some areas > 2300 mm/year
- Complex geological systems in Dien Bien: ($\gamma\delta P_3-T_1db$), S_2-D_1nc formation, T_{2-3}/c formation, and $NPnc_2$ formation
- FSA1 and HH: Kaolinite-gibbsite-hydromica weathered with mixing of silixit with other weathering crusts
- Distribution of weathered crust types: FS4, SD1, SD2, SD3.
- High lineament density about >1 km/km²
- High runoff density, including areas > 2 km/km²

Statistical index and multiple linear regression methods appear to yield rapid, accurate and relatively low-cost results. Results depend on the accuracy of the data. Nevertheless, these methods also have several disadvantages, including:

- Input of statistical data is not automatic. Values (e.g., $-\infty$ or $\ln 0$) must be assigned.
- Statistical index and multiple linear regression methods have alphanumeric type or categories of classes of database (e.g., weathering crust units, geological formation units and geomorphologic units) that cannot be immediately processed; these alphanumeric type or categorical types are assigned a frequency ratio value.

When flood hazards occur, the risk to life and livelihoods is high due to the lack of preparedness, human development in high-risk areas, and general lack of hazard-proof construction materials and planning. Based on the final landslide zonation map, the following areas have high risk of landslides: Phuong Le Loi, Bia Le Loi, Phuong La Nay, Muong Tung, Tin Toc, Cong Troi, Nam He stream, Huoi Cha stream, Huoi Lo and Huoi Leng stream.

CHAPTER 6.

CONCLUSIONS AND RECOMMENDATIONS

6.1. CONCLUSIONS

This study was carried out by combining Remote Sensing technology and GIS models. The most advanced input data were obtained from LandSat TM image and aerial-photos of scale 1:50,000, which were used for landslide occurrence mapping, geological structure and land use change studies. Spatial GIS model is a powerful analysis technology using statistical models with GIS-software. The study evaluated and estimated the landslide hazard in relations with naturally different elements of conditions, such as: geology, hydrology, land use, rainfall, etc.

Based on the combination of the field survey and major factors affecting the process of landslide in the research area, 88 landslides in the area were detected and analyzed based on the RS and field surveys. Nine (9) factors influenced the stability of the landslides in the research area: 1) rainfall, 2) slope; 3) geology; 4) geomorphology; 5) weathering crusting; 6) land cover; 7) lineament density; 8) drainage density; and 9) elevation.

The research generated a series of landslide susceptibility maps using “statistical index method” and “multiple linear regression method.” Comparison of the obtained results shows that there are large differences between “bivariate statistical method” and “multivariate statistical method.” Moreover, similar methods yielded different results.

The study also generated a prediction map of landslide hazard in Muong Lay based on the GIS. The landslide hazard zonation map of the research area shows that the area of the prediction groups of very low, low, moderate, high and very high landslide hazard are 2.91%, 33.14 %, 40.87%, 19.61%, and 3.47%. A significant percentage (23%) of the research area has high to very high risk of landslide hazard.

An assessment of the research results was conducted and found that at least 80% of landslide area and 85% of the landslides in the research area have been accurately predicted. This result is a relatively high with model predictions, therefore results of landslide hazard zonation is relatively accurate and can be applied to practical landslide risk and vulnerability assessments in the region. Several causal factors were determined, including: rainfall, slope degree, geology, geomorphology, weathering crust, land cover, lineament density, drainage density, and elevation. With land-use planning, improved civil engineering techniques and increased investment, the model indicates that several key factors could be “changed” with human engineering to effectively reduce the risk of landslides to local populations. Hence, the resulting landslide prediction model is of great

utility to government land-use planners, engineers, and resettlement officers to promote the socio-economic development of poor villagers in Muong Lay region of Vietnam.

6.2. RECOMMENDATIONS

The Muong Lay region of North Western Vietnam is a relatively remote, mountainous region, inhabited primarily by ethnic minorities. Despite two decades of government investment and overseas development assistance aimed to improve the socio-economic status of local inhabitants, the area remains very poor.

The people of Muong Lay region inhabit an area that experiences high frequency of natural hazards, especially tropical storms, flash floods and landslides. Using GIS and RM technologies, landslide modeling can be applied to improve socio-economic planning through its application in land-use, transport and housing plans, risk and vulnerability assessments, and resettlement planning.

This research culminated in the development of a new landslide zonation map. It is hoped that this landslide map will be useful for saving lives and improving the livelihoods of the people of Muong Lay, ensuring that future infrastructure projects are not only designed with landslide risks in mind, but also to ensure that the few development projects that are built are not “wasted” by future, predicted events. To facilitate this supreme goal, some recommendations for remedying and preventing serious damages from landslides include:

- In areas Phuong Le Loi, Bia Le Loi area, Phuong La Nay, Muong Tung, Tin Toc, Cong Troi, Nam He stream, Huoi Cha stream, Huoi Lo and Huoi Leng stream, there is a high or very high risk of landslides. Commercial, industrial or residential land-use plans for these areas should be reexamined in light of landslide risk and vulnerabilities. Existing infrastructure and human settlement should be examined with the potential for the need of mitigation planning (i.e., moving these structures to areas of lower risk). Any existing or future resettlement plans to move ethnic minority households and villages closer to economic and transport hubs should strongly consider using the landslide maps in their planning processes.
- Many forest areas in Muong Lay have been deforested by local people in recent decades due to traditional swidden agriculture practices and the need for fuelwood and housing materials. This deforestation on a landscape scale creates favorable conditions for localized erosion and landslides, particularly after heavy rain events. In an effort to reduce the harmful effects of landslides caused by erosion and subversion on barren lands, the Government of Vietnam has initiated limited afforestation projects with the support, cooperation and labor of local people. With the application of landslide modeling, future afforestation efforts could be targeted in areas of highest risk and highest vulnerability to potential loss of life and property.

REFERENCE

1. **Abdel-Salam, M.M., 1982.** *Some institutional aspects and future prospects of the Sudan Gezira Scheme*. DSRC seminar series; discussion paper 26. Khartoum, Development Studies and Research Centre Faculty of Economic and Social Studies University of Khartoum.
2. **Aleotti, P., Chowdhury, R., 1999.** Landslide hazard assessment: summary review and new perspectives. *Bulletin engineering geology and environment*, 58: 21-44.
3. **Anbalagan, R., 1992.** Landslide hazard evaluation and zonation mapping in mountainous terrain. *Engineering geology*, 32: 269-277.
4. **Ashis, K., 2004.** An approach for GIS-based statistical landslide susceptibility zonation-with a case study in the Himalayas. *Journal Article*. Volume 2, Number 1/April, 2005, 61-69.
5. **Atkinson, P., Massari, R., 1998.** Generalised linear modelling of susceptibility for landsliding in the Central Apennines, Italy. *Computers & Geosciences*, 24(4): 373-385
6. **Ballard, T.M., Willington, R.P., 1975.** Slope instability in relation to timber harvesting in the Chilliwack Provincial Forest. *The forestry chronicle*, 51: 59-62.
7. **Benda, L.E., Cundy, T.W., 1990.** Predicting deposition of debris flows in mountain channels. *Canadian Geotechnical Journal* 27:409-417
8. **Bolt, B.A., Horn, W.L., MacDonald, G.A., Scott, R.F., 1975.** *Geological Hazards*, 328 pp. Springer-Verlag, New York. 328 pp.
9. **Bozzano, F., Floris, M., Valentini, G., 1996.** Il ruolo delle piogge nelle instabilità di pendio sul versante ionico della Basilicata: Primi risultati. *Proc. of the International Conference ALBA 1996, Prevention of Hydrogeological Hazards: The Role of Scientific Research*, November 5-7, 1996, Alba, Italy, Vol. I: 357-367.
10. **Brabb, E.E., 1984.** Innovative approaches to landslide hazard and risk mapping. In *Proc. 4th Inter. Sym. on Landslides*, Toronto, Ont. J. Seychuk (editor). Volume 30, pp. 307- 324
11. **Bull, W.B., 1996.** Prehistorical earthquakes on the Alpine fault, New Zealand. *Journal of geophysical research*, 101: 6037-6050.
12. **Cardinali, M., Carrara, A., Guzzetti, F., Reichenbach, P., 2002.** Landslide hazard map for the upper Tiber river basin. *CNR Gruppo Nazionale per la Difesa dalle Catastrofi Idrogeologiche Publication n. 2116*, scale 1:100,000.
13. **Carrara, A., 1983.** Multivariate models for landslide hazard evaluation. *Mathematical Geol.*, v. 15, n. 3, p. 403-426.
14. **Carrara, A., 1991.** GIS techniques and statistical models in evaluating landslide hazard. *Earth Surf. Proc. and Landforms*. Vol. 5:pp.427-445.
15. **Cevik, E., Topal, T., 2003.** GIS-based landslide susceptibility mapping for a problematic segment of the natural gas pipeline, Hendek (Turkey). *Environmental geology*, 44: 949-962.
16. **Chi, K.H., Park, N.W., Chung, C.J., 2002.** Fuzzy logic integration for landslide hazard mapping using spatial data from Boeun, Korea. *Symposium on Geospatial Theory, Processing and Applications*, Ottawa 2002, pp.1-6
17. **Chung, C.F., Leclerc, Y., 1994.** A quantitative technique for zoning landslide hazard. *International association for mathematical geology annual conference*, Mont Tremblant, Québec: 87-93.
18. **Chung, C.F., Fabbri, A.G., Van Westen, C.J., 1995.** Multivariate regression analysis for landslide hazard zonation. *Geographical information systems in assessing natural hazards* (A. Carrara and F.Guzzetti, editors, Kluwer Academic Publishers, Dordrecht, The Netherlands): 107-133.
19. **Chung, C.F., Fabbri, A.G., 1998.** Three Bayesian prediction models for landslide hazard. In: A. Buccianti, (ed.) *Proceedings of International Association for Mathematical Geology 1998*

- Annual Meeting (IAMG 98), Ischia, Italy, October 3-7, 1998, eds. A. Bucciante, R. Potenza, & G. Nardi, 204-211.
20. **Chung, C.F., Fabbri, A.G., 1999.** Probabilistic prediction models for landslide hazard mapping. *Photogrammetric Engineering & Remote Sensing*, 65(12): 1389-1399.
 21. **Chung, C.F., Fabbri, A.G., 2001.** Prediction models for landslide hazard zonation using a fuzzy set approach. *Geomorphology & Environmental Impact Assessment*, Balkema Publishers: 31-47.
 22. **Churchill, R.R., 1982.** Aspect-induced differences in hillslope processes. *Earth Surface Processes and Landforms*, 7(2): 171-182.
 23. **Crosta, G.B., Dal Negro, P., 2003.** Observations and modelling of soil slip-debris flow initiation processes in pyroclastic deposits: the Sarno 1988 event. *Natural Hazards and Earth System Sciences*, 3(1-2): 53-69.
 24. **Crosta, G.B., Agliardi, F., 2004.** Parametric evaluation of 3D dispersion of rockfall trajectories. *Natural Hazards and Earth System Sciences*, 4: 583-598.
 25. **Crozier, M.J., 1982.** A technique for predicting the probability of mudflow and rapid landslide occurrence. In *Proc. Inter. Seminar on Landslides and Mudflows*, Alma-Ata USSR, October 1981, UNESCO, Paris.
 26. **Crozier, M.J., 1984.** Field assessment of slope instability. In: Brunsden, D. and Prior, D.B. (eds.), *Slope Instability*, John Wiley & Sons Ltd., Chichester, Chapter 4, 103-142.
 27. **Crozier, M.J., 1989.** *Landslides: Causes, consequences and environment*. Routledge, London, 252.
 28. **Crozier, M.J., Glade, T., 2005.** Landslide Hazard and risk: Issues, concepts, and approach. In: Glade, T., Anderson, M. & Crozier, M. (Eds): *Landslide hazard and risk*. Wiley, Chichester: 1-40.
 29. **Cruden, D.M., Varnes, D.J., 1996.** Landslide Types and Processes. In *Landslides Investigation and Mitigation*. Transportation Research Board, US National Research Council, Turner, A.K. and Schuster, R.L. (editors). Special Report 247, Washington, DC 1996, Chapter 3.
 30. **Dai, F.C., Lee, C.F., Xu, Z.W., 2001.** Assessment of landslide susceptibility on the natural terrain of Lantau Island, Hong Kong. *Environmental geology*, 40(3): 381-391.
 31. **Dai, F.C., Lee, C.F., Zhang, X.H., 2001.** GIS-based geo-environmental evaluation for urban land-use planning: a case study. *Engineering geology* 61(4): 257-271.
 32. **Dai, F.C., Lee, C.F., 2002.** Landslide characteristics and slope instability modeling using GIS, Lantau Island, Hong Kong. *Geomorphology*, 42: 213-228.
 33. **Dai, F.C., Lee, C.F., 2003.** A spatiotemporal probabilistic modelling of storm-induced shallow landsliding using aerial photographs and logistic regression. *Earth Surface Processes and Landforms*, 28(5): 527-545.
 34. **David, J.W., Paul, F.H., 2000.** Mapping landslide susceptibility in Travis County, Texas, USA. *Geology journal*, 51: 245-253.
 35. **Davis, J.C., 1986.** *Statistical and data analysis in geology*, 2nd edn. John Wiley & Sons, Inc., New York, 646 p.
 36. **Davis, T.J., Keller, C.P., 1997.** Modelling uncertainty in natural resource analysis using fuzzy sets and Monte Carlo simulation: slope stability prediction. *International Journal of Geographical Information Systems* 11 (5): 409-434.
 37. **De La Ville, N., Diaz, A.C., Ramirez, D., 2002.** Remote sensing and GIS technologies as tools to support sustainable management of areas devastated by landslides. *Environment, development and sustainability*, 4 (2): 221-229.
 38. **Dietrich, W.E., Dunne, T., 1978.** Sediment budget for a small catchment in mountainous

- terrain. *Zeitschrift fur Geomorphologie*, 29: 191-206.
39. **Dietrich, W.E., Reiss, R., Hsu, M.L., Montgomery, D.R., 1995.** A process-based model for colluvial soil depth and shallow landsliding using digital elevation data. *Hydrological process*, 9: 383-400.
 40. **Dietrich, W.E., Bellugi, D., Real de Asua, R., 2001.** Validation of the shallow landslide model, SHALSTAB, for forest management. in: *Land Use and Watersheds: Human influence on hydrology and geomorphology in urban and forest areas*, edited by: Wigmosta, M.S. and Burges, S.J., Amer. Geophys. Union, Water Science and Application, 2: 195-227
 41. **Duncan, S.H. 1989.** Slope stability analysis in timber harvest planning, Smith Creek, Pacific County. In *Engineering Geology in Washington*. Wash. State Dept. Nat. Res., pp. 927-932.
 42. **Duncan, S.H., Ward, J.W., Anderson, R.W., 1987.** A method for assessing landslide potential as an aid in forest road placement. *North West Sci.*, 61:152-159.
 43. **Dunne, T., 1984.** The prediction of erosion in forests. In *Proc. Sym. on Effects of Forest Land Use Erosion and Slope Stability*, Univ. Hawaii, Honolulu, pp. 3-11.
 44. **Dymond, J.R., Jessen, M.R., Lovell, L.R., 1999.** Computer simulation of shallow landsliding in New Zealand hill country. *International Journal of Applied Earth Observation and Geoinformation*, 1(2): 122-131.
 45. **Ellen, S.D., Mark, R.K., Cannon, S.H., Knifong, D.C., 1993.** Map of debris flow hazards in the Honolulu District of Oahu, Hawaii. U.S.G.S. Open File 93-213.
 46. **Ercanoglu, M., Gokceoglu, C., 2002.** Assessment of landslide susceptibility for a landslide-prone area (north of Yenice, NW Turkey) by fuzzy approach. *Environmental Geology*, 41:720-730.
 47. **Ercanoglu, M., 2005.** Landslide susceptibility assessment of SE Bartın (West Black Sea region, Turkey) by artificial neural networks. *Natural Hazards and Earth System Sciences*, 5: 979-992
 48. **Evans, S.G., Gardiner, J.S., 1989.** Geological hazards in the Canadian Cordillera. In *Quaternary geology of Canada and Greenland*. R.J. Fulton (editor). *Geol. Surv. Can. No. 1*, pp. 702-713.
 49. **Evans, S.G., Hungr, O., 1993.** The assessment of rockfall hazard at the base of talus slopes. *Can. Geotech. J.* 30:620-636.
 50. **Fannin, R.J., Rollerson, T.P., 1993.** Debris flows: some physical characteristics and behaviour. *Can. Geotech. J.*, 30:71-81.
 51. **Fell, R. 1994.** Landslide risk assessment and acceptable risk. *Can. Geotech J.* 31:261-272.
 52. **Fookes, P.G., Dale, S.G., Land, J.M., 1991.** Some observations on a comparative aerial photography interpretation of a landslipped area. *Quarterly Journal of Engineering Geology*, 24, 249-265.
 53. **Fridland, V.M., 1973.** Soil and the humid tropical weathring crust for instance in North Viet. Hanoi Techical Publishing House, Vietnam. Galang, J.S., 2004. Master thesis "A Comparison of GIS Approaches to slope instability zonation in the central Blue Ridge mountains of Virginia". Faculty of Virginia Polytechnic Institute and State University, Blacksburg, Virginia. p 99.
 54. **Gao, J., 1993.** Identification of topographic settings conducive to landsliding from DEM in Nelson County. *Earth surface Process and Landforms*, 18: 579-591.
 55. **Glade, T., 1998.** Establishing the frequency and magnitude of landslidetriggering rainstorm events in New Zealand. *Environmental geology*, 35(2-3): 160-174.
 56. **Glade, T., 2001.** Landslide hazard assessment and historical landslide data - an inseparable couple? In: *The use of historical data in Natural Hazard Assessments*,
 57. **Glade, T., Albini, P., Francés, F., Aksoy, H., 1996.** Landslide susceptibility mapping of the

- slopes in the residual soils of the Mengen region (Turkey) by deterministic stability analyses and image processing techniques. *Engineering Geology*, 44: 147-161.
58. **Gomez, H., Kavzoglu, T., 2005.** Assessment of shallow landslide susceptibility using artificial neural networks in Jabonosa River Basin, Venezuela. *Engineering Geology* 78: 11-27.
 59. **Gorsevski, P.V., Gessler, P., Foltz, R.B., 2000.** Spatial prediction of landslide hazard using logistic regression and GIS. 4th International Conference on Integrating GIS and Environmental Modeling (GIS/EM4): Problems, Prospects and Research Needs. Banff, Alberta, Canada, September 2 - 8, 2000.
 60. **Gorsevski, P.V., Gessler, P.E., Jankowski, P., 2003.** Integrating a fuzzy kmeans classification and a Bayesian approach for spatial prediction of landslide hazard. *Journal of geographical systems*, 5(3): 223-251.
 61. **Govi, M., 1977.** Photo interpretation and mapping of the landslides triggered by the Friuli earthquake of 1976. *Bull. Inter. Assoc. Eng. Geol.* 15:67-72.
 62. **Guzzetti, F., Cardinali, M., 1990.** Landslide inventory map of the Umbria Region, Central Italy. In *Proc. 6th Inter. Conference and Field Workshop on Landslides*, pp. 273-283.
 63. **Guzzetti, F., Cardinali, M., Reichenbach, P., 1994.** The AVI project: a bibliographical and archive inventory of landslides and floods in Italy. *Environmental Management*, 18: 623-633.
 64. **Guzzetti, F., Carrara, A., Cardinali, M., Reichenbach, P., 1999.** Landslide hazard evaluation: a review of current techniques and their application in a multi-scale study, Central Italy. *Geomorphology*, 31(1-4): 181-216.
 65. **Guzzetti, F., 2000.** Landslide fatalities and the evaluation of landslide risk in Italy. *Engineering Geology*, 58: 89-107.
 66. **Guzzetti, F., Crosta, G.B., Detti, R., Agliardi, F., 2002.** STONE: a computer program for the three-dimensional simulation of rock-falls. *Computers & Geosciences*, 28(9): 1079-1093.
 67. **Guzzetti, F., Reichenbach, P., Wieczorek, G.F., 2003b.** Rockfall hazard and risk assessment in the Yosemite Valley, California, USA. *Natural Hazards and Earth System Sciences*, 3(6): 491-503.
 68. **Guzzetti, F., Reichenbach, P., Ghigi, S., 2004.** Rockfall hazard and risk assessment in the Nera River Valley, Umbria Region, central Italy. *Environmental Management*, 34(2): 191-208.
 69. **Guzzetti, F., Reichenbach, P., Cardinali, M., Galli, M., Ardizzone, F., 2005.** Landslide hazard assessment in the Staffora basin, northern Italian Apennines. *Geomorphology*, 72: 272-299.
 70. **Guzzetti, F., Reichenbach, P., Ardizzone, F., Cardinali, M., Galli, M., 2006.** Estimating the quality of landslide susceptibility models. *Geomorphology*, 81: 166-184.
 71. **Hack, J.T., Goodlett, J.C., 1960.** Geomorphology and forest ecology of a mountain region in the central Appalachians. U.S. Geological Survey professional paper 347, 66 p.
 72. **Hall, D.E., Long, M.T., Remboldt, M.D., 1994.** Slope stability reference guide for National Forests in the United States. U.S.D.A., For. Serv., Washington, DC., EM7170-13.
 73. **Hammond, C., Hall, D., Miller, S., Swetik, P., 1992.** Level 1 stability analysis (LISA), documentation for Version 2.0. U.S.D.A., For. Serv., Moscow, ID, Intermountain Res. Sta. Gen. Tech. Rep. INT-285.
 74. **Hansen, A. 1984.** Landslide hazard analysis. In *Slope Instability*. D. Brunsten and D.B. Prior (editors). John Wiley and Sons, pp. 523-602.
 75. **Hansen, A. Franks, C.A.M., 1991.** Characterization and mapping of earthquake triggered landslides for seismic zonation. In *Proc. 4th Inter. Conference Seismic Zonation*, Stanford, CA., pp. 149-195.

76. **Hansen, B.E. 1990.** The significance of lithology in debris torrent occurrence in three regions of British Columbia. M.A. Thesis, Dept. Geog., Univ. BC, Vancouver, BC.
77. **Hartlen, J., Viberg, L., 1988.** Evaluation of landslide hazard. In Proceedings 5th Inter. Sym. on Landslides. C. Bonnard (editor). Lausanne, Switzerland, pp. 1037-1057.
78. **Haruyama, M., Kitamura, R., 1984.** An evaluation method by the quantification theory for the risk degree of landslides caused by rainfall in active volcanic area. In Proc. 4th Inter. Sym. on Landslides, Toronto, Ont. J. Seychuk (editor). pp. 435-440.
79. **He, Y.P., Xie, H., Cui, P., Wei, F.Q., Zhong, D.L., Gardner, J.S., 2003.** GIS-based hazard mapping and zonation of debris flows in Xiaojiang Basin, southwestern China. *Environmental Geology*, 45: 286-293.
80. **Hicks, B.G., Smith, R.D., 1981.** Management of steep lands impacts by landslide hazard zonation and risk evaluation. *N.Z. J. of Hydrology*, 20:63-70.
81. **Hoang, L.N., Khanh, N.Q., 2003.** Article: "Satellite image geometric correction", Youth journal, Research Institute of Geology and Mineral Resources, Hanoi, Vietnam. (Vietnamese)
82. **Hogan, D.L., Wilford, D.J., 1989.** A sediment transfer hazard classification system, linking erosion to fish habitat. In Proc. Watershed '89 Conference U.S.D.A., For. Serv., Juneau, Alaska, pp. 143-155.
83. **Hollingsworth, R., Kovacs, G.S., 1981.** Soil slumps and debris flows: prediction and protection. *Bull. Assoc. Engng. Geol.* 18:17-28.
84. **Honda, K., Philipps, G.P., Yokoyama, G.P., 2002.** Identifying the threat of debris flow to major arterial roads using Landsat ETM+ imagery and GIS modeling-an example from Catanduanes island, Republic of the Philippines. Proceedings of the Asian conference on remote sensing, <http://www.gisdevelopment.net/aars/acrs/2002/>
85. **Howes, D.E., Sondheim, M., 1989.** Quantitative definitions of stability classes as related to post-logging clearcut landslide occurrence (II). BC Min For. Land Man. Rep. No. 56:167-187.
86. **Hung, L.Q., 2001.** Remote sensing based hydrogeological analysis in Suoi Muoi. Catchment – Vietnam. IUPWARE MSc thesis, Vrije Universiteit Brussel, 88pp
87. **Hung, L.Q., 2002.** Report on: "Applying GIS and Remote sensing in Landslide susceptibility research of Coastal provinces in Central of Vietnam, from Quang Binh provinces to PhuYen province". VIGMR, 7-2002. (Vietnamese).
88. **Hung, L.Q., Khanh, N.Q., 2002.** Article: "Apply remote sensing analysis method and GIS in researching geological hazards", Youth journal, Research Institute of Geology and Mineral Resources, Hanoi, Vietnam. (Vietnamese)
89. **Hung, N.V., 2008.** Ph.D in Geo-informatics. Thesis: "*Remote Sensing and Geographical Information System Tools for Decision Support of Specific Crops with focus on Soil Erosion Risk in Hoa Binh province, Vietnam*". Institute of Geography and Geology, Ernst - Moritz - Arndt - University of Greifswald, Germany.
90. **Hungr, O., Sobkowicz, J., Morgan, G.C., 1993.** How to economize on natural hazards. *Geotech. News*, 11:54-57.
91. **Hutchinson, J.N., 1988.** General report: morphological and geotechnical parameters of landslides in relation to geology and hydrology. 5th International Symposium on Landslides, Balkema, Rotterdam, 1: 3-35.
92. **Hutchinson, N., 1992.** Landslide hazard assessment. In Proc. 6th Inter. Sym. on Landslides. D.H. Bell (editor). Christchurch, N.Z. pp. 1805-1842.
93. **Hylland, M.D., Lowe, M., 1997.** Regional landslide-hazard evaluation using landslide slopes, western Wasatch Country, Utah. *Environment and engineering geoscience*, 3(1): 31-43.
94. **Ibetsberger, H.J., 1996.** The Tsergo Ri landslide: an uncommon area of high morphological activity in the Langthang valley, Nepal. *Tectonophysics*, 260: 85-93.

95. **Iverson, R.M., Major, J.J., 1987.** Rainfall, ground-water flow, and seasonal movement at Minor Creek landslide, northwestern California: physical interpretation of empirical relation. Geological survey. America bulletin, 99: 579-594.
96. **Iverson, R.M., 2000.** Landslide triggering by rain infiltration. Water Resources Research, 36(7): 1897-1910.
97. **Ives, J.D., Bovis, J.M., 1978.** Natural hazards maps for land-use planning, San Juan Mountains, Colorado, U.S.A. Arct. Alp. Res., 10:185-212.
98. **Ives, J.D., Mears, A.I., Carrara, P.E., Bovis, M.J., 1976.** Natural hazards in mountain Colorado. Ann. Assoc. Am. Geogr., 66:129-143.
99. **Jackson, L.E. 1987.** Debris flow hazard in the Canadian Rocky Mountains. Geol. Surv. Can., Paper 86-11.
100. **Jackson, L.E., Hungr, O., Gardner, J.S., Mackay, C., 1989.** Cathedral mountain debris flows. Bull. Inter. Assoc. Engng. Geol., 40:35-55.
101. **Jacobson, R.B., Cron, E.D., McGeehin, J.P., 1989.** Slope movements triggered by heavy rainfall, Nov. 3-5, 1985 in Virginia and West Virginia, U.S.A. Geol. Soc. Am. Special Paper 236:1-14.
102. **Jibson, R.W., Harp, E.L., Michael, J.A., 1998.** A method for producing digital probabilistic seismic landslide hazard maps: an example from the Los Angeles, California, area. U.S. Geological Survey Open File Report 98-113.
103. **Jibson, R.W., Jibson, M.W., 2001.** Programs to using Newmark's method to model slope performance during earthquakes. U.S. Geological Survey Open File Report 01-116.
104. **Juang, C.H., Lee, D.H., Sheu, C., 1992.** Mapping slope failure potential using fuzzy sets. Journal of Geotechnical Engineering ASCE 118 (3): 475-493.
105. **Kienholz, H., 1978.** Maps of geomorphology and natural hazards of Grindelwald, Switzerland. Arct. Alp Res., 10:169-184.
106. **Kingsbury, P.A., Hastie, H.J., Bentley, S.P., 1992.** Regional landslip hazard assessment using a geographic information system. In Proc. 6th Inter. Sym. on Landslides. D.H. Bell (editor). Christchurch, N.Z., pp. 995-999.
107. **Keefer, D.K., 2002.** Investigating landslides caused by earthquakes-a historic review. Sum. of Geophysics, 23: 473-510.
108. **Khanh, N.Q., 1996.** Bachelor of science of Geology. Thesis: “ *Applying Remote sensing in geological structure research of Van Chan, Yen Bai province, Vietnam* ”. Faculty of Geology and Geography, *Hanoi University of Science*, 1996. (Vietnamese)
109. **Khanh, N.Q., 2000.** Master of Science. Thesis: “ *Using GIS to assessment of capability fluctuation of environmental Geology in SonLa hydro-electric lake and surrounding* ”. Faculty of Environment Science, *Hanoi University of Science*. (Vietnamese)
110. **Lang, A., Moya, J., Corominas, J., Schrott, L., Dikau, R., 1999.** Classic and new dating methods for assessing the temporal occurrence of mass movements. Geomorphology, 30: 33-52.
111. **Lessing, P., Erwin, R.B., 1977.** Landslides in West Virginia. Reviews in Engineering Geology, Vol. 3. D.R. Coates (editor). Geol. Soc. Am., pp. 245-254.
112. **Lee, S., Min, K., 2001.** Statistical analysis of landslide susceptibility at Yongin, Korea. Environmental Geology, 40 1095-1113.
113. **Lee, S., Choi, J., Min, K., 2002.** Landslide susceptibility analysis and verification using a Bayesian probability model. Environmental Geology, 43: 120-131.
114. **Lee, S., Ryu, J.H., Min, K., Won, J.N., 2004.** Landslide susceptibility analysis using GIS and artificial neural network. Earth Surface Processes and Landforms, 28(12): 1361-1376.

115. **Lee, S., 2005.** Application and cross-validation of spatial logistic multiple regression for landslide susceptibility analysis. *Geosciences*, 9(1): 63-71.
116. **Lee, S., Pradhan, B., 2006.** Probabilistic landslide hazards and risk mapping on Penang Island, Malaysia. *Earth System Science*, 115(6): 661-672
117. **Lineback, G.M., Marcus, W.A., Aspinall, R., Custer, S.G., 2001.** Assessing landslide potential using GIS, soil wetness modeling and topographic attributes, Payette River, Idaho. *Geomorphology*, 37: 149-165.
118. **Lohnes, R.A., Handy, R.L., 1968.** Slope angles in friable loess. *Geology journal*, 76(3): 247-258.
119. **Lomtdaze, V.D., 1997.** Geoengineering - tectonical geoengineering. Nedra Publishing House, Moskva.
120. **Long, N.T., 2008.** Ph.D in Physical Land Resources. Thesis: "*Landslide Susceptibility Mapping of the mountainous area in A Luoi District, Thua Thien Hue Province, Vietnam*". Vrije Universiteit Brussel (VUB), Belgium. 7-2008.
121. **Long, N.T., Khanh, N.Q., 2008.** Report on: "*Application of Geographic – Geological Information System for landslide potential assessment, supporting for social and economic and sustainable development in Son La hydroelectric catchments – including of Muong Lay, Tua Chua, Tuan Giao, Muong Te and Sin Ho*". Department of Remote Sensing and Geomatics, VIGMR. (Vietnamese).
122. **Luzi, L., Pergalani, F., 1999.** Slope instability in static and dynamic conditions for urban planning: the "Oltre Po Pavese" case history (Regione Lombardia – Italy). *Natural hazards*, 20: 57-82.
123. **Luzi, L., Pergalani, F., 2000.** A correlation between slope failures and accelerometric parameters: the 26 September 1997 earthquake (Umbria- Marche, Italy). *Soil Dynamics and Earthquake Engineering*, 20: 301-313
124. **Maharaj, R., 1995.** Engineering-geological mapping of tropical soils for land-use planning and geotechnical purposes: a case study from Jamaica, West Indies. *Engineering geology*, 40: 243-286.
125. **Mathew, J.A., Brunsden, D., Frenzel, B., Gläser, B., Weiß, M.M., 1997.** Rapid mass movement as a source of climatic evidence for the Holocene Palaeo climate. *Research*, v19, Gustav Fischer, Stuttgart.
126. **Matula, M., 1971.** Engineering geology mapping and evaluation in urban planning. In *Environmental Planning and Geology*, U.S. Dept. of Housing and Urban Dev., Washington, DC., pp. 144-150.
127. **McClelland, D.E., Foltz, R.B., Wilson, W.D., Cundy, T.W., Heinemann, R., Saurbier J.A., Schuster, R.L., 1997.** Assessment of the 1995 & 1996 floods and landslides on the Clearwater National Forest, Part I: landslide assessment. Report to the regional Forester Northern Region U.S. Forest Service.
128. **McClung, D., 1990.** A model for scaling avalanche speeds. *J. Glaciol.* 36:188-196.
129. **McNutt, J.A., McGreer, D., 1985.** Pitfalls in the strict reliance on expert opinion in assessing slope stability hazard. In *Proc. Workshop on Slope Stability*. U.S.D.A. For. Serv., Portland, Oregon. Gen. Tech. Rep. PNW-180, pp. 30-35.
130. **Mehmet Lütfi SÜZEN, 2002.** Ph.D Geol. Eng. Thesis: "*Data Driven Landslide Hazard Assessment using Geographical Information Systems and Remote Sensing*". Geological Engineering Department, METU 06531 Ankara TURKEY
131. **Mehrotra, G.S., Sarkar, S., Dharmaraju, R., 1992.** Landslide hazard assessment in Rishikesh-Tehri, Garwhal Himalaya. In *Proc. 6th Inter. Sym. on Landslides*. D.H. Bell (editor). Christchurch, N.Z., pp. 1001-1007.
132. **Miles, S.B., Ho, C.L., 1999.** Rigorous landslide hazard zonation using Newmark's method

- and stochastic ground motion simulation. *Soil Dynamics and Earthquake Engineering*, 18(4): 305-323.
133. **Montgomery, D.R., Dietrich, W.E., 1994.** A physically-based model for the topographic control on shallow landsliding. *Water resources research*, 30: 1153-1171.
 134. **Morgan, G.C., Rawlings, G., Sobkowicz, J., 1992.** Evaluating total risk to communities from large debris flows. In *Proc. Geohazards '92 Sym.*, Can. Geotech. Soc., Vancouver, BC, pp. 225-235.
 135. **Nagarajan, R., Roy, A., Vinod Kumar, R., Mukherjee, A., Khire, M.V., 2000.** Landslide hazard susceptibility mapping based on terrain and climatic factors for tropical monsoon regions. *Bulletin of engineering geology and environment*, 58: 275-287.
 136. **Nasmith, H.W., Gerath, R.F., 1979.** Application of the ELUC terrain classification system to engineering projects. *BC Prof. Engng.*, 30.
 137. **Newmark, N.M., 1965.** Effects of earthquakes on dams and embankments. *Geotechnique*, 15: 139-160.
 138. **Nielsen, T.H., Brabb, E.E., 1977.** Slope stability studies in the San Francisco Bay region, California. *Reviews in Engineering Geology*, Vol. 3. D.R. Coates (editor). *Geol. Soc. Am.*, pp. 235-243.
 139. **Niemann, K.O., Howes, D.E., 1992.** Slope stability evaluations using digital terrain models. *BC Min. For., Victoria, BC, Land Man. Rep.* 74.
 140. **Nossin, J.J., 1989.** Aerospace survey of natural hazards. *ITC Journal*, 3-4: 183-188.
 141. **Nyland, D., Miller, G.E., 1977.** Geological hazards and urban development of silt deposits in the Penticton area. *BC Dept. Hwys., Geotech. Mat. Br. Victoria, BC Intern. Rep.*
 142. **O'Loughlin, E.M., 1986.** Prediction of surface saturation zones in natural catchments by topographic analysis. *Water Resources Research*, 22(5): 794-804.
 143. **O'Neill, M.P., Mark, D.M., 1987.** On the frequency distribution of land slope. *Earth surface Process and Landforms*, 12: 127-136.
 144. **Oyagi, N. 1984.** Landslides in weathered rocks and residual soils in Japan and surrounding areas. In *Proc. 4th Inter. Sym. on Landslides*, Toronto, Ont. J. Seychuk (editor). pp. 1-31.
 145. **Oztekin, B., Topal, T., 2005.** GIS-based detachment susceptibility analyses of a cut slope in limestone, Ankara–Turkey. *Environmental geology*, 49: 124–132.
 146. **Pachauri, A.K., Pant, M., 1992.** Landslide hazard mapping based on geological attributes. *Engineering geology*, 32: 81-100.
 147. **Pachauri, A.K., Gupta, P.V., Chander, R., 1998.** Landslide zoning in a part of the Garhwal Himalayas. *Environmental geology*, 36(3-4): 325-334.
 148. **Pack, R.T., Tarboton, D.G., Goodwin, C.N., 1998.** The SINMAP approach to terrain stability mapping. In: *Proceedings of 8th Congress of the International Association of Engineering Geology*, Vancouver, British Columbia, Canada. pp. 1157-1165.
 149. **Pack, R.T., Tarboton, D.G., Goodwin, C.N., 2005.** SINMAP 2 - A stability index approach to terrain stability hazard mapping. <http://www.engineering.usu.edu/dtarb/sinmap.html>.
 150. **Petley, D.N., Crick, W.D.O., Hart, A.B., 2002.** The use of satellite imagery in landslide studies in high mountain areas. *Proceedings of the 23rd Asian Conference on Remote Sensing (ACRS'2002)*, Kathmandu.
 151. **Pistocchi, A., Luzi, L., Napolitano, P., 2002.** The use of predictive modeling techniques for optimal exploitation of spatial databases: a case study in landslide hazard mapping with expert system-like methods. *Environmental Geology* 41: 765–775.
 152. **Popescu, M.E., 1994.** A suggested method for reporting landslide causes. *Bull. Inter. Assoc. Engng. Geol.*, 50:71-74.

153. **Radbruch-Hall, 1982.** Landslide overview map of the conterminous United States. U.S. Geol. Surv. Prof. Paper 1183.
154. **Rao, P., Mukherjee, D., 1992.** Kathgodam-Naintal Highway - a case study in landslide hazard zonation. In Proc. 6th Inter. Sym. on Landslides. D.H. Bell (editor). Christchurch, N.Z., pp. 1051-1056.
155. **Rautela, P., Lakhera, R.C., 2000.** Landslide risk analysis between Giri and Tons Rivers in Himachal Himalaya (India). International Journal of applied earth observation and geoinformation, 2: 153–160.
156. **Reilly, T., Powell, B., 1985.** Applications of geotechnical data to forest management. In Proc. Workshop on Slope Stability: Problems and Solutions in Forest Management. U.S.D.A. For Serv., Portland, Ore., Gen. Tech. Rep. PNW-180, pp.87-93.
157. **Reger, J.P., 1979.** Discriminate analysis as a possible tool in landslide investigations. Earth Surface Processes and Landforms, 4: 267-273.
158. **Rice, R.M., Pillsbury, N.H., 1982.** Predicting landslides in clearcut patches: recent developments in the explanation and prediction of erosion and sediment yield. In Proc. Exeter Symp. Inter. Assoc. Hydrological Sci. Publ. 137:303-311.
159. **Roth, R.A. 1983.** Factors affecting landslide-susceptibility in San Mateo County, California. Bull. Eng. Geol. 20:353-372.
160. **Ryder, J.M., MacLean, B., 1980.** Guide to the preparation of a geological hazards map. BC Min. Environ., Res. Anal. Br. Rep. 1980-04-17.
161. **Sarkar, S., Kanungo D.P., Mehrotra G.S., 1995.** Landslide hazard zoning: a case study in Garhwal Himalaya, India. Mountain Research and Development, 15(4): 301-309.
162. **Shrestha, D.P., 1991.** Lecture notes on digital image processing of remote sensing data. Enschede, Netherlands, ITC.
163. **Sidle, R.C., Chigira, M., 2004.** Landslides and debris flows strike Kyushu, Japan. Transactions American Geophysical Union, 85(15): 145-151.
164. **Sidle, R.C., Ochiai, H., 2006.** Landslides: processes, prediction, and landuse. American Geophysical Union, Washington, D.C. Water Resources Monograph No.18: 312p.
165. **Sobkowiec, J., Hungr, O., Morgan, G.C., 1995.** Probabilistic Mapping of a debris flow hazard area: Cheekeye Fan, British Columbia. In Proc. Can. Geot. Conf. Vancouver, BC, pp. 519-529.
166. **Soeters, R., Van Westen, C.J., 1996.** Slope instability recognition analysis and zonation. In: Turner KT, Schuster RL (eds) Landslide: investigation and mitigation. Spec Rep 47. Transportation Research Board, National Research Council, Washington, DC, 129–177
167. **Styles, K.A., Hansen A., Burnett, A.D., 1986.** Use of a computer-based land inventory for delineation of terrain which is geotechnically suitable for development. In Proc. 5th Inter. Cong. Inter. Assoc. Engng. Geol., Buenos Aires, Argentina. pp. 1841-1848.
168. **Süzen, M.L., Doyuran, V., 2004.** A comparison of the GIS based landslide susceptibility assessment methods: multivariate versus bivariate. Environmental geology, 45: 665–679.
169. **Swanston, D.N., Dyrness, C.T., 1973.** Stability of steep land. Forest journal, 71: 264-269.
170. **Swanston, D.N., 1978.** Effect of geology on soil mass movement activity. Proc. 5th North American Forest Soils Conference: 89-115.
171. **Tangestani, H.M., 2004.** Landslide susceptibility mapping using the fuzzy gamma approach in a GIS, Kakan catchment area, southwest Iran. Australian Journal of Earth Sciences 51 (3): 439 – 450.
172. **Terlien, M.T.J., Van Asch, T.W.J., Van Westen, C.J., 1995.** Deterministic modelling in GIS-based landslide hazard assessment. In: Carrara A, Guzzetti F (eds) Geographical

- information systems in assessing natural hazards. Kluwer Academic Publishing, The Netherlands, pp 57-77.
173. **Thach, N.N., 2005.** Teaching material: “*Remote sensing base*”, Hanoi University of Science, Hanoi National University, Vietnam. (Vietnamese)
 174. **Thien, T., 2004.** Master of Sciences in Physical Land Resources, Thesis: “*GIS and Remote sensing based for quantitative prediction of Landslide Hazard Zonation, case study Thua Thien Hue province of Vietnam*”, Vrije Universiteit Brussel (VUB), Belgium.
 175. **Thomson, S., 1971.** Analysis of a failed slope. Canadian geotechnical journal, 8: 596-599.
 176. **Tuyet D., 1991.** Report on: “*Initial studying results of landslides in Son La Town* “. Proc. 2nd Conf. Geol. Indochina, 1:470-472, Hanoi. (Vietnamese)
 177. **Tuyet D., 1997.** Report on: “*Landslide alarm sign for constructions and inhabitants in the eastern of Ong Tuong hill, SonLa, Vietnam*”. Geology and Mineral magazine, 2 : 32-34, Hanoi. (Vietnamese)
 178. **Tuyet D., 1999.** Report on: “*The predicted impacts and events of environmental Geology in SonLa hydro-electric lake and surrounding*”. VIGMR; Geology and Mineral magazine, Hanoi. (Vietnamese)
 179. **Văn, T.T., 2001.** Project report “*Assessment and prediction of geohazards in the 8 coastal provinces of Central Vietnam from Quang Binh to Phu Yen - present situation, causes, prediction and recommendation of remedial measures*”. Research Institute of Geology and Mineral Resources, Hanoi, Vietnam.
 180. **Van Westen, C.J., Alzate, J.B., 1990.** Mountain hazard analysis using a PC based GIS. In: AGID report no. 13 : environmental geology and natural hazards of the Andean region : 30 April - 2 May 1990, Medellin, Colombia / ed. by M. Hermelin, pp. 527-536.
 181. **Van Westen, C.J. 1993.** Geographic information systems in slope stability zonations. UNESCO. ITC Publ. No. 15.
 182. **Van Westen, C.J., Soeters, R., Rengers, N., 1994.** GISSIZ: training package Geographical Information Systems in slope instability zonation. In: STOP Disasters, (1994)18, pp. 24-25. - Also published as ITC publication ; 15.
 183. **Van Westen, C.J., Saldaña López, A., Uria cornejo, S.P., (1997).** ILWIS 2.1 for Windows : Applications guide : the Integrated Land and Water Information System. Enschede, ITC, 1997. 352 p.
 184. **Van Westen, C.J. Daag, A.S., 1998** Estimating erosion in volcanic deposits on mount Pinatubo, Philippines: using a DTM overlaying technique. In: EOM : The magazine for geographic, mapping, earth information = Earth Observation Magazine, (1998)2, pp. 18-20.
 185. **Van Westen, C.J., Vargas Franco, R.D., 2004.** GIS case studies : the use of geographic information systems for the assessment of natural hazards, vulnerability and risk in central America. Enschede, Centro de Coordinación para la Prevención de los Desastres Naturales en América Central (CEPREDENAC), UNESCO, ITC, Delft University of Technology (TUD), 2004.
 186. **Van Westen, C.J., 2008.** GIS for urban multi - hazard risk assessment : the RiskCity training package. In: European geologist, (2008)26, pp. 5-7,9.
 187. **Varnes, D.J., 1978.** Slope movements, types and processes. In landslide analysis and control, Schuster, R.L., Krizek, R.J (eds). National Academy Sciences. Washington DC. 11-33.
 188. **Varnes, D.J., 1984.** International Association of Engineering Geology Commission on Landslides and Other Mass Movements on Slopes: Landslide hazard zonation: a review of principles and practice, UNESCO, Paris. 63 pp.
 189. **Wakatsuki, T., Tanaka, Y., Matsukura, Y., 2005.** Soil slips on weathering-limited slopes underlain by coarse-grained granite or finegrained gneiss near Seoul, Republic of Korea. Catena, 60(2): 181-203.

190. **Ward, T.J., Li, R.M., Simons, D.B., 1982.** Mapping landslide hazards in forest watersheds. *Am. Soc. Civ. Engng., J. Geotech. Eng. Div.* 108:319-324.
191. **Wieczorek, G.F., 1984.** Preparing a detailed landslide-inventory map for hazard evaluation and reduction. *Bull. Assoc. Engng. Geol.* 21:337-342.
192. **Wilson, R.J., 1993.** Predicting earthquake-induced landslide displacements using Newmark's sliding block analysis. *Transportation Research Record*, 1411: 9-17.
193. **Yalcin, A., 2007.** GIS-based landslide susceptibility mapping using analytical hierarchy process and bivariate statistics in Ardesen (Turkey). *Catena* (2007), doi : 10.1016/j.catena.2007.01.003.
194. **Yamaguchi, Y., Tanaka, S., Odajima, T., Kamai, T., Tsuchida, S., 2003.** Detection of a landslide movement as geometric misregistration in image matching of SPOT HRV data of two different dates. *International journal of remote sensing*, 24(18): 3523 - 3534.
195. **Yokota, S., Iwamatsu, A., 1999.** Weathering distribution in a steep slope of soft pyroclastic rocks as an indicator of slope instability. *Engineering geology*, 55: 57-68.
196. **Zheng, G., Lang, Y., Takano, B., Matsuo, M., Kuno, A., Tsushima H., 2002.** Iron speciation of sliding mud in Toyama Prefecture, Japan. *Journal of Asian Earth Science*, 20: 955-963.

CURRICULUM VITAE

1. Personal information:

1	Full name	Khanh, Nguyen Quoc	Birth date/place	02/09/1975	Hanoi	Sex: M <input checked="" type="checkbox"/>
2	Institution & address:	Vietnam Institute of Geosciences and Mineral resources (VIGMR)				
	Department/ division/ faculty :	Remote sensing and Geomatics Department				

2. Qualifications:

<i>Years</i>	<i>Academic institutions</i>	<i>Major/ Specialty</i>	<i>Academic degree</i>
6/1996	Hanoi University of Science	Geography and Geology	Bachelor of science (Excellent)
6/1999	University of Foreign Languages– Hanoi National University	English Language	Bachelor in Foreign Language (Ordinary)
6/2000	Hanoi National University	Environment	Master of Science (Excellent)

3. Professional experience:

<i>Years</i>	<i>Institution</i>	<i>Professional address</i>	<i>Position</i>
1996-now	Vietnam Institute of Geological and Mineral resources	Thanh Xuan - Hanoi	Researcher
2004-now	Institute of Geography and Geology. University Greifswald, Germany	Friedrich-Ludwig-Jahn-Str 16, 17487 Greifswald , Germany	PhD

4. Expertise and research interests

4.1. List all the research grants/ projects received/ participated during the last 5 years

<i>No</i>	<i>Project name</i>	<i>Funding institution & funded amount</i>	<i>Project duration</i>	<i>Position/ role in the project</i>
1	Landslide hazard assessment in Muong Lay, Vietnam. Applying GIS and remote sensing	- Institute of Geography and Geology. University Greifswald, Germany - Vietnam Institute of Geology and Mineral Resources, Hanoi Vietnam	5 years	PhD thesis

2	<i>Application of Geographic – Geological Information System for landslide potential assessment supporting for social and economic sustainable development in Son La hydroelectric catchments – including of Muong Lay, Tua Chua, Tuan Giao, Muong Te and Sin Ho</i>	<i>Ministry of Natural Resources and Environment, Hanoi, Vietnam</i>	<i>3 years</i>	<i>Researcher</i>
3	<i>Building methods of geological hazard risk assessment in northern highland urban areas of Vietnam by Using GIS and Remote sensing model. Case study in Yen Bai city</i>	<i>Ministry of Natural Resources and Environment, Hanoi, Vietnam</i>	<i>2 years</i>	<i>Researcher</i>
4	<i>Geological hazard risk assessment in in Ha Giang, Cao Bang, Tuyen Quang and Bac Kan province.</i>	<i>Ministry of Natural Resources and Environment, Hanoi, Vietnam</i>	<i>2 years</i>	<i>Researcher</i>

4.2. Publications and accomplishments:

(List all the published scientific papers, monographs, patents, awards for the last 10 years)

No	Authors	Name of publication (papers, patents, monographs)	Journals/ Publisher	Year
1	Nguyen Quoc Khanh	<i>Applying remote sensing for structure geology research in Van Chan, Yen Bai, Vietnam. (Vietnamese)</i>	<i>Thesis. Hanoi University of Science</i>	1996
2	Nguyen Quoc Khanh	<i>Applying GIS for assessment Water and Land resources in Son La hydroelectric and surrounding, Vietnam. (Vietnamese)</i>	<i>Master's Thesis. Hanoi University of Science</i>	2000
3	Nguyen Quoc Khanh	<i>Applying GIS and remote sensing in Geology reseaching (Vietnamese)</i>	<i>Youth journal, Vietnam Institute of Geology and Mineral Resources, Hanoi</i>	2002
4	Nguyen Quoc Khanh, Le Nguyen Hoang.	<i>Satellite image geometric correction, (Vietnamese)</i>	<i>Youth journal, Vietnam Institute of Geology and Mineral Resources, Hanoi</i>	2003
5	Tran Tan Van, Le Quoc Hung, Nguyen Quoc Khanh	<i>Apply remote sensing analysis method and GIS in researching geological hazards in Central of Vietnam from</i>	<i>Vietnam Institute of Geology and Mineral Resources, Hanoi,</i>	2002

		<i>Quang Binh to Phu Yen. (Vietnamese)</i>	<i>Vietnam</i>	
6	<i>Le Quoc Hung, Nguyen Thanh Long, Nguyen Quoc Khanh,</i>	<i>Results of satellite image interpretation in Poco area, (Vietnamese)</i>	<i>Vietnam Institute of Geology and Mineral Resources, Hanoi, Vietnam.</i>	2004
7	<i>Nguyen Quoc Khanh</i>	<i>Method of spatial statistical analysis in zoning of landslide predicting in Muong Lay Townlet</i>	<i>Journal of Geology, Department of Geology and Mineral of Vietnam</i>	2010
8	<i>Nguyen Quoc Khanh</i>	<i>Ph.D. thesis: “Landslide hazard assessment in Muong Lay, Vietnam. Applying GIS and remote sensing”</i>	<i>Institute of Geography and Geology. University Greifswald, Germany</i>	2010